Incorporating cinnamaldehyde into concrete for corrosion mitigation

by

Hajar Jafferji

A Dissertation

Submitted to the Department of Civil and Environmental Engineering

at

WORCESTER POLYTECHNIC INSTITUTE

In partial fulfillment of the requirements for the

Degree of Doctor of Philosophy

in

Structural Engineering

in the Department of Civil and Environmental Engineering

2016

APPROVED:

Dr. Aaron R. Sakulich, Advisor _____

Dr. Tahar El-Korchi, Department Head _____
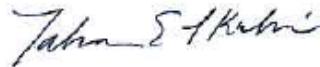
Doctoral Committee:

Dr. Mingjiang Tao _____

Dr. Leonard D. Albano _____

DEDICATION

In loving memory of my mother who taught me to always reach for the stars.

To my father, sister, and brother. Dad, you have always supported me no matter how crazy my dreams can sometimes be. Summer, you are my best friend and are always there to bring me back to reality when I get carried away with all my dreams. Mohammad, you always understand me and are the one person I can always rely for good and practical advice.

There is no way I would be able to get through anything in life without you all.

ABSTRACT

Concrete structures can prematurely deteriorate due to the corrosion of reinforcing steel. Corrosion can occur through chloride ingress due to exposure to aggressive media such as seawater and deicing salts. Corrosion causes over $100 billion in damage annually.

There are many corrosion mitigation techniques on the market today; these techniques have limited effectiveness as demonstrated by the fact that billions of dollars are still being expended each year due to corrosion-related damage. Therefore, there is a need for innovative approaches to corrosion prevention. This research program used cinnamaldehyde (CA), a bioactive agent derived from cinnamon bark, as a method for corrosion mitigation. Although CA can prevent the corrosion of metals, its hydrophobicity has a negative effect on hydration when incorporated in cementitious systems. In order to avoid these negative consequences while harnessing the anti-corrosive properties, CA was incorporated in a cementitious mixture through the use of lightweight aggregate (LWA). Several tests were carried out to investigate the potential chemical and mechanical effects due to the addition of LWA pre-wet with CA. Promising results were observed, in which the time to corrosion was prolonged by 91 %.

TABLE OF CONTENTS

LIST OF FIGURES

LIST OF TABLES

NOMENCLATURE

LWA   Lightweight aggregate

CA   Cinnamaldehyde

PCI   Penetrating corrosion inhibitor

CHAPTER 1: INTRODUCTION

This chapter discusses the processes of corrosion in concrete as well as corrosion prevention methods available on the market today. The innovative research program is then introduced. This research program is the first of its kind to incorporate the bioactive agent, cinnamaldehyde, as a corrosion inhibitor in concrete.

1.1 Background

Cement-based concrete, as it is known today, dates back to the Romans and has been noted for its durability as well as its versatility. The Pantheon in Rome that still remains standing since 126 AD is a classic illustration of a concrete structure and is particularly noted for its expansive concrete dome that spans 138 ft. (42 m) in diameter [1]. Concrete has become a staple building material with nearly 5.5 billion tons (5 billion tonnes) produced annually worldwide – approximately 1 tonne (1.1 tons) per person per year [2]. Although fundamental components of concrete generally remain the same, there have been many advances in constructing with concrete.

Engineers and architects try to constantly push the envelope by designing longer span bridges to taller buildings. For instance, the Barrios de Luna Bridge in Spain is a concrete cable-stayed bridge with a main span of 1444 ft. (440 m) [3]. Moreover, the Burj Khalifa in Dubai, UAE, currently holds the record as the tallest building in the world, rising 2717 ft. (828 m) in height, and was constructed from high-performance concrete [4].

Regardless of the size or scope of a project, each design goal consists of four main objectives: the design must be safe, serviceable, economically viable, as well as aesthetically pleasing [3]. A major part in achieving these goals depends on the durability of the concrete

used. Durability of a concrete structure is not solely based on the strength of the material but also its ability to prevent the ingress of aggressive media (i.e. sea water and deicing salts) [5]. Research and technology aim to create the most ideal concrete compositions/mixes for structures depending on a case by case basis. Common factors that govern a mix design are the location, weather conditions, function of structure, etc. Although structures are designed to be as durable as possible, American infrastructure is considered to be in poor condition with an overall "grade" of D+ and a need for $3.6 trillion for full restoration [6]. Moreover, an estimated $100 billion is spent each year around the world on maintaining and repairing corrosion related damage [7, 8].

1.2 Corrosion of concrete

The three main components of concrete are ordinary portland cement (OPC), aggregates, and water [9]. OPC is made from a mixture of components: lime or calcium oxide (CaO) commonly from limestone; silica (SiO_2) usually from sand or clay; alumina (Al_2O_3) commonly from recycled aluminum or clay; iron (Fe_2O_3) commonly from clay, iron ore, scrap iron or fly ash; and gypsum ($CaSO_4 \cdot 2H_2O$) found with limestone. All components, except for gypsum, are combined together and are heated in a kiln up to 2,642 °F (1450 °C) which produces pellets known as clinker. The clinker is then cooled and finely ground and gypsum is then added to control setting time. The main components of cement are shown in Table 1 *(overleaf)* and the main chemical composition of clinker is shown in Table 2 *(overleaf)*; other components such as sodium and potassium oxides are usually present but at variable amounts and not listed on Table 2. Due to the complexity of cement, chemical compounds are usually denoted in shorthand "chemist's notation". Each component of clinker plays a role in the final properties of cement [10]:

2

Table 1: Main raw components of cement [11]

Compound	Formula	Chemist's notation
Calcium oxide	CaO	C
Silicon dioxide	SiO_2	S
Aluminum oxide	Al_2O_3	A
Iron oxide	Fe_2O_3	F
Magnesium oxide	MgO	M
Water	H_2O	H
Sulfate	SO_3	$\bar{S}$

Table 2: Main chemical composition of clinker [11]

Compound	Formula	Chemist's notation
Tricalcium silicate (Alite)	$3\ CaO \cdot SiO_2$	C_3S
Dicalcium silicate (Belite)	$2\ CaO \cdot SiO_2$	C_2S
Tricalcium aluminate	$3\ CaO \cdot Al_2O_3$	C_3A
Tetracalcium ferroaluminate	$4\ CaO \cdot Al_2O_3 \cdot Fe_2O_3$	C_4AF
Gypsum	$CaSO_4 \cdot 2H_2O$	$C\bar{S}$

- Tricalcium silicate: hydrates and hardens quickly to assist in initial set and early strength development;

- Dicalcium silicate: hydrates and hardens at a slower rate to assist in strength increase after one week;

- Tricalcium aluminate: responsible for creating a large amount of heat during hydration and hardening during the first few days, also slightly helps in early strength increase;

- Tetracalcium ferroaluminate: reduces temperature during cement manufacture and largely responsible for the gray color of cement; and,

- Gypsum: added during final grinding of cement to react with C_3A to produce ettringite (calcium trisulfoaluminate) in order to control the hydration of C_3A to prevent rapid set.

One of the most important factors of OPC is that it is a hydraulic cement. This means that properties such as strength begin developing only when in contact with water; the mixture of cement and water is referred to as cement paste. The aluminates in cement contribute to the setting and solidification of cement paste. The hydration of C_3S and C_2S creates calcium silicate hydrate (C-S-H) which is the main source of compressive strength in the paste. Additionally, calcium hydroxide (CH) is formed during the hydration of calcium silicates. Portlandite is responsible for creating the high alkalinity of the cementitious mixture [11-13].

To create concrete aggregates, commonly gravel and sand, are added to cement paste; the cement paste holds the aggregates together creating a matrix. Aggregates are added to reduce creep and shrinkage and also reduce the amount of cement needed in a mixture, as cement is relatively expensive [12]. Reinforcing steel is often added to the concrete in order to aid in tension (concrete performs well in compression but not in tension) [14].

Concrete without any reinforcing steel is quasi-brittle and exhibits strain-softening behavior. The steel reinforcement, however, displays ductile behavior and can produce large deformations prior to failure. Thus, the load-displacement responses of these two materials can be observed in Figure 1 *(overleaf)*, where the failure behaviors are compared and displays how the steel reinforcement assists with tension; the tension strength of concrete is roughly 1/10 of its compressive strength. The areas under the load-displacement curves also show the toughness of the materials; toughness is described as the material's ability to consume energy. Concrete has a low toughness, close to 1/50 to 1/100 of steel [15].
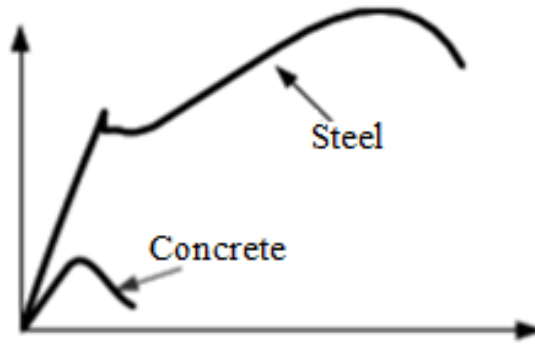
Figure 1: Failure behaviors of concrete and steel **[15]**

The mechanical and chemical properties of steel reinforcement are important to the performance of the overall concrete structure. Aspects including strength, ductility, bond to the concrete (bars are usually ribbed to ensure proper adhesion with the concrete.), and weldability are considered during design. Some standards, such as the European design requirements of concrete structures, describe strength as the tensile strength and yield strength of the reinforcement; the ductility is the ratio of the tensile and yield strength or the strain at the maximum load. Additionally, there have been limitations regarding the chemical content of the carbon steel. Quantities of elements such as carbon, potassium, and manganese are managed since past experience shows that an increase of these elements helps with increasing the strength of the reinforcement but causes issues with its welding [11].

Concrete structures can prematurely deteriorate through the corrosion of the reinforcing steel [16, 17]. Concrete typically has an alkaline pore solution (pH > 13.5) due to the presence of calcium, sodium, and potassium oxides [18]. This protects the reinforcing steel by stabilizing a thin, passive iron oxide layer on the surface of the steel [19]. The iron oxide layer can become depassivated and allow the rebar to corrode through two methods: the carbonation of concrete and chloride attack [20].

1.2.1 Carbonation

Carbonation of concrete is a chemical process. As carbon dioxide from the atmosphere comes in contact with concrete, half of the carbon dioxide will interact with calcium hydroxide (equation 6) and the other half will decalcify the C-S-H. Both reactions will produce calcium carbonate [21, 22]:

$$CO_2 + Ca(OH)_2 \xrightarrow{H_2O} CaCO_3 + H_2O \qquad (6)$$
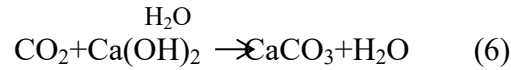
The depth of carbonation can be determined using Fick's first law [23]:

$$x = \sqrt{\frac{2Dc}{a}} \sqrt{t} \qquad (7)$$

where x is the carbonation depth at time t; D is the diffusion coefficient of CO_2 in carbonated concrete; a is the concentration of the reactive compounds (the amount of CO_2 necessary to carbonate alkaline material); and c is the CO_2 concentration in the atmosphere.

1.2.2 Chloride ingress

When chloride ingresses into concrete, it is capable of destroying the passivating film of the rebar, lowering the pore solution pH by lowering the solubility of $Ca(OH)_2$, raising the moisture content because of the formation of salts such as NaCl in the concrete, and increasing the electrical conductivity of the concrete, accelerating the corrosion of the rebar. If elements of the concrete are contaminated with chlorides during mixing, corrosion can begin early on. The ingress of chloride through reinforcing concrete can be described by Fick's second law [20]:

$$c(x,t) = c_s \left[1 - erfc\left(\frac{x}{2\sqrt{D_{eff}, c \cdot t}} \right) \right] \qquad (8)$$

6

where $c(x,t)$ is the chloride content at depth x and time t; *erfc* is the error function; $D_{eff,C}$ is the effective chloride diffusion coefficient; c_s is the surface or near surface chloride content; and x is the depth and t is the time.

1.2.3 Electrochemical process

Corrosion of the embedded steel in concrete is an electrochemical process where corroded steel is transferred into the pore solution and gives up electrons at the anode as shown in Figure 2 *(overleaf)*. Two electrons are given up in the anodic reaction that are consumed along with water and oxygen at the cathode (equations 9 and 10). One way that a reaction can continue and form rust is through ferrous hydroxide turning into ferric hydroxide, which in turn becomes ferric oxide (rust) (equations 11-13) [24, 25].

$$\text{Anode:} \quad Fe \rightarrow 2Fe^{2+} + 2e^- \quad\quad\quad (9)$$

$$\text{Cathode:} \quad \tfrac{1}{2} O_2 + H_2O + 2e^- \rightarrow 2(OH^-) \quad\quad\quad (10)$$

$$Fe^{2+} + 2OH^- \rightarrow Fe(OH)_2 \quad\quad\quad (11)$$

$$4Fe(OH)_2 + O_2 + 2 H_2O \rightarrow 4Fe(OH)_3 \quad (12)$$

$$2Fe(OH)_3 \rightarrow Fe_2O_3H_2O + 2H_2O \quad\quad\quad (13)$$
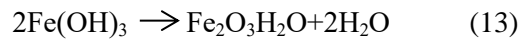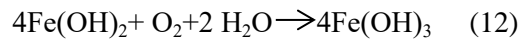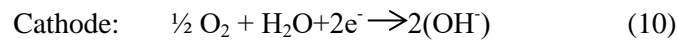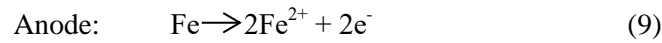
The main issue with the formation of rust is volumetric expansion, which creates a buildup of pressure causing cracking and eventually spalling of the concrete cover if the tensile strength of the concrete is exceeded. Cracks are particularly undesirable because they immediately reduce many mechanical properties of concrete, most importantly compressive strength, and provide aggressive media access to the reinforcing steel, which accelerates the cycle of deterioration [26, 27]. Additionally, the corrosion of reinforcing steel can cause mass
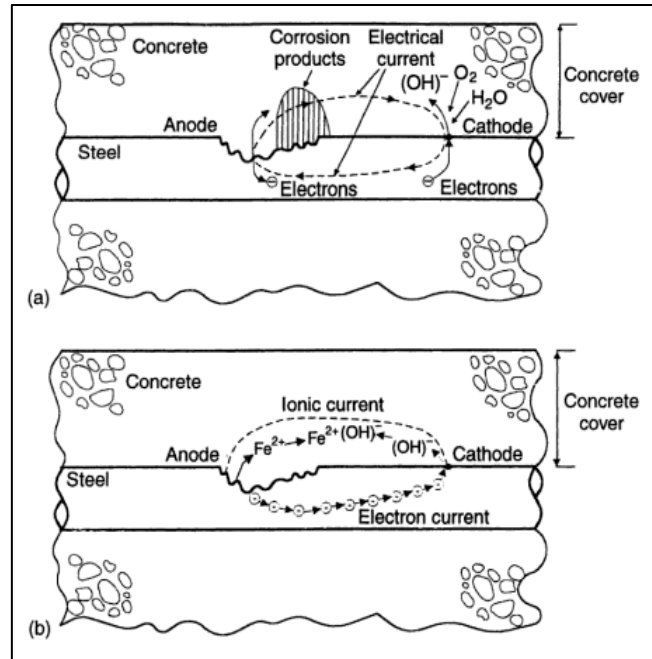
Figure 2: Process of corrosion of steel reinforcement in concrete
"Bentur, A., N. Berke, and S. Diamond, Steel corrosion in concrete: fundamentals and civil engineering practice. 1997: CRC Press."

loss and therefore create a reduction of its cross-sectional area; this can result in a reduction of the mechanical properties of the steel as well as impact the cosmetics of the structure [20, 21, 24]. The Tutti model describes corrosion of reinforcing steel due to both carbonation and chloride ingress as shown in Figure 3 (a) *(overleaf)*. Once CO_2 or chlorides diffuse through the concrete, corrosion is initiated until it reaches its threshold; once the threshold is reached corrosion is propagated and will continuously increase over time [28]. Cusson *et al.* produced a more detailed model of corrosion, based on the Tutti model as shown in Figure 3 (b) *(overleaf)* [29]. This model accounts for premature causes for deterioration such as early-age cracking as well as the gradual processes that lead to a concrete structure's failure.

1.2.4 Prevention methods

In the late 1960s, there was concern regarding the premature deterioration of highway bridge decks where large repairs were necessary just a few years after construction. It was concluded

8
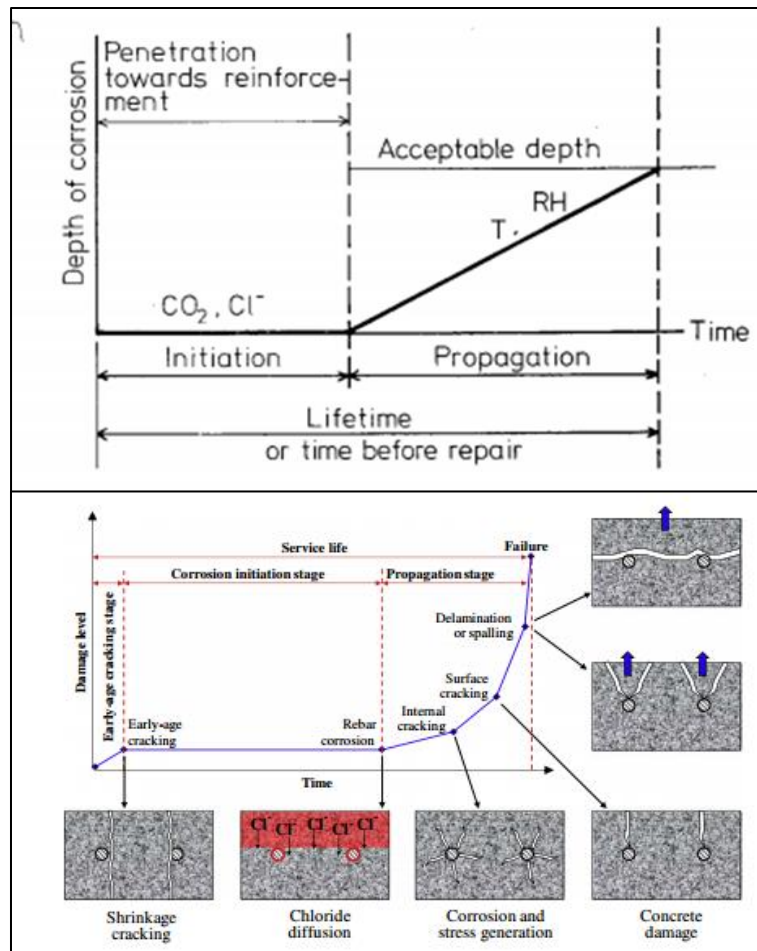
Figure 3: (a) Tutti's model of corrosion *(top)* [28] and (b) expanded corrosion model *(bottom)* [29]

that the corrosion of reinforcing steel was mainly to blame. These failures were more prevalent in snow-belt states since deicing salts were heavily used. This created a movement to increase design regulations, reevaluate concrete cover and quality of concrete regulations, and require more careful inspections and practices during construction [30-32]. Moreover, the need for new corrosion mitigation techniques became apparent. This led to the development of various methods for corrosion prevention in concrete, which will be discussed.

9

<u>Waterproofing membrane</u>

As a direct response to the increase of premature deterioration of highway bridges, the Federal Highway Administration (FHWA) urged states to use a protective system to prevent future damage. Since the issue of corrosion was quite recent, available protection techniques were limited. In 1970, National Experimental Evaluation Program (NEEP) Project No. 12 advised the use of protective membranes along with denser concrete [33]. In 1972, all federally-funded bridges with possible contact to aggressive agents were required to use protection on bridge decks. This created a boom in waterproofing membranes as it was one of the options on the market.

Waterproofing membranes were developed for prevention of both corrosion of steel reinforcement as well as freeze/thaw damage in concrete bridge decks [33]. By creating a barrier, the rebar could be protected from corrosion induced by chloride ions, water, and oxygen [24, 33]. The deck of a bridge requires the most maintenance of a bridge and can greatly impact the service life of the structure [34]. If a bituminous surface (asphalt) is applied to the deck with potential exposure to aggressive media, a membrane must be placed as asphalt is permeable. Figure 4 shows the results of a study that was conducted in 1994 by the National Cooperative
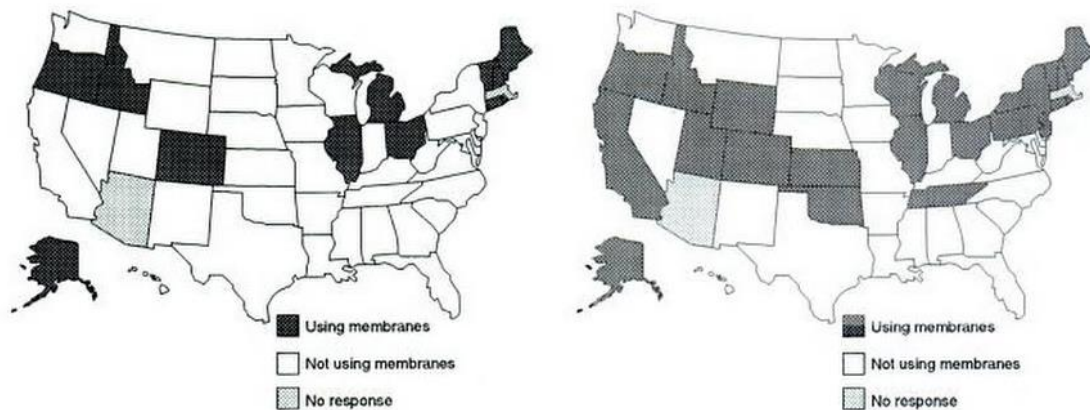
Figure 4: Waterproofing membrane usage in new construction *(left)* and in rehabilitation *(right)* [33]

Highway Research Program (NCHRP) to identify the usage of these membranes across the US and Canada. All 50 states were surveyed along with the ten provinces of Canada; however, only 48 states and six provinces responded. These results are shown in Figure 4 where it highlights the states that use and do not use the membrane in both new structures and in rehabilitation. It was determined that the Northeast U.S. has had a long history with using membranes, whereas the rest of the U.S. uses them sporadically.

Waterproofing membranes can be preformed or liquid barriers. Preformed membranes are commonly installed by first placing a primer onto the concrete deck as way to strengthen the bond between the membrane and the deck. Following the primer, the membrane can be laid; many times the membrane is a sheet that can be rolled on top of the deck (and primer) with a self-adhesive back. Some membranes can adhere to the deck by the use of heat (e.g., a hand torch). As for a liquid membrane, it also has a primer placed first as with the preformed membranes. The liquid membrane is then applied through spray or roller and is described as similar to rubberized asphalt, two-component polymer, polyurethane, methyl methacrylate, rubber polymer, polymer-modified asphalt, or rubberized bitumen [34]. Many times, in order to avoid destruction of the membrane during construction, a protection board is used. The material of the protection board can be roofing felt or an asphalt-felt. A finishing bond, known as the tack coat, is placed to create a stronger bond between protection board and the layer of asphalt concrete commonly made of a layer of bituminous material a base course. The asphalt concrete becomes the wearing course [33, 35]. The two waterproofing membranes are illustrated in Figure 5 *(overleaf)*.
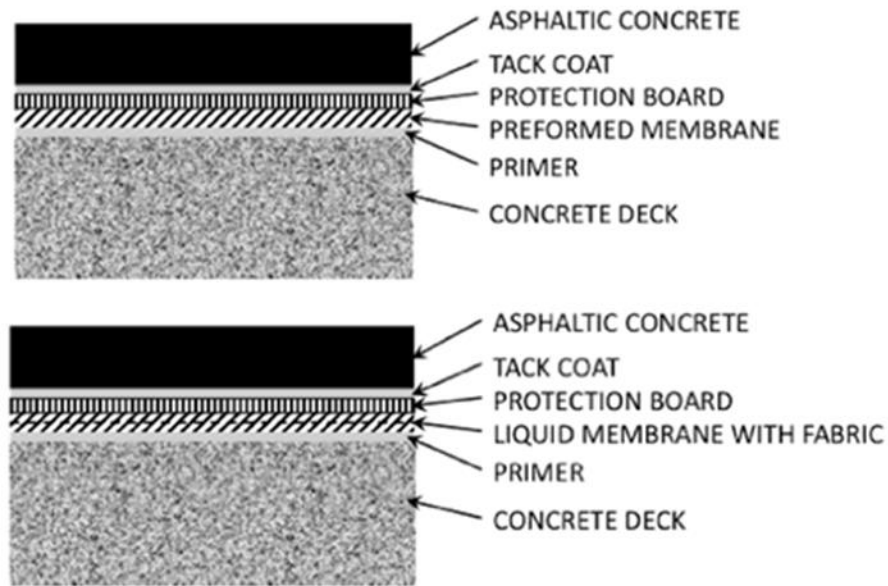
Figure 5: A common technique of preformed waterproofing membrane *(top)* as well as liquid membrane *(bottom).* [34].

According to the surveys conducted by the NCHRP in 1994 the service life of the membranes (both preformed and liquid) range from 10 to 30 years. There have been some complications with these membranes causing the replacement of the membranes in less than ten years. Some decks faced debonding that caused issues with the asphalt wearing course whereas in other cases, the membrane failed due to traffic stresses and age [33, 35].

<u>Epoxy-coated reinforcement</u>

The FHWA and the National Bureau of Standards (now the National Institute of Standards and Technology – NIST) focused on determining an effective method to alleviate the corrosion issue. This resulted in four powder epoxy coatings to be used in fusion bonded epoxy steel reinforcement [30, 36, 37]. Epoxy resin was first commercially available in 1947 [38]. The process of fusion bonded epoxy-coating on steel reinforcement came about in the early 1970s. This method has become one of the most widely used products for corrosion prevention [32]. The application of epoxy to steel reinforcement stems from a concept used in the petroleum

industry, where an epoxy coating was placed on small diameter pipes. The first step is to clean and remove existing rust on the steel, usually by grit blasting. The steel is then heated to around 446 °F (230 °C). Epoxy powder is then sprayed and melted onto the steel and is followed by a curing and quenching process. Epoxy-coated reinforcing steel is very beneficial to corrosion prevention since it is a dielectric which prevents charged chloride ions and oxygen from passing through. The coating also increases the electrical resistance between neighboring reinforcement [30, 32]. If the epoxy does become damaged, or chloride contents become extremely high, epoxy-coated reinforcement should still reduce the rate of corrosion. This is illustrated in Figure 6 where it shows the epoxy-coated reinforcement facing corrosion but it is more likely to remain localized rather than accelerating deterioration [24].

The first structure to use epoxy-coated steel reinforcement was in a suburb of Philadelphia in 1973, where four spans of a bridge across the Schuylkill River included epoxy-coated bars [39]. In 1976 the Florida Department of Transportation (FDOT) and FHWA included epoxy-coated bars in the new designs of bridges in the Florida Keys region. This was due to the fact that they were highly exposed to marine environments. In 1981 epoxy coated bars became
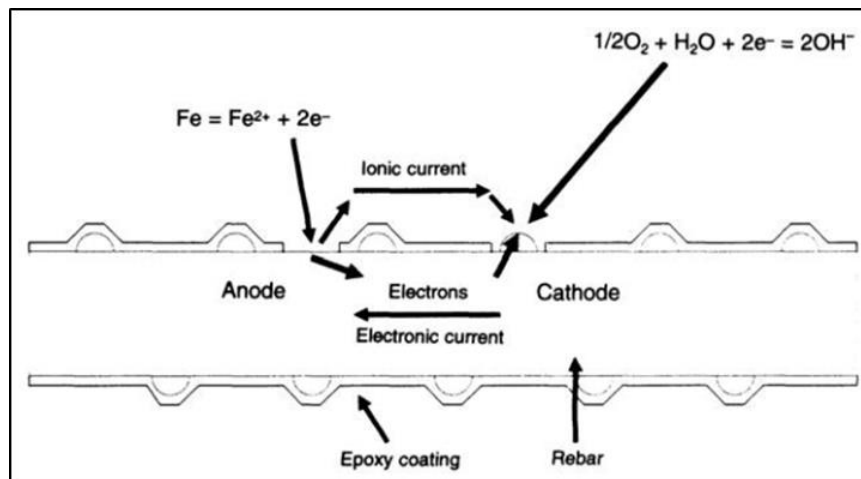
Figure 6: Epoxy-coated steel reinforcement undergoing corrosion. Corrosion remains localized [24].

13

the main means of corrosion prevention in bridge decks, and later for all bridge reinforcement components in Florida. It was not until 1986 that issues began to arise; the Long Key Bridge started to show corrosion only six years after being built. After a thorough investigation, it was determined that the cause of the damage was that the epoxy debonded from the steel bar without the influence of chloride [40]. Debonding could be caused by deposits of grit left on the surface of the bars prior to coating [24].

Epoxy-coated steel reinforcement does have many benefits and remains a method that can be improved. It is commonly used as a protection method against corrosion since it is affordable and simple to incorporate in a design (where just an increase in lap length is needed due the lower bond strength) [24, 35]. Future research and developments can potentially make this corrosion prevention technique to be more effective.

<center>Stainless steel reinforcement</center>

Another option for corrosion mitigation is stainless steel reinforcement. Stainless steel rebar is particularly known for its resistance to corrosion due to its chromium-rich passivating film [11, 41]. Alloy additions (such as nickel, molybdenum, nitrogen, titanium, etc.) may differ depending on the desired uses, such as level of corrosion protection, cost, and weldability [20]. Sometimes clad reinforcement is used, in which a layer of stainless steel is added around a carbon steel center. Issues arise with clad reinforcement if the outer surface layer becomes disturbed or destroyed, leaving the reinforcement susceptible to corrosion. There are four categories of stainless steel reinforcement, depending on their microstructure: ferritic, austenitic, martensitic, and austenitic-ferritic (duplex). Table 3 *(overleaf)* lists common stainless steel reinforcements along with their typical chemical compositions. Martensitic is not listed on Table 3 because it is not commonly used. It is, however, quite similar to ferritic steel, but has a higher hardness and

<center>14</center>

greater strength due to a larger content of carbon which makes martensitic more prone to stress corrosion cracking. Stainless steel is expensive because it contains nickel, which is costly [11, 42]. Table 4 compares the prices of common corrosion prevention methods. Stainless steel reinforcement is about six times the cost of epoxy-coated reinforcement.

The mechanical properties of stainless steel reinforcement are similar to those of carbon steel; it has similar yield strength, elastic modulus, and ductility. Stainless steel reinforcement can be easily used during construction. It does not have concerns commonly found in other corrosion prevention methods such as epoxy-coated reinforcement, where the protective epoxy barrier can be damaged during construction [20, 42].

Table 3: Common stainless steel reinforcements [11, 41]

Microstructure	Cr (% by mass)	Ni (% by mass)	Mo (% by mass)	Other elements (% by mass)
Austenitic	17.5-19.5	8-10	-	-
	16.5-18.5	10-13	2-2.5	-
Duplex	21-23	4.5-6.5	2.5-3.5	0.1-0.22 N
	22-24	3.5-5.5	0.1-0.6	0.05-0.2 N
	21-22	1.4-1.7	0.1-0.8	4.0-6.0 Mn, 0.2-0.25 N
Ferritic	16.0–18.0	-	-	
	17.5–18.5	-	-	
	17.0–20.0	-	1.8–2.5	

Table 4: Cost comparison of corrosion prevention methods(t= tonnes, m=meter l= liter). [20, 42]

Corrosion Prevention	Cost (in Germany)
Unalloyed steel	250 [€/tonne] (236 USD/ton)
Galvanized steel	600 [€/tonne] (567 USD/ton)
Epoxy-coated steel	440 [€/tonne] (416 USD/ton)
Stainless steel 1.4571	2875 [€/tonne] (2717 USD/ton)
Nitrite inhibitor	33 [€/m] (11 USD/ft)
Cathodic protection	120 [€/m] (38 USD/ft)

In the early 1960s, the construction of the Gateway Arch in St. Louis sparked great interest regarding the use of stainless steel as structural reinforcement. This then led to the development of the first American specification regarding the design of structural stainless steel in 1968. International standards in countries such as Australia, New Zealand, and South Africa regarding this material in construction originated in the American standard. Japan published the *Design and Construction Standards of Stainless Steel Buildings* in 1995. However, the use of stainless steel stems from much earlier. The Progreso Pier in Mexico was constructed in the 1940s where 200 tonnes (220.462 tons) of stainless steel reinforcement was placed; there have been no signs of deterioration to date [41].

Galvanized reinforcement

Galvanized reinforcement (which corrodes sacrificially) can be used as a corrosion prevention method [24]. These reinforcement bars are made by a hot-dip galvanizing process. Steel reinforcement are pickled (where they are placed in acid, commonly hydrochloric or sulfuric acid, in order to clean the steel's surface) and dipped into a zinc bath at about 842 °F (450 °C). The zinc coats the steel and creates an iron-zinc alloy layered effect that adheres to the reinforcement. An outer layer of about 0.0039 - 0.0059 in. (100-150 μm) zinc is left remaining on the reinforcement's surface [11].

The pH of the concrete stabilizes the zinc [43]. When the pH ranges between 8 and 12.6 the zinc is more stable. If the pH drops below 8 or above 12.6, corrosion rates increase. Therefore, galvanized reinforcement is more effective in a concrete system facing corrosion due to carbonation rather than corrosion due to chloride ingress. When carbonation occurs, the pH of the pore solution is drastically reduced. However, when concrete faces chloride ingress,

16

galvanization does not prevent corrosion but will reduce the rate of corrosion due to the zinc sacrificially corroding [43].

<div align="center">Cathodic protection</div>

Cathodic protection can also be used as a corrosion mitigation technique. It is commonly used in the petroleum industry as a protection method for pipelines. Cathodic protection can be installed during the construction of a new structure for protection against possible corrosion or applied to an existing structure to control corrosion rates. Cathodic protection can be done by two methods: using a sacrificial anode or by impressing a current [43].

The concept of using a sacrificial anode was introduced by Sir Humphrey Davy in 1824. It was used to protect ships from corrosion when in contact with water. Over time, the use became more widespread and is now used in underground pipelines. Figure 7 illustrates the use of a sacrificial anode in concrete. When a sacrificial anode is used in concrete, a metal (usually zinc) that has an electrochemical series higher than the steel reinforcement is put in place. This
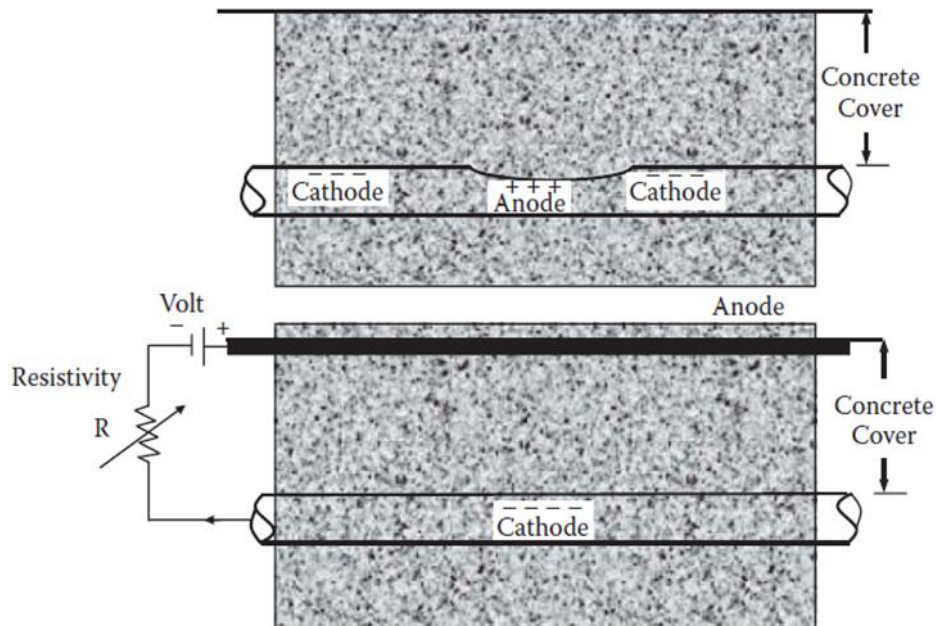
Figure 7: Cathodic protection method using sacrificial anode [43]
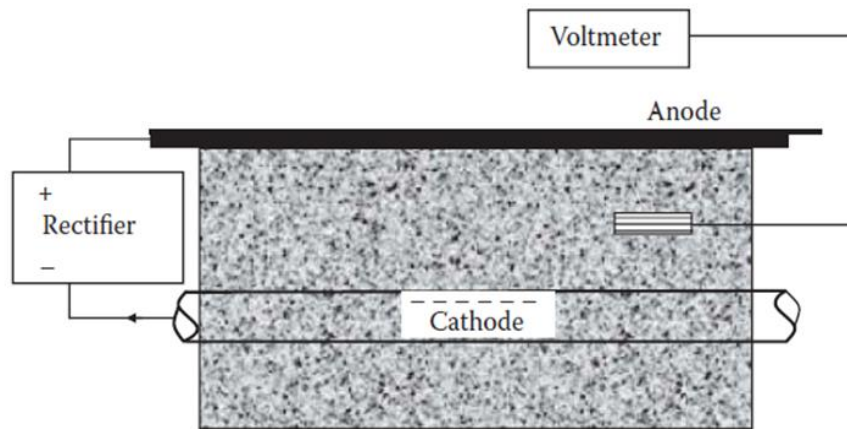
Figure 8: Cathodic protection method using an impressed current [43]

causes the steel reinforcement to become cathodic and the zinc to be anodic, dissolving over time as it oxidizes and imparting electrons to the steel reinforcement. The second type of cathodic protection, impressing a current, requires an external source of electricity to create the needed electrons for the steel reinforcement and is shown in Figure 8. An anode (such as a wire titanium mesh) is placed onto the surface of concrete and batteries can be the source of electricity [43].

Using cathodic protection, however, can negatively affects the concrete's interface with rebar [44]. Additional considerations when using cathodic protection are that it is quite expensive due to its routine checks and measurements to ensure the proper function as well as that the anode itself is costly [43].

Corrosion inhibitors

Commercially available corrosion inhibitors have become quite common in concrete because of their easy addition/application to a concrete structure. When a corrosion inhibitor is added into the mixture of fresh concrete, the inhibitor can behave as a protection method by preventing or prolonging the initiation to corrosion or reducing the rate of depassivation of the steel if corrosion has begun [11, 24].

A common corrosion inhibitor is calcium nitrite. Calcium nitrite is an anodic inhibitor that is capable of strengthening the passivating protective oxide film on the reinforcing steel bar. Therefore, calcium nitrite increases the chloride threshold level of the cementitious matrix and prevents or delays corrosion. Ferrous ions from the concrete interact with the calcium nitrite to produce the oxide film [45]:

$$2Fe^{2+} + 2OH^- + 2NO_2^- \longrightarrow 2NO + Fe_2O_3 + H_2O \qquad (14)$$
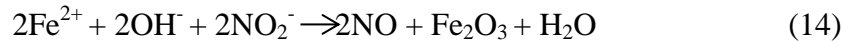
However, calcium nitrite accelerates the hydration reactions of the concrete and usually requires the use of water-reducing and/or retarding admixtures [11].

Another common corrosion inhibitor available on the market is penetrating corrosion inhibitor (PCI). PCIs are normally applied to the surface of hardened concrete structures by spraying, painting, or rolling of the liquid solution. They are meant to penetrate through the surface and migrate throughout the concrete and reach the reinforcing steel [46, 47]. Most PCIs are monoflurophosphate-based (MFP) or amino alcohol-based (AMA) inhibitors and can be transported through concrete in three ways: capillary suction, diffusion, or through a gaseous phase [48]. PCIs containing MFP cannot be added to fresh concrete due to its reaction with the calcium ions within concrete where insoluble products can be formed (such as calcium phosphate and calcium fluoride) [11].

Although the use of commercially available PCIs is quite popular, field studies have shown their lack of effectiveness. Schiegg *et al.* conducted a three-year field study using PCIs (MFP and commercially available Ferrogard-903) on the chloride-contaminated side walls of the Naxberg road tunnel in Lucerne, Switzerland [49]. Prior to the application of the two PCIs, a 2 % chloride concentration was present in the walls. The PCIs were then applied to the surface of the structure according to the manufacturer. After three years of monitoring the chloride

concentrations in the tunnel, the study concluded the PCIs to be ineffective in reducing the rate of corrosion [11, 49].

1.3 Research program

The corrosion of steel reinforcement within concrete has been a major issue since the 1960s. Although there have been great strides with research and commercially available products created to alleviate this critical issue, there is yet no product which mitigates corrosion as demonstrated by the fact that $100 billion of corrosion related damage is still occurring annually [7, 8]. Therefore, new and innovative corrosion prevention methods are a necessity. This research program focuses on developing a new approach to corrosion mitigation.

Research has demonstrated that natural bioactive agents such as cinnamaldehyde (CA) mitigate corrosion by forming a protective film on the surface of metals [50, 51]. CA, a derivative of cinnamon bark, has been used as a flavor enhancer in food and in the medical field for generations to alleviate health concerns such as diabetes [52, 53]. When incorporated in a cementitious matrix, bioactive agents can coat cement particles and inhibit the hydration of the cement, reducing compressive strengths at all ages [54, 55]. This experimental program incorporates these bioactive agents without interfering with the properties of the concrete; this is achieved by encapsulation of the agents in lightweight aggregate (LWA).

LWA is a porous aggregate that can absorb liquids using capillary action. The use of lightweight aggregates dates back to the construction of the Pantheon where natural LWA such as pumice was used as a method to reduce the density of the dome as its height increased [56]. In 1918, Stephen J. Hayde patented process for firing clay, shale, and slate to create LWA. His

patent became significant during World War I when the U.S. government used this technology to produce lightweight concrete ships [56].

Conventionally, LWA is pre-wet with water and included into a cementitious mix to reduce early age cracking; this can be referred to as *internal curing* as shown in Figure 9. Once the pre-soaked LWA is added to a mix, over time an internal drop in humidity due to cement hydration will occur and cause the liquid absorbed by the LWA to be released [57]. The purpose of internal curing stems from the need to alleviate effects due to cement hydration and chemical shrinkage, which cause early-age cracking (see *Mix design*, section 2.7, below). Chemical shrinkage occurs when the reactants (cement and water) take up more space than the products. After the cement paste is set, it may further shrink due to self-desiccation if it is not exposed to
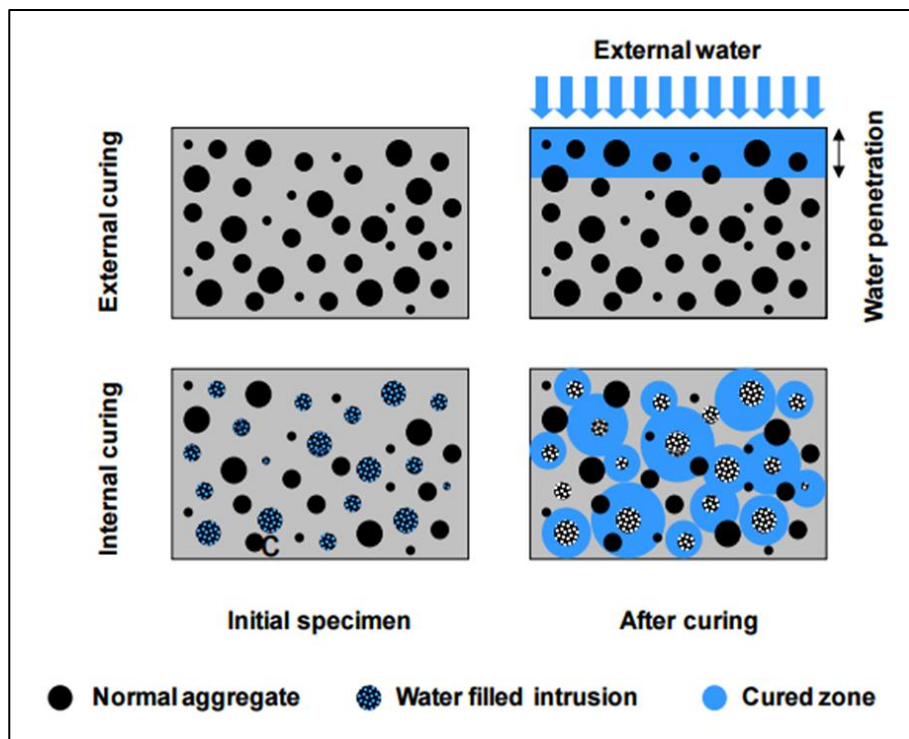
Figure 9: Illustration of the use of LWA for internal curing as opposed to the traditional external curing. When concrete is externally cured, water penetrates from the surface and does not hydrate the cement particles within the specimen. However, by including LWA pre-soaked in water, the cement within the specimen can become hydrated and prevent early age cracking [58]

an additional water supply. Therefore, by adding pre-soaked LWA into a cementitious matrix, the shrinkage can be reduced since an internal supply of water will be available [57]. Figure 9 compares the curing processes between traditional external curing (where no water-filled LWA is present) and internal curing. Preventing early-age cracking is critical to reducing premature deterioration of a concrete structure.

This research program is the first of its kind to incorporate CA into a cementitious matrix. CA can mitigate the corrosion of metals but cannot be added to a cementitious mixture because CA can coat cement particles and prevent the hydration of the cement. Therefore, the proposed strategy to include CA within a cementitious matrix stems from the concept of internal curing. If the LWA is soaked in CA instead of water, the CA will be released after the concrete's early-age properties have developed, and thus it will not impact the system's mechanical properties [25]. As shown in Figure 10, after release, the bioactive agent will migrate towards the reinforcing
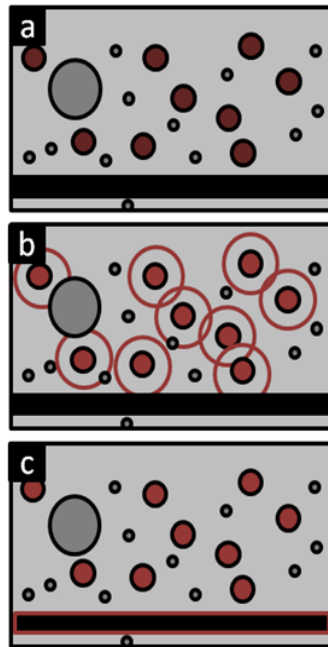
Figure 10: Schematic representation of the composite system, CA encapsulated in LWA a) the fresh mix contains cement (light gray), normal aggregate (dark gray spheres), LWA filled with bioactive agent (red), and a piece of rebar (black bar). Because the bioactive agent is 'locked away' it cannot interfere in the development of early age properties. b) After set, water is consumed in hydration reactions, leading to a pressure gradient that forces some bioactive agent to migrate out of the LWA. c) Over time, bioactive agent builds up on the surface of rebar and begins to play a role in corrosion mitigation.

steel and protect against corrosion.

This paper is divided into four sections: Section 1 is an introduction and background to corrosion in concrete; Section 2 describes the materials and methods used in the research program; Section 3 presents and discusses the results found in this experimental program; and Section 4 explains the conclusions and future works from this program.

Since the research program progressed over time, discussions will be split into three studies: Study 1, Study 2, and Study 3. Study 1 was the preliminary investigation of the use of LWA pre-soaked in CA in a cementitious matrix. The study also looked as using the same concept for a commercially available PCI. Since PCI is sprayed on the surface of a concrete structure and is meant to penetrate through the concrete and create a protective film on the steel reinforcement, this research program looked at possibly accelerating the protection by encapsulating the PCI into LWA, from which the PCI could be released after hydration reactions occur. Therefore, by having the PCI inside the cementitious matrix, it can travel to the steel reinforcement and create a protective barrier at a faster rate than through surface application. The setting time, compressive strength, heat evolution (via semi-adiabatic calorimetry), and autogenous shrinkage of the experimental mixtures were measured and an accelerated corrosion test (ACT) was used to quantify performance in a corrosive environment. Study 2 focused on improving the mix design of LWA pre-wet with CA. In doing so, five tests were carried out: isothermal calorimetry, rebar pullout, chloride threshold level and sorptivity. Since mechanical interferences due to the inclusion of CA-LWA were found in Studies 1 and 2, Study 3 coated LWA with cement as a means to prevent the interferences seen in previous studies. After carrying out all three studies, it was concluded that the inclusion of CA into a cementitious system was shown to greatly reduce the time to corrosion.

CHAPTER 2: MATERIALS AND METHODS

This research program was divided into three studies. As the research progressed tests, materials, and methods varied in order to find a solution to the use of CA in concrete for corrosion mitigation. All materials used in the experimental program were safely stored along with their Material Safety Data Sheets (MSDS) in a labeled cabinet in the laboratory[1].

2.1 Research program

2.1.1 Sand

Local sand with a specific gravity of 2.61 was used throughout. All sand was oven dried at a temperature of 104 °F (40 °C) and cooled for at least 24 h prior to being used. A sieve analysis was carried out according to ASTM C136 in order to determine the size distribution of the sand Figure 11 [58]. The smooth curve of the sand distribution indicates that the particle sizes of the sand are well distributed. This is important because the distribution impacts both the workability
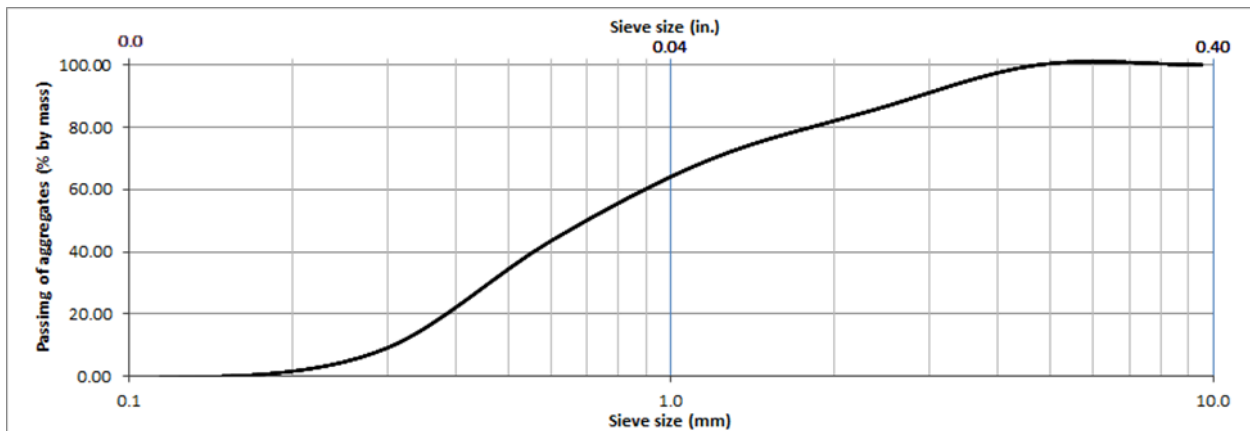
Figure 11: Sieve distribution of sand

---

[1] Materials described in the study are not meant for endorsement nor are the methods used meant to imply the best possible way for conducting tests.

and void content of a cementitious mixture. Additionally, the sand particle distribution determines the amount of paste (cement and water) necessary to fill the voids as well as coat the sand; this can be seen in Figure 12. In Figure 12.a, uniform particle sizes are only used which results in large voids; Figure 12.b illustrates well-distributed aggregates and therefore less voids in the mixture. Another way to reduce void size can be by using smaller particle sizes (Figure 12.c); however, there would be a reduction in the material's strength. Gap-graded aggregates are shown in Figure 12.d where the intermediate sizes (sizes between larger particles and finer particles) are removed, and Figure 12.e is a no-fines mixture where smaller particles are removed. These cases result in yet larger voids within the mixture [59].
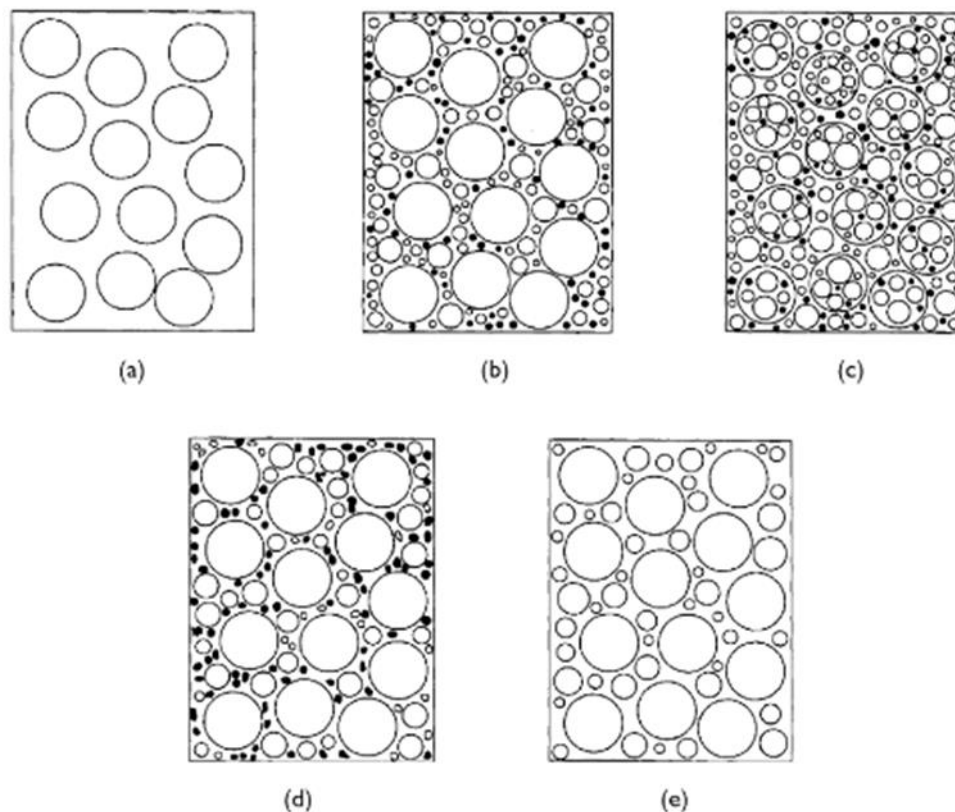
Figure 12: (a) uniform distribution, (b) well distribution, (c) smaller particle size distribution, (d) gap-graded distribution, (e) no fines in distribution [60]

Table 5: Sand and LWA distribution

Sieve No.	Mesh size	Percent retained (%)
8	0.0937 in. (2.36 mm)	14.6
16	0.0469 in. (1.18 mm)	16.0
30	0.0234 in. (600 μm)	26.2
50	0.0117 in. (300 μm)	34.2
100	0.0059 in. (150 μm)	9.0

Since lower void sizes create a denser microstructure, lower void sizes are commonly desired for designs attempting to prevent the ingress of aggressive media. Besides the strength being lower in designs with larger voids, cracks of the cementitious mixture as well transport of aggressive media through the pore solution are more likely to occur more quickly [60]. Thus, it is important that the sand is well distributed.

No. 8, 16, 30, 50, and 100 were included in all mix designs – particles larger than sieve size No. 4 and smaller than No. 100 were not used. Sieve sizes as well as their corresponding mesh size and percent retained per mesh size are detailed in Table 5. Therefore, all sample mixtures were mortar samples as opposed to concrete samples. Since the main concern with the addition of liquids (CA, PCI, or water) regarded cement hydration, it was not necessary to include coarse aggregates.

2.1.2 Lightweight Aggregate (LWA)

Lightweight aggregate (LWA) is porous aggregate and has the ability to use capillary action to absorb liquids it is soaked in. It can be used as a method to introduce liquids into a cementitious mix. In all experiments the LWA used was expanded shale with a specific gravity of 1.5 and was provided by Northeast Solite Corporation. All LWA was oven dried at a temperature of 40 °C

(104 °F) and cooled for at least 24 h prior to being used. When including LWA in a mortar mix, it partially replaced the sand on a volumetric basis. This way, the size distribution of aggregates remained constant regardless of whether or not LWA was used as detailed in Table 5 [61].

2.2 Cement

All mixes were prepared with commercially available ASTM C150 Type I/II cement. X-ray diffraction (XRD) and Fourier transform infrared spectroscopy (FTIR) were conducted on the as-received ordinary portland cement (OPC) for quality control purposes as illustrated in Figure 13. Alite (C_3S), belite (C_2S), and celite (C_3A) were detected by XRD. Five bands were identified with FTIR. Bands at 601.8 cm^{-1} and 663.5 cm^{-1} were due to Si-O vibrations; the band at 881.5 cm^{-1} was due to Si-O, Al-O, CO_3^{2-} vibrations; the band at 1153.4 cm^{-1} was due to S-O vibrations; and the band at 1438.9 cm^{-1} was due to CO_3^{2-}. These results are consistent with standard ready-mix OPC.
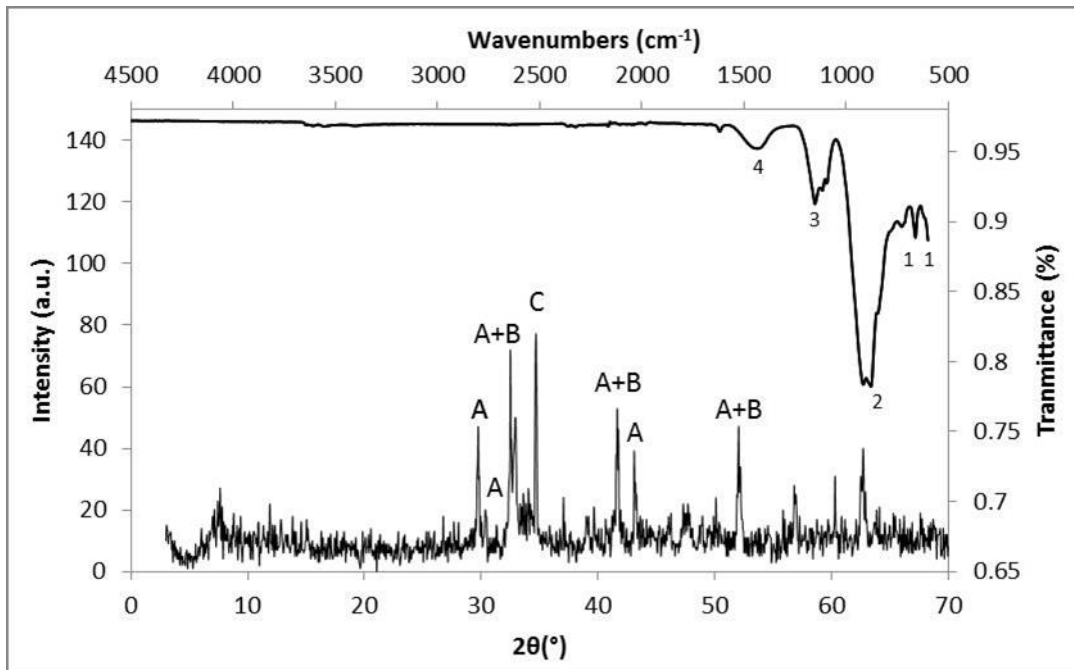
Figure 13: XRD (primary axes) and FTIR spectra (secondary axes) of the OPC. A = alite; B = belite; C = celite. Bands at 1 = 601.8 cm^{-1} and 663.5 cm^{-1} were due to Si-O vibrations; the band 2 = 881.5 cm^{-1} was due Si-O, Al-O, CO_3^{2-} vibrations; the band at 3 = 1153.4 cm^{-1} was due to S-O vibrations; and the band at 4 = 1438.9 cm^{-1} was due to CO_3^{2-}

27

2.3 Cinnamaldehyde (CA)

Cinnamaldehyde (C_9H_8O) was obtained from Sigma-Aldrich and had a specific gravity of 1.5. LWA was used to encapsulate and transport CA into the cementitious mix. CA was always kept in an airtight bottle, and when used with LWA, it was stored in an airtight container as CA tends to crystalize when exposed to air. This research program is the first of its kind in regards to using CA encapsulated in in LWA for corrosion prevention of reinforcing steel in concrete.

2.4 Penetrating corrosion inhibitor (PCI)

A commercially available, surface-applied penetrating corrosion inhibitor (PCI), Sika FerroGard 903, with a specific gravity of 1.14 was used. Sika FerroGard 903 is a liquid corrosion inhibitor meant to be used on hardened reinforced concrete as a method to retard the corrosion of the reinforcing steel. It is a formula made of an amino alcohol base and salts of amino alcohol (the exact formula is a trade secret) where it controls the cathodic and anodic reactions. This inhibitor is meant to be applied to the surface of concrete by spray, roller, or brush. The inhibitor then migrates through the concrete and towards the reinforcing steel to create a protective film on the steel as shown in Figure 14 [62]. For this research program PCI was used in two manners: in its
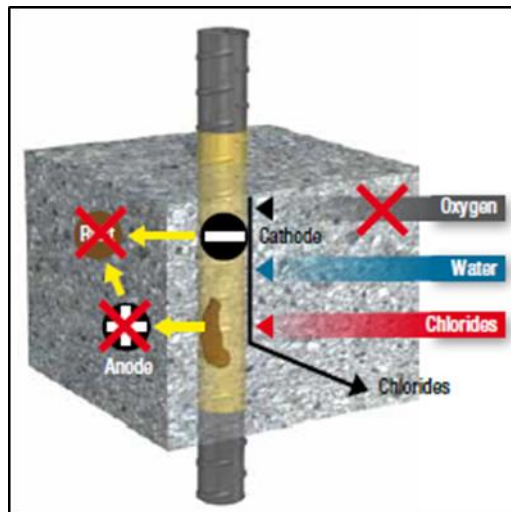
Figure 14: A protective film is created by the PCI and creates a barrier to deter aggressive media [63]

conventional method of surface application, where it was sprayed on the surface of a mortar sample and intended for comparison purposes; and encapsulated in LWA (in the same manner of encapsulating LWA with water or CA) in order to investigate whether the time for the PCI to reach the reinforcing steel could be shortened by reducing necessary diffusion distance. This approach has not been previously studied in research.

2.5 Additional materials

Tap water at room temperature was used in all mixes, including water encapsulated in LWA (when applicable). A water:cement (w/c) ratio of 0.4 (not including any water added via LWA, if applicable) was used in all mixes. A mold release (WD-40) was applied to the surface of some equipment (i.e. compressive strength and Vicat needle sample molds) to facilitate demolding.

2.6 Absorption study

The absorption of water by LWA was provided by the manufacturer as 17.5% of its mass. Since CA has a different specific gravity and other properties than water, it was necessary to conduct an absorption study. For Study 1, this was carried out by first oven drying the LWA at a constant temperature of 40 °C (104 °F) for 24 h. The LWA were then sieved to separate their particle sizes (No. 8, 16, 30, 50, 100) and the separate sizes were placed in mesh holders. The mesh holders containing LWA were soaked in CA for 24 h at room temperature and were then placed in an oven at 40°C (104°F). The weight was recorded each day for a week. A similar method was used in a previous study [63]. However, this method became non-applicable for the absorption of CA into LWA. When the CA was exposed to air or the oven, it crystalized on the surface of the LWA, as opposed to fully entering and storing in the pores.

Therefore, to encapsulate the liquids into the LWA, LWA was soaked at room temperature in the liquid for at least 24 h in an airtight container. The amount of liquid encapsulated into the LWA was determined by the absorption capacity provided by the manufacturer of LWA (17.5 % by mass of LWA). The CA, PCI, or water-impregnated LWA was then incorporated into the mix at a saturated-surface-dry (SSD) state. This method was used for Study 1 and Study 2. For Study 3, a more accurate representation of the absorption of CA into LWA was desired. Therefore, a further study was carried out similar to that of Castro *et. al* to determine the actual absorption of CA into the LWA [64].

Castro *et. al* used a 'volumetric flask' method to observe the absorption of water into LWA as a function of time [64]. This study investigated the absorption of water into fifteen different types of LWA from different regions and of varying gradations. LWA (oven dried and cooled to room temperature) was added to a 250 ml (8.5 oz.) volumetric flask. Water was added to the flask and once the flask reached about 80% of its capacity, the water and LWA were agitated manually to release air bubbles that may exist between the LWA particles; then water was added to fill the flask completely. At 10 min, 20 min, 30 min, 1 h, 2 h, 3 h, 4 h, 5 h, 6 h, 24 h, 36 h, and 48 h, and then under a vacuum, the water and LWA were agitated manually. At each reading, the mass of the flask and its contents were weighed and then water was added to the flask until the 250 ml capacity was achieved; the flask was then weighed again. Castro *et. al* concluded that all samples of LWA continued to absorb water over time.

A similar approach to Castro *et. al* was carried out for this program and is illustrated in Figure 15 *(overleaf)*. A 50 ml volumetric flask was filled with ~9.8 g (0.35 oz.) of LWA following the distribution described in section *2.1.2* and water was poured on top to fill the flask up to its meniscus. The same method carried out by Castro *et. al* was used, in which the flask
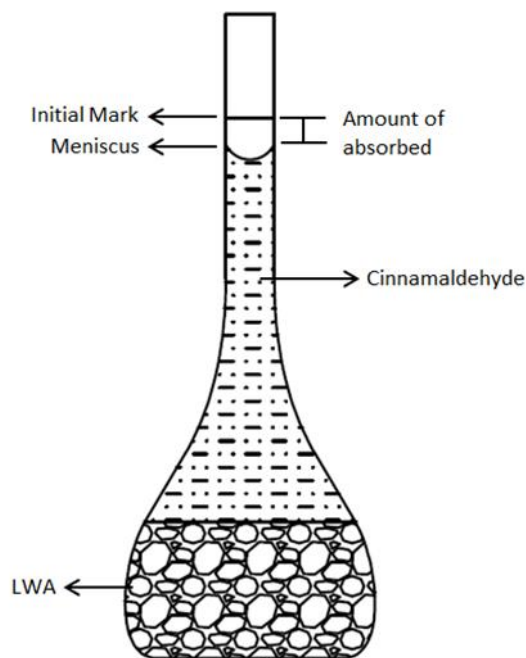
Figure 15: Schematic of absorption study of LWA

was agitated in order to reduce the air bubbles between particles and water was added to bring the volume back up to 50 ml.

Over time, the LWA continued to absorb water, and thus the mass of water absorbed was recorded at 0, 1, 2, 3, 4, 24, and 48 h; at each time the flask was agitated and water was added to keep the volume at 50 ml and the mass of the flask was recorded. This experiment was carried out in both a room temperature environment as well as in a vacuum in order to determine the optimal way to fill the pores of the LWA. The same method was also conducted using CA in order to determine the absorption of CA into LWA. Figure 16 *(overleaf)* compares the absorption findings.

Although the recordings were taken at 0, 1, 2, 3, 4, 24, and 48 h, the time of particular interest was at 24 h since the maximum time for which LWA was soaked in liquid (CA or water)
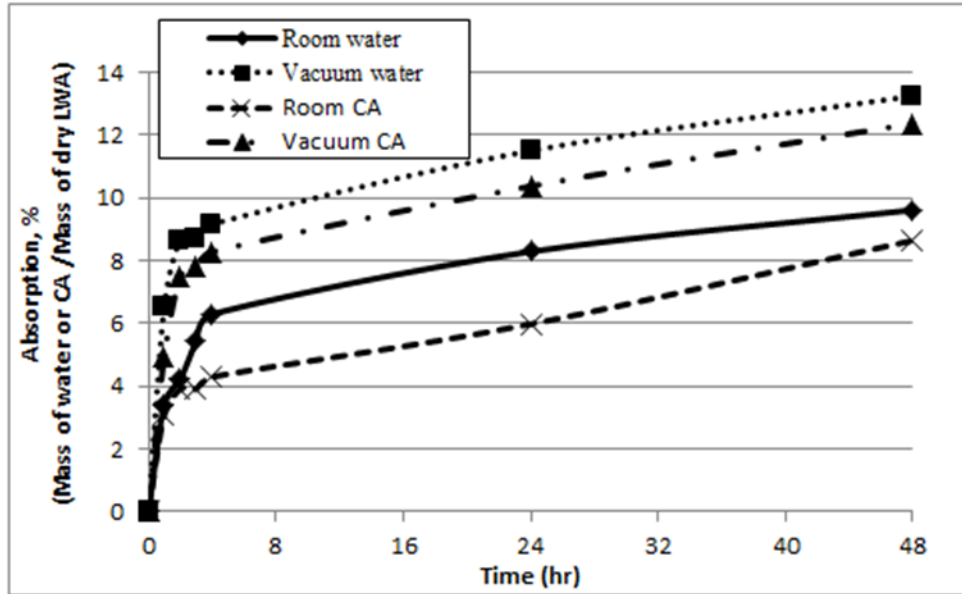
Figure 16: Absorption results

and incorporated in mortar samples was 24 h. An 8.3 % of absorption by mass was determined

for the LWA soaked in water at room temperature whereas in the vacuum it absorbed 11.5 %.

Less absorption occurred when LWA was soaked in CA. At room temperature, the LWA

absorbed 6 % by mass and 10.4 % when under a vacuum as shown in Figure 16. This reduction

in absorption of CA compared to water was expected since CA is a more viscous material as well

as has a higher specific gravity than water. The same trend was observed as in the experiment

conducted by Castro *et. al*.

2.7 Mix design

A water:cement (w/c) ratio of 0.4 (not including any water added via LWA, if applicable) and a

55 % vol. fraction of aggregate were used in all mix designs. Aggregates were either sand or a

mix of LWA and sand. LWA replaced sand on a volumetric basis in order to ensure a constant

particle size distribution and accurate comparison between mixtures. For mixing, cement was

first placed in a Hobart mixer and stirred for 30 s. Water was then added while the cement was

	Mix	Sand (cm^3)	Cement (cm^3)	Mixing Water (cm^3)	LWA (cm^3)	Internal Water (cm^3)	PCI (cm^3)	Cinnamaldehyde (cm^3)
Study 1	Mix 1	1375.0	464.6	585.4	-	-	-	-
	Mix 2	1127.6	464.6	585.4	247.4	-	-	75
	Mix 3	1127.6	464.6	585.4	247.4	75	-	-
	Mix 4	1106.5	464.6	585.4	268.5	-	75	-
	Mix 5	1106.5	464.6	585.4	268.5	75	-	-
	Mix 6	1375.0	464.6	585.4	-	-	-	-
Study 2	Mix 7	1375.0	464.6	585.4	-	-	-	-
	Mix 8	1046.7	464.6	585.4	328.3	86.2	-	-
	Mix 9	1046.7	464.6	585.4	328.3	-	-	86.2
Study 3	Mix 10	1375.0	464.6	585.4	-	-	-	-
	Mix 11	1046.7	464.6	585.4	328.3	-	-	48.8
	Mix 12	1046.7	464.6	585.4	328.3	-	-	48.8
	Mix 13	1046.7	464.6	585.4	328.3	56.6	-	-
	Mix 14	1046.7	464.6	585.4	328.3	56.6	-	-

stirring and allowed to mix together for 1 min. Finally, the aggregates were added to the cement paste as it was being mixed and mixed for 2 min. The mix designs of all three studies are shown in Table 6.

Study 1 investigated a total of six mortar mixes. Mix 1 was a control where only sand, cement and water were used. Mix 2 included CA-LWA; Mix 3 was the same as Mix 2, but included internal water instead of CA. Mix 4 contained PCI-LWA; Mix 5 was the same as Mix 4, but with internal water in place of the PCI. In this way, Mixes 1, 3, and 5 served as controls enabling the identification of changes in physicochemical properties due to the incorporation of LWA (as opposed to due to the actions of the CA and PCI). In a final mix, Mix 6, penetrating corrosion inhibitor was applied to the surface in three 24 h intervals which started 24 h after demolding. Mix 6 was used for comparison purposes and underwent only accelerated corrosion testing, where it was evaluated for electrical resistivity and steel mass loss (setting time,

compressive strength, air content, semi-adiabatic calorimetry, and autogenous shrinkage were not tested on Mix 6 since penetrating corrosion inhibitor was applied to the surface of a hardened sample).

Study 2 consisted of three mortar mixes. Mix 7 served as the control and was composed of sand, cement, and water. The two other mixes (Mix 8 and Mix 9) were experimental and consisted of the same components as Mix 7, but included a partial replacement of the sand with presoaked LWA. Mix 8 contained water-LWA and Mix 9 contained CA-LWA. LWA was soaked in water for at least 24 h in a sealed container. After 24 h, the presoaked LWA was then incorporated into Mix 8 in a saturated surface dry (SSD) state. The same method was used for encapsulating CA in the LWA for Mix 9. In order to determine the appropriate amount of LWA to be added to the mix, the amount of LWA was calculated by [13]:

$$M_{LWA} = \frac{C_f \times CS \times \alpha_{max}}{S \times \Phi_{LWA}} \qquad (15)$$

where M_{LWA} is the mass of LWA; C_f is the cement factor; CS is the chemical shrinkage of the binder (determined using ASTM C1608 [65] – Figure 17); α_{max} is maximum degree expected for
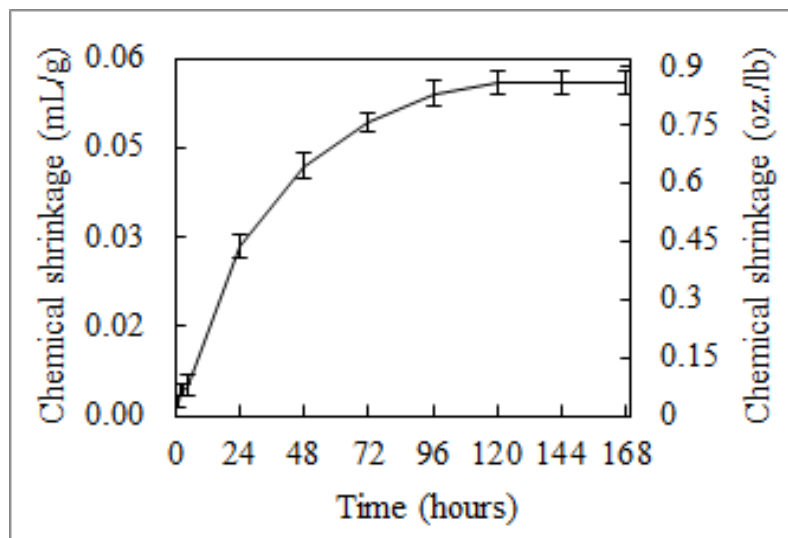
Figure 17: Chemical shrinkage of cement paste measured over seven days (168 h).

34

Table 7: Values used to calculate M_{LWA}

Variable	Value
C_f	585 kg/m^3 (36.5 lb/ft^3)
CS	0.056 mL/g (0.86 oz./lb)
α_{max}	1
S	0.95
Φ_{LWA}	0.175

the reaction of the binder; S is the saturation level; and Φ_{LWA} is the sorption capacity of the LWA listed in Table 7.

Chemical shrinkage is the volumetric reduction due to the hydration of cement. Tawaza *et al.* proved by calculation that the products of cement hydration occupy less volume than its reactants [66]. Chemical shrinkage was measured by ASTM C1608 [65]. Cement paste with a w/c of 0.4 was place in a glass vial (five replicate samples were used). Water was then poured over the cement paste and filled to the top of the vial. A rubber stopper with a pipet embedded in the center capped the vial. The vials were then placed in a water bath at a constant temperature of 23 °C (73.4 °F). Pipet readings were obtained for the first 4 h and daily measurements were taken thereafter. As time increased, the chemical shrinkage of the cement paste increased as shown in Figure 17.

Five mixes were investigated in Study 3. The mix designs were similar to Study 2 but with a few differences. The absorption quantity of the liquids into LWA differed (as it was determined by the flask method described above in section 2.6 *absorption study*). A vacuum was used to encapsulate any liquids (either water or CA) into LWA. Liquids were poured on the LWA and were manually mixed to ensure consistent distribution of the liquid. The pre-wet LWA was then placed into a vacuum for 8 h and then placed in an airtight container for the remaining 16 h (LWA was soaked in its liquid for a total of at least 24 h). Mix 10 served as the control and

was composed of sand, cement, and water. Mix 11 contained CA-LWA, and Mix 13 contained water-LWA. Mixes 12 and 14 were similar to Mixes 11 and 13, respectively, but included an additional step of coating the LWA with dry cement. After soaking and vacuum treatment, the pre-wet LWA was placed in a plastic bag containing 241.8 g of cement. The cement and LWA were manually shaken in the bag in order to distribute the cement throughout the LWA. Next, the cement-LWA mixture was placed on a No. 100 mesh sieve and shaken for 20 min. to remove excess cement. Therefore, the LWA was left with a thin coating of cement on its surface and mixed into the cementitious matrix as in Mixes 11 and 13.

2.8 Compressive strength

Compressive strength tests were performed according to ASTM C109 [67]. Mortar was placed in pre-lubricated (with W-D40), stainless steel, 2-in. (50 mm) cube molds, which were then placed in a plastic bag, stored in a fog room, and demolded after 24 h. The cubes were stored uncovered at 70 °F (21 °C) and 99 % humidity during curing. Three mortar cubes from each mix design were tested at ages of 3, 7, and 28 d. The compressive strength test was used as a method to evaluate whether the mechanical properties of the cementitious mixtures were impacted due to the experimental additions of liquid (water, CA, or PCI) encapsulated by LWA.

2.9 Setting time

Setting time was determined in accordance with ASTM C191 using the Vicat apparatus shown in Figure 18 *(overleaf)* [68]. The Vicat test method uses a 1-mm needle to measure the penetration depth of the needle into the cementitious sample. After mixing the sample, it was immediately placed into a lubricated cone-shaped mold with a glass bottom plate. The sample was then leveled off with a metal spatula to ensure accurate penetration measurements across the top
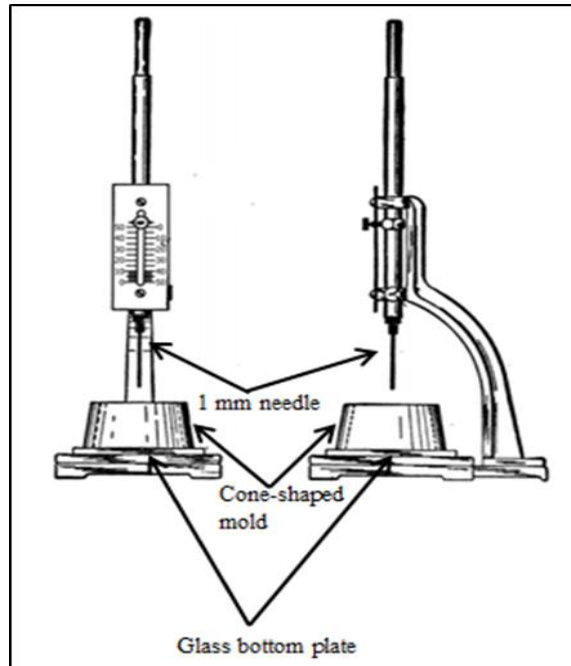
Figure 18: Vicat apparatus [69]

surface of the sample. For this research program, once water was added to cement during the mixing process of mortar, the time was recorded. After 30 min., the first penetration was taken and recorded. Thereafter, every 15 min. a penetration reading was taken until final set was achieved.

The setting time suggests whether the experimental materials added to the mortars are interfering with the chemical processes (i.e. prolonged or retarded set times). The set time is defined as the time in which it takes a fresh mixture to lose its malleable consistency but prior to it reaching its hardened phase at which properties such as strength can be measured [69]. The initial set time through the ASTM Vicat technique can be described as the time it takes once water and cement come in contact until the needle penetration is at 25 mm. The final set time is considered to be when the needle penetration only leaves a slight impression on the sample's surface.

2.10　Air content

The air content of the mortar was measured in accordance with ASTM C185 [70]. Air contents were measured to be 3.8 % (Mix 1), 2.2 % (Mix 2), 3.5 % (Mix 3), 4.4 % (Mix 4), and 3.1 % (Mix 5). Since the ASTM method allows a wider range for bias between similar mixes, the results suggest that the air content is not significantly impacted by the experimental agents, and was not further investigated.

2.11　Calorimetry

2.11.1 Semi-adiabatic Calorimetry

The reaction between water and cement is exothermic [69]. In order to assess whether this reaction is being disturbed by the experimental agents, semi-adiabatic calorimetry was used. A disturbance in hydration reactions would appear as an alteration of heat evolution during the exothermic cement hydration processes.

Mortar specimens were cast in 4 x 8 in. (100 x 200 mm) cylinder molds with type K thermocouples embedded in the center. The entire cylinder was insulated, and the rise in sample temperature was recorded by a data acquisition system for 3 d as shown in Figure 19. It was only necessary to collect the heat released during hydration for 3 d since the main rise in temperature occurs after several hours (primarily due to the hydration of C_3S and the production of C-S-H and portlandite) [69].

A similar custom-built setup has been used in previous research when evaluating the temperature rise of phase change materials (PCMs) in mortar [71]. Mortar samples were cast in 2 x 4 in. (47 x 97 mm) cylindrical molds where a type J thermocouple was embedded within the center of the sample and placed inside microporous insulation. This kind of custom-made semi-
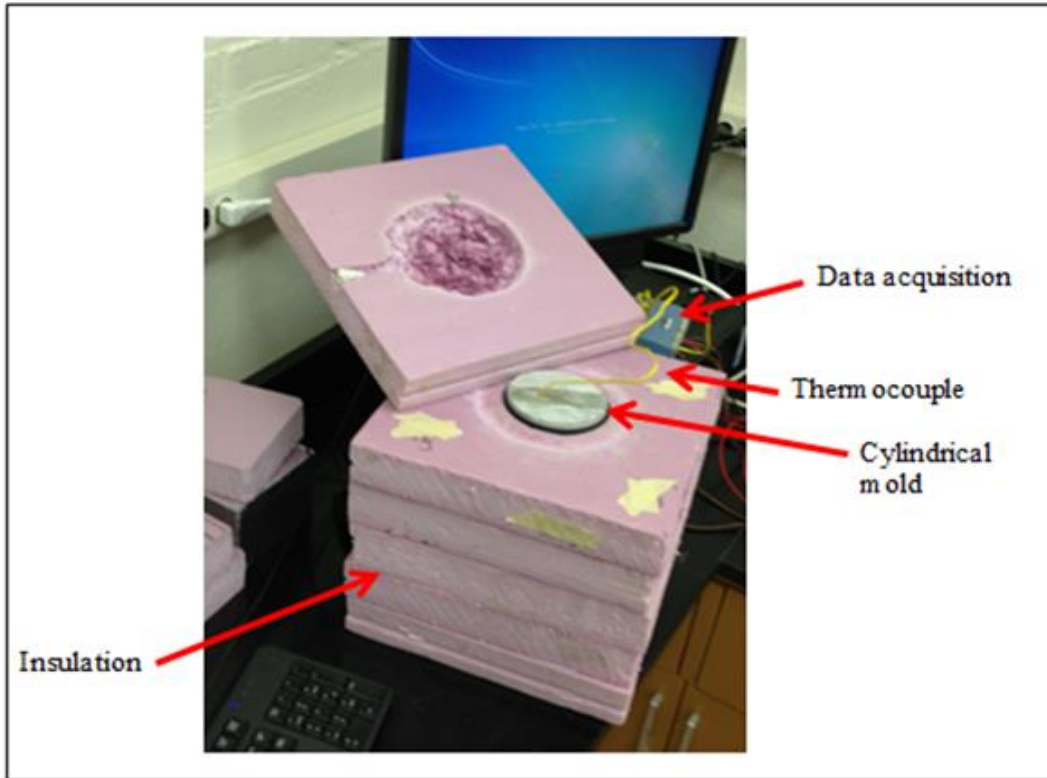
Figure 19: Semi-adiabatic calorimetry setup

adiabatic calorimeter was also used to measure the heat of hydration when using a viscosity modifier in mortar [72].

2.11.2 Isothermal Calorimetry

Isothermal calorimetry was measured with a TAMair instrument to assess the hydration kinetics of the mortars. For each mortar design, two ampoule samples were used in neighboring chambers. This was conducted to reduce variability between chambers. If the results did not indicate concern of variability, the two findings were averaged. It was critical that once the mortar was mixed, it was immediately prepared, measured, and placed in the ampoules, as the goal was to capture the heat evolution of the sample.

Each ampoule consisted of a measured amount of mortar dependent on the specific heat capacities of individual material components of the mixture. The heat flows of the mortars were

39

evaluated during the initial 24 h of hydration. For each sample placed in the calorimeter there was a 45-minute normalization period which made it impossible to measure early heat flow of the samples. The specific heat of sand and LWA was 0.76 J/K·g (0.182 BTU/lb°F), cement of 0.75 J/K·g (0.179 BTU/lb°F), and water of 4.18 J/K·g (0.998 BTU/lb°F); the specific heat of CA was not accounted for since only a very small amount was included in the mix. Two 10 g reference samples of cement were used. All samples were normalized by the cement content. The chamber of the calorimeter was kept at a constant temperature of 25 °C (77 °F).

2.12 Autogenous shrinkage

Autogenous shrinkage was measured for the mortar samples according to ASTM C1698 [73]. This test quantifies the bulk strain of a sample. Since chemical shrinkage is due to the hydration of cement particles it results in an 'internal' volume reduction. Autogenous shrinkage causes a net deformation to the system and therefore is considered as an 'external' volume change. The two forms of shrinkage are compared in Figure 20 [74]. This test was conducted as an indirect
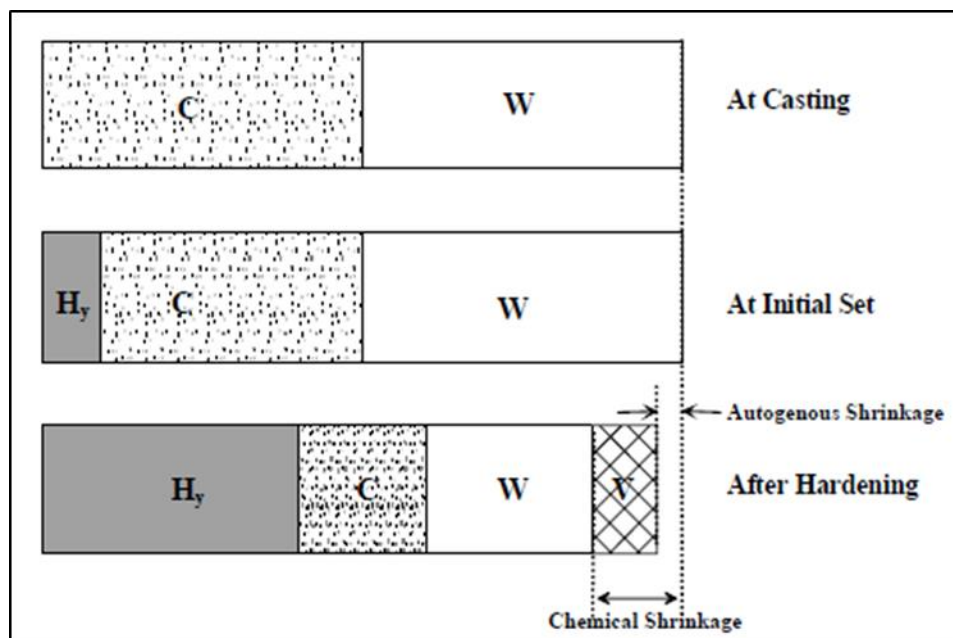
Figure 20: Schematic of relationship of chemical and autogenous shrinkage of a cement paste. C = unhydrated cement, W= water, Hy = hydration products, V = void created by hydration [75].

40

way of determining whether the liquids encapsulated in the LWA are diffusing out of the LWA –

a reduction of autogenous shrinkage would indicate that the internal agents are entering the pore

system and filling in the empty voids caused during chemical shrinkage.

In order to measure the autogenous shrinkage of the mortars, the mortars were placed in

corrugated plastic tubes that were tightly sealed with plugs on each end and stored at a constant

temperature with no exposure to external forces. Specimens (at least three per mix design) were

stored in two layers of plastic bags on a plastic board (so that samples were not bent or disturbed

during the duration of the test) and placed in a 70 °F (21 °C) and 99 % humidity environment to

ensure constant curing conditions. Samples were measured using a dilatomer where the length

from the time of final set to 28 d was recorded. The length of the mortar sample, *L(t),* at time *t*

was calculated:

$$L(t) = L_{ref} + R(t) - 2 \cdot L_{plug} \qquad (16)$$

where L_{ref} is the length of the reference bar (mm), *R(t)* is the reading of the length gauge with

sample in dilatomer (mm), and L_{plug} is the average length of the end plugs.

The autogenous strain was then calculated by:

$$\varepsilon_{autogenous} = \frac{L(t) - L(t_{fs})}{L(t_{fs})} \cdot 10^6 = \frac{R(t) - R(t_{fs})}{L(t_{fs})} \cdot 10^6 \ \mu m/m \quad (17)$$

where t_{fs} is the time of final setting when the first length measurement was taken (min.) and $R(t_{fs})$

is the reading of the length gauge at t_{fs}.

2.13   Accelerated corrosion tests (ACT)

Accelerated corrosion tests (ACT) were conducted on experimental samples based on designs

found in the literature. There are several ACTs with varying setups. Detwiler *et al.* used an ACT

to study durability in terms of prevention of corrosion to reinforcing steel. The experiment investigated concrete samples at varying curing temperatures as well as reduced w/c ratios and tested their impact on chloride penetration. Concrete cylinders of 4 x 11 in. (10 x 28 cm) with a 0.4 in. (10 mm) piece of wire-brushed reinforcing steel (to remove existing corroded particles) were poured and cast. Due to their shape, these samples can be referred to as "lollipop" specimens. These samples were then placed in seawater at room temperature and a 12 V power source was impressed on the reinforcing steel. This caused the reinforcing steel to become anodic and the steel plates to be cathodic. Both visual inspection and use of the data logger recording current assisted with corrosion detection. A spike in current indicated corrosion and cracking [75].

A similar method was conducted by Shaker *et al.* and Okba *et al.* when investigating the durability of styrene-butadiene latex modified concrete (LMC) [76, 77]. Elmoaty also used a similar ACT when studying the corrosion resistance of concrete when cement is partially replaced by granite dust [78]. Güneyisi *et al.* used ACT when observing the behavior of chloride contaminated concrete when metakaolin is and is not incorporated into the concrete [79]. Güneyisi *et al.* also used the ACT setup for investigating the corrosion of concrete when using both plain and blended cements as well as at varying curing conditions [80].

Here, three samples were investigated per mix design. Mortar was placed into a 4 x 8 in. (100 x 200 mm) cylinder, and a jig was used to hold a 0.5 in. (12.7 mm) piece of wire-brushed steel rebar in the center. Although wire brushing may not be the ideal pre-treatment of reinforcing steel due to the possibility of residual rust remaining on the steel, it was consistently carried out and therefore reduced the risk of error in the testing process. Epoxy coating was used
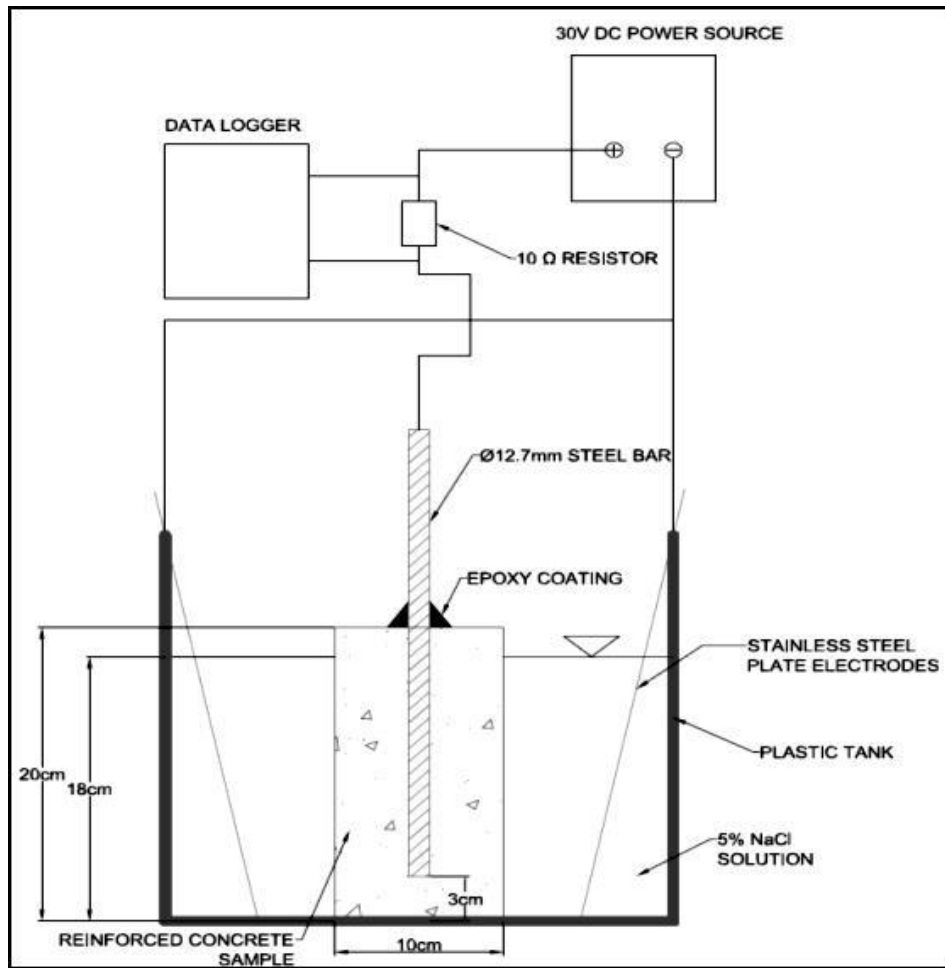
Figure 21: Schematic of accelerated corrosion test (ACT)

around the top of the rebar to prevent crevice corrosion. The lollipop samples were placed in a plastic tank containing 5 wt.% NaCl solution after 28 days of curing; two stainless steel plates were placed near the sample; and a 30 V DC power source was used to accelerate the corrosion. A data logger recorded current through the rebar, with a rapid increase in current signifying cracking. The schematic of the ACT setup is shown in Figure 21, and Figure 22 *(overleaf)* shows a sample that has undergone ACT. While it is known that accelerated tests do not resemble field conditions, an ACT is useful for drawing comparisons between techniques and proving concepts.
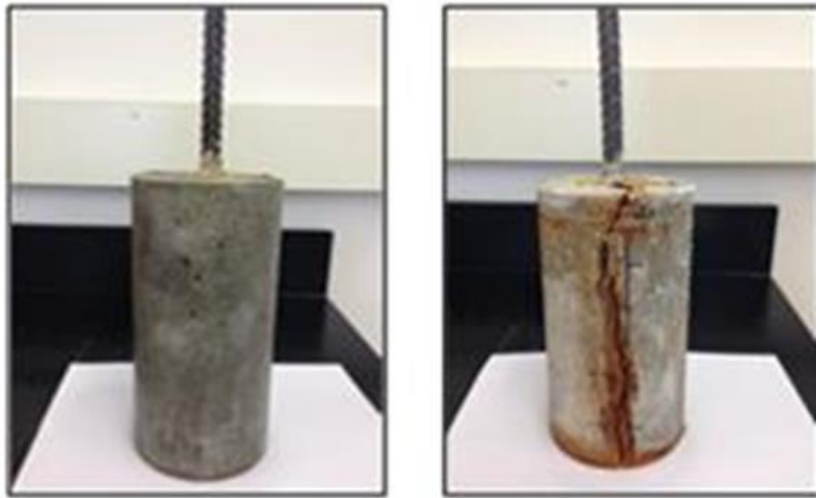
Figure 22: Lollipop sample prior to ACT (left); failure of sample after undergoing ACT (right)

2. 13. 1 Electrical resistivity

In addition to the current readings, the electrical resistivity of each sample was quantified using the Wenner technique [81]. Four readings were taken for each of the lollipop samples from the beginning of the ACT until cracking failure of the sample. The current was recorded until complete failure of the lollipop sample; complete failure was determined by both a spike in current and visual inspection of severe cracking in the sample (Figure 22). Similar trends have been observed in various other studies which have conducted accelerated corrosion tests [75-77, 80, 82].

The mass loss of the reinforcing steel over the course of the ACT was calculated using Faraday's law:

$$M = \frac{A_w \cdot \int I dt}{n \cdot F} \tag{18}$$

where, M = mass loss (g); A_w = atomic weight of iron (55.86 g/mole); $\int Idt$ = current x time relation (A•sec) which was evaluated numerically from the ACT test; n = ferrous valency (2); F = Faraday's constant (96,485.3 coulombs/mole of ferrous).

2.14 Fourier transformation infrared spectroscopy (FTIR) and X-ray diffraction (XRD)

Chemical changes in the mortars were determined through XRD and FTIR experiments. Samples for each analysis method were prepared in the same manner. A small piece of hardened mortar was manually ground to a fine powder by mortar and pestle. XRD was measured from an angle of 0 – 80 degrees reflected from the angle of the X-ray beam and FTIR was tracked between wavelengths of 500 cm^{-1} and 4500 cm^{-1}.

2.15 Scanning electron microscopy (SEM)

To investigate the impact of the addition of CA via LWA as well as water via LWA to mortar, SEM was used. To prepare samples, a piece of hardened mortar was cast into a mold using two-part epoxy. Once the epoxy hardened, the sample was removed from its mold and polished using sandpaper (#120, #240, #600, 1μm, 0.3μm, 0.05μm). The top surface was then sputter-coated with gold to make it conductive. The main objective for this test was to investigate the interfacial transition zone (ITZ) between the LWA and its absorbed material.

Concrete is composed of both the cement paste and the aggregate. In a fresh mixture of concrete, the aggregate can interfere with mix of the cement paste [83]. The cement particles are suspended in the mixing water and will have difficulty packing together if it is near a solid object such as an aggregate. During mixing the cement paste faces shearing stresses from the aggregates thus causing the water to separate from the cement particles (commonly referred to as
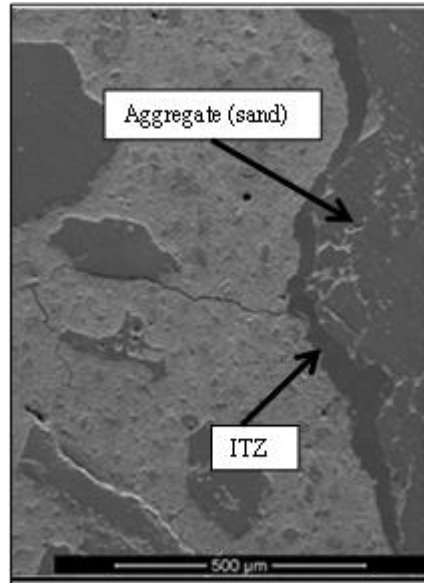
Figure 23: ITZ in a mortar sample

the wall effect") therefore creating a narrow area, called the ITZ, around the aggregates where there are fewer cement particles and more water (Figure 23) [83, 84]. The strength of concrete can be impacted by large regions of ITZ. A concrete specimen with regions of large ITZs can have an overall lower strength and stiffness due to the ITZ region itself having lower strength and stiffness. Moreover, durability of the concrete partly relies on the ITZ. Regions of an ITZ are more permeable; permeability negatively impacts the durability since it allows aggressive media to diffuse through the cementitious mixture at a faster rate and potentially corrode the steel reinforcement which can prematurely deteriorate the structure [83, 84].

2.16 Sorptivity

Sorptivity tests were conducted following ATSM C1585 [85]. Mortar was placed into 4 x 2 in. (100 x 50 mm) cylinders, stored in a fog room, demolded after 24 h, and placed back in the fog room to cure for 28 d (three samples per mix). On day 28, the samples were removed from the fog room and placed in an oven at 105 °C to dry for 24 h. Once removed from the oven and cooled, the circumference of each cylinder was sealed using duct tape in order to ensure

unidirectional sorption. The samples were then placed on supports at the bottom of an enclosed

plastic tank. Water was filled into the tank such that it was 0.08 ± 0.04 in. (2 ± 1 mm) above the

bottom of the sample; the water level was maintained throughout the experiment. Absorption, I,

was calculated by:

$$I = \frac{m_t}{a \times d} \tag{19}$$

where I was the absorption; m_t is the change in mass at time t ($\Delta m = m_t - m_0$) where m_0 is initial

mass at $t = 0$; a is the exposed area of the sample (mm^2); and d is the density of water (g/mm^3).

Both the initial and secondary rates of water sorptivity were identified as the slopes of the

lines of the absorption plotted against the square root of time. To characterize initial sorptivity,

the masses of the sample were taken at 60 s, 5 min, 10 min, 20 min, 30 min, 60 min, and every

hour for the following 6 h. The secondary rate of absorption is found in the same manner as the

initial rate but at later ages. Masses were recorded once every ~ 24 h for a total of 7 d.

2.17   Diffusion of NaCl

The diffusion of NaCl through sample mortars was examined. Previous literature describes

similar diffusion tests using silver nitrate (AgNO$_3$) as a visual detection method with image

processing software for accurate measurement of chloride diffusion within samples. Bentz *et al.*

conducted a study regarding viscosity modifiers in mortar where the penetration depths of

chloride ions were analyzed [72]. The cylindrical samples were cast in 2 x 4 in. (50 x 100 mm)

molds. After 7 d and 28 d of curing, the samples were fully submerged in a chloride bath where

600g of chloride was dissolved and sealed. The samples were then tested for chloride penetration

at 28, 56, 180, and 365 d by splitting the samples lengthwise and spraying with silver nitrate. The

silver nitrate causes a color difference due to the 'free' chlorides which react with silver nitrate to produce silver chloride [86].

$$Ag^+ + Cl^- \longrightarrow AgCl \downarrow \text{ (light gray)} \quad\quad (20)$$
$$Ag^+ + OH \longrightarrow AgOH \longrightarrow Ag_2O \downarrow \text{(brown)} \quad\quad (21)$$
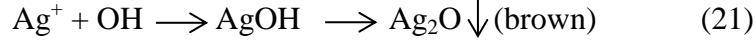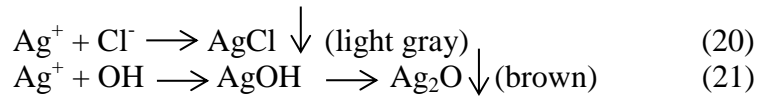
Baroghel-Bouny *et al.* used this method to detect uniaxial diffusion of chloride into concrete as well as in saturated conditions [87, 88]. Several other studies have used this technique as well including Aldea *et al.* which focused on the impact of curing conditions when cement was replaced by slag [89]. For that study, image processing software was not used; physical measurements of penetration depth were taken instead.

In this research program, mortar (three samples per mix) was placed in 4 x 8 in. (100 x 200 mm) cylinder molds. After 28 d curing, the cylinders were each immersed in a 5 % (by mass) NaCl solution stored in a sealed plastic tank for 3 m. The samples were removed from the solution, split lengthwise, and sprayed with silver nitrate. As seen in Figure 24 (left) the silver
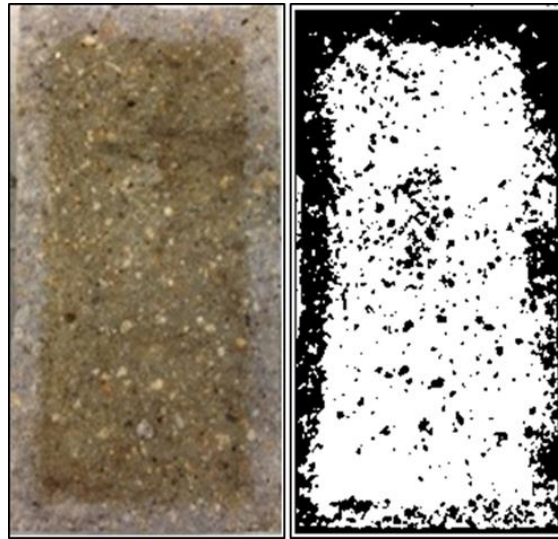
Figure 24: Split cylindrical sample after sprayed with silver nitrate. The light gray around sample indicates the depth of chloride ingress (left) and the binarization of the sample using ImageJ where the black indicates chloride ingress (right).

48

nitrate changes the color of the mortar such that where there is a concentration of chloride ions, the mortar is lighter in color (normally around the top, bottom, and sides). The ImageJ program developed by the National Institute of Health (NIH) was used to determine color variations and calculate the area through which the chloride had diffused Figure 24 (right) [90].

2.18 Chloride threshold level (CTL)

The chloride threshold level (CTL) can be described as the chloride content at the steel surface that breaks down the passive layer and initiates corrosion [88]. In order to determine the CTL, two steps had to take place: corrosion initiation and measurement of the chloride content. In order to initiate corrosion, an accelerated corrosion test (ACT) was carried out (see section 2.13 *Accelerated corrosion test)* [80, 91]. After 28 d of curing, the samples were placed into the ACT, and a data logger recorded the current. Once a sharp increase in current (indicating the initiation of corrosion) was observed, the test was immediately terminated. To determine the chloride content, ion chromatography (IC) was used. The corrosion-initiated cylinders were split lengthwise and a sample of mortar was taken at four different depths shown in Figure 25 *(overleaf)*: from the surface to ½ in. (12.7 mm) deep into the sample; 1 ½ in. (38.1 mm); 2 in. (50.8 mm); and along the length of the mortar-rebar interface. These samples were obtained with a masonry drill. 1 g of powder was added to a 150 ml beaker which was then filled with 100 ml of deionized water and left to soak for about 15 h. After soaking, the samples were heated on a hotplate at 184 °F (84.4 °C) for 3 h. The solution was then filtered using a No. 4 filter into a 100 ml flask and washed with deionized water to fill the 100 ml. The concentration of chloride ions in the original sample was determined by:

$$Cl = \frac{R \times Fl}{W} \qquad (22)$$

where *Cl* is the concentration of chloride ions in the original sample (ppm); *R* is the concentration of chloride ions in the sample from the ion chromatograph (ppm); *Fl* is the volume of the flask containing undiluted sample (ml); and *W* is the weight of the original powdered sample (g).

2.19   Bond strength

To identify if the experimental mixes interfered with the bond strength between mortar and reinforcing steel, rebar pullout tests were conducted. This test is significant since reinforced concrete is a composite building material, and therefore the bond strength impacts its mechanical behavior. Several variations of this test have been conducted in literature. Yeih *et al.* used both a mathematical model and experimental analyses on rebar pullout to study the interface of steel and concrete [92]. Samples were cast in 4 x 8 in. (100 x 200 mm) cylinders with either a No. 3 or No. 4 rebar embedded in the concrete. A universal testing machine was used to perform the pullout, and two linear variable differential transformers (LVDTs) were used for the readings.
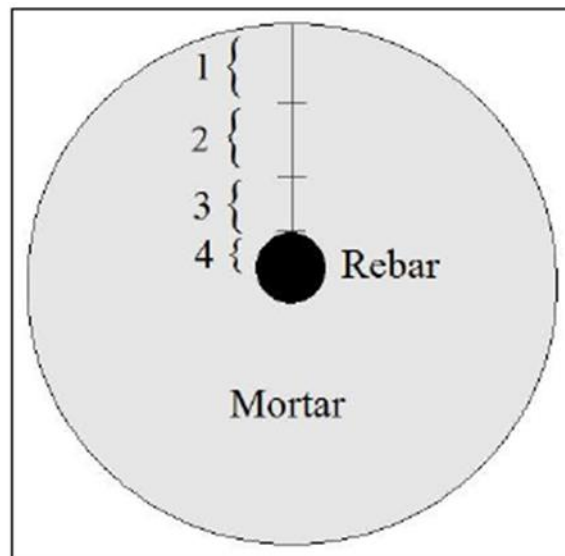
Figure 25: A top view of the sample section along with the four depths that were drilled out and tested for chloride content through ion chromatography. (1) is the powdered mortar collected from the depth of surface to ½ in.; (2) is the powdered mortar collected from the depth of ½ in. to 1 ½ in.; (3) is the powdered mortar collected from the depth of 1 ½ in. to 2 in.; (4) is the powdered mortar collected along the length of the mortar-rebar interface.

Similarly, Baena *et al.* and De Lorenzis *et al.* focused on the bond between FRP bar and concrete [93, 94]. Additionally, pullout tests have been carried out on the impact of bond strength and gaps at the concrete-steel interface due to issues such as segregation, enamel coated steel, concrete with slag replacement, and corrosion-protected reinforcing steel [95-98].

Samples were prepared by placing mortar into 6 x 12 in. (152.4 x 304.8 mm) cylinders and embedding a ¾ in. (19.1 mm) wire-brushed rebar of 3 ft. (91.4 cm) length in the center. To ensure perpendicular alignment a jig was made to hold the rebar in place. Once cured for 28 d, the samples (three for each mix) were placed on the top crosshead of a load frame where the rebar ran through the lower crosshead and was secured by jaws as shown in Figure 26. A shim
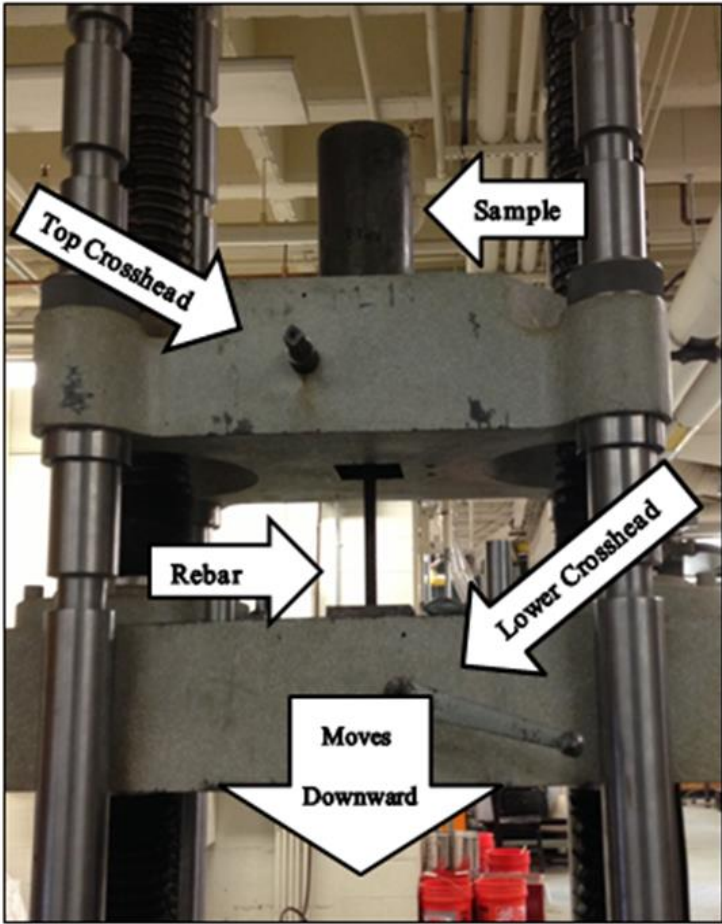
Figure 26: Pullout setup

51

was put between the top of the tensile frame and the cylinder to reduce the effects of eccentricity. A displacement rate of 0.1 in/min was used as it was a convenient rate to obtain the data necessary.

Table 8 summarizes all tests carried out along with the Study in which each test was performed. Study 1 considered seven tests, Study 2 carried out nine tests, and Study 3 completed three. Chapter 3 presents and discusses the results found in each study.

Table 8: Studies 1, 2, and 3 along with the tests carried out

Test	Study 1	Study 2	Study 3
Absorption study	-	-	✓
Compressive strength	✓	✓	✓
Setting time	✓		-
Air content	✓	-	-
Semi-adiabatic Calorimetry	✓	-	-
Isothermal Calorimetry	-	✓	✓
Autogenous shrinkage	✓	-	-
ACT	✓	✓	-
Electrical resistivity	✓	-	-
FTIR and XRD	-	✓	-
SEM	-	✓	-
Sorptivity	-	✓	-
Diffusion of NaCl	-	✓	-
CTL	-	✓	-
Bond strength	-	✓	-

This research program was broken into three studies. Study 1 was a preliminary investigation of incorporating CA into a cementitious mixture by encapsulation into LWA. Additional to studying the encapsulation of CA into LWA, a commercially available PCI was also investigated. Six tests were carried out to study both the chemical and mechanical impacts due to the inclusion of CA and PCI into a cementitious matrix. Based on the results found in Study 1, further investigations (Studies 2 and 3) were conducted to investigate strategies to improve the mechanical properties due to the incorporation of CA into a cementitious matrix.

3.1 Study 1

Study 1 was a preliminary investigation of the inclusion of CA via LWA in cementitious system. Seven tests were carried out and these are discussed below.

3.1.1 Setting time

The setting times of Mixes 1-5 were determined. The addition of liquids (CA, water, or PCI) encapsulated into LWA increased the setting times of all mixes as shown in Table 9. Although Mix 2 produced the same initial setting time as Mix 1, its final setting time was prolonged by 45 min. The initial setting time of both Mixes 3 and 4 were prolonged by 90 min (55 %); that of Mix 5 was prolonged by 45 min (38 %). Final setting times for Mixes 3, 4, and 5 increased by 90 min (38 %), 195 min (57 %), and 60 min (29 %), respectively.

Table 9: Initial and final setting times for each mix

Mixture	Contents of Mixture	Initial Setting Time (min)	Final Setting Time (min)
Mix 1	Control	75	150
Mix 2	CA-LWA	75	195
Mix 3	Internal curing	165	240
Mix 4	PCI-LWA	165	345
Mix 5	Internal curing	120	210

The extended initial and final setting times of Mixes 3 and 5 can be explained by the additional stage they undergo as they dry, as illustrated in Figure 27. The first stage is known as the initial drying period. During this time, Mixes 1, 3 and 5 all experience the same effect where some evaporation begins from the top layer of the specimen. Next is the constant rate period where menisci form at the upper surface and evaporation continues from that point. Finally, the falling rate period occurs where menisci travel into the sample. For specimens with water encapsulated in LWA, as in Mixes 3 and 5, the constant rate period becomes extended and therefore causes the lengthened setting time since the LWA may release some of its stored water [99, 100].

However, admixtures impact the setting time of a cementitious system. CA and PCI are both organic materials. The lengthened setting times of Mixes 2 and 4 are likely due to CA and PCI remaining on the surface of the LWA after pre-soaking. This material then enters the mix water and hinders the reaction between cement particles and water [101]. CA or PCI remaining on the surface of the LWA comes in contact with the cement and coats the cement particles.
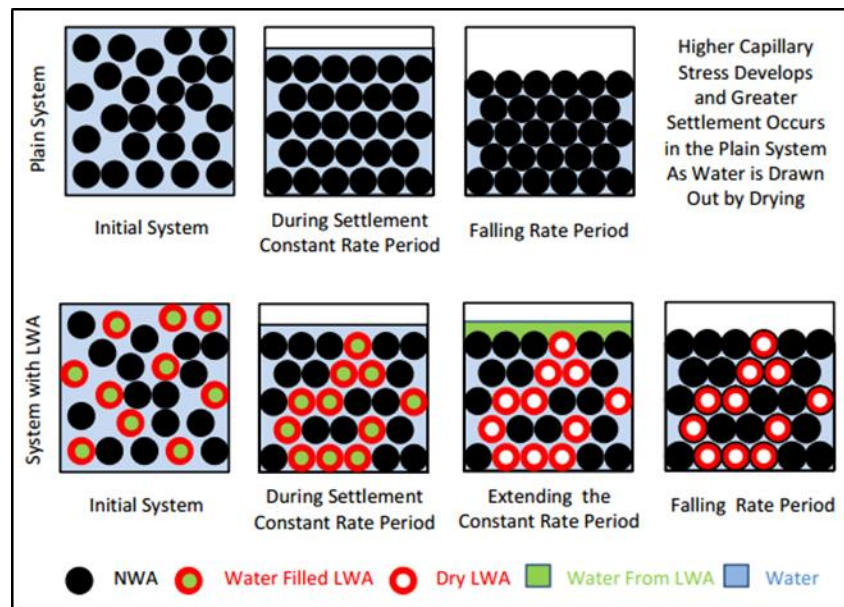
Figure 27: Comparison of drying in a plain system vs. internal curing [99]

54

When cement is coated with an oil (CA or PCI) it does not allow the water to hydrate the cement. Therefore the hydration reaction between cement and water is retarded.

3.1.2 Compressive strength

The compressive strength of a mortar should increase with time due to the hydration of the cement particles. Additional considerations such as the mixture proportions, curing conditions, and age of testing all impact the resulting strengths as well [57]. Since the curing conditions and age of testing remained constant for all mixture designs, those two factors can be eliminated from consideration. Mixes that did not incorporate CA or PCI had similar strength profiles as compared in Figure 28. Mix 3 and Mix 5 achieved comparable but slightly lower strengths than Mix 1. This is due to the LWA being mechanically weaker (because it is porous) than the
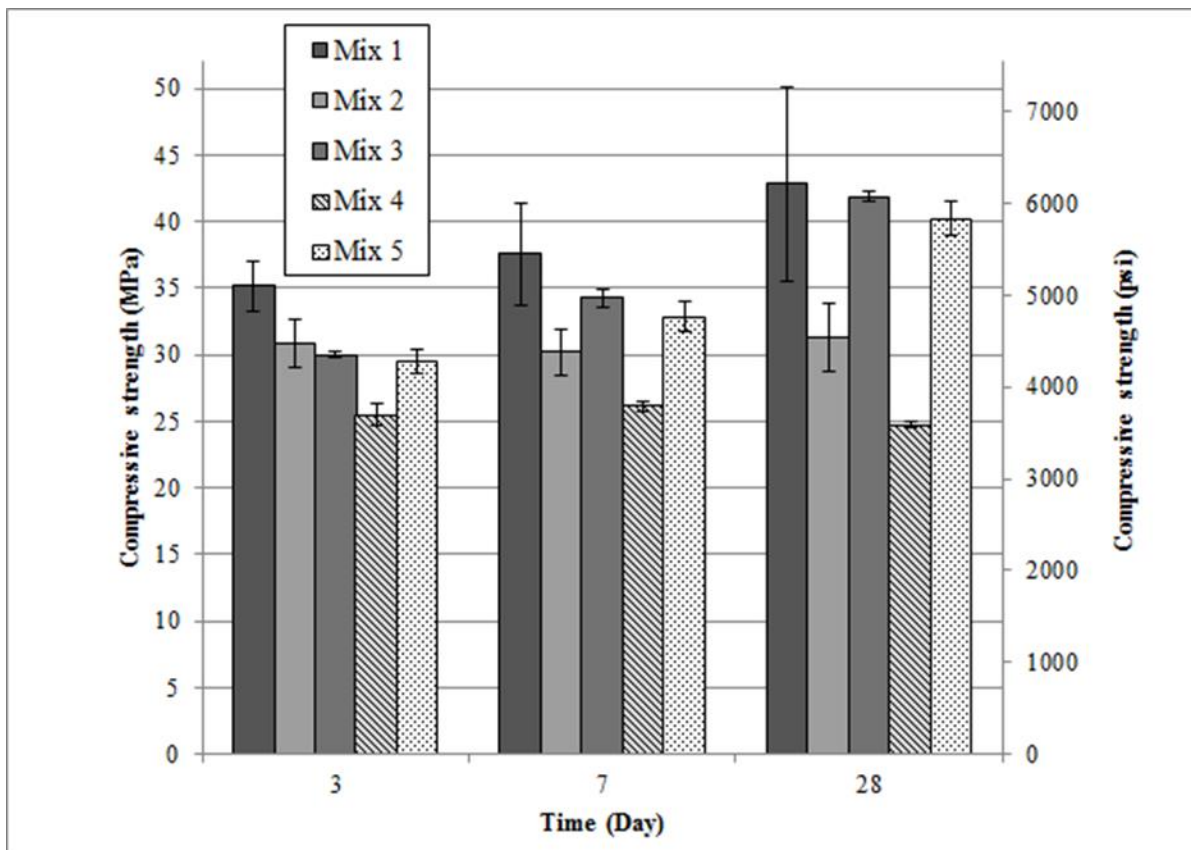
Figure 28: Compressive strength of mortars at days 3, 7, and 28 as tested by ASTM C109

aggregate it replaces. Since internal curing can provide an additional supply of water (and therefore extra hydration of the cement) it can increase the specimen's strength. However, the LWA is porous and thus mechanically weaker than the aggregates that it replaces and therefore can negatively impact the strength of the specimen. Many studies have observed either an increase in compressive strength or a slight decrease in strength when partially replacing normal weight aggregates with LWA.

Bentz studied the use of blended cements for high-performance mortars [102]. Three blended cements (silica fume blended cement contained 8 % silica fume by mass, the slag cement contained 20 % slag by mass, and the fly ash cement contained 25 % of a Class F fly ash by mass) were used and compared both with and without internal curing. All three blended cements showed long-term increases of 10 % in compressive strength when using internal curing [102]. Similar results were determined by de la Varga *et al.* where experimental testing was conducted on large percentage replacements (40 % or 60 % by volume) of cement by Class C fly ash as well as the inclusion of internal curing [103]. It was found that the specimens containing the fly ash with internal curing displayed an increase in strength. On the other hand, a study determined that the porous nature of the LWA contributed to the lower compressive strength found when embedding phase change materials (PCMs) into LWA to reduce freeze/thaw damage [63, 104].

The strengths of Mix 2 did not significantly increase with time. The same trend was observed with Mix 4. Although some of the decreases in the strengths of both Mixes 2 and 4 are due to the LWA, which is mechanically weak, further reductions in compressive strength are likely due to either the CA and the PCI diffusing out of the LWA and interfering with the hydration reactions, or surplus liquid remaining on the surface of the LWA, entering the mix

56

water and causing interference. Similar results have been observed in a previous study when encapsulating PCMs within LWA [63, 104]. In addition to the LWA being weaker than conventional aggregates, the reduction of strength was also explained that the degree of hydration may be lowered if the LWA exchanges PCM with water from the system. Moreover, the LWA could be releasing the PCM into the cementitious mixture prior to the cement particles becoming fully hydrated where the PCM would coat the cement particles prior to the water and retard the specimen by preventing the interaction of the water and cement [63, 104]. The same could be occurring with the CA and PCI in this study. Further investigations explain the weakness occurring *(see section 3.2.4 Scanning electron microscopy).*

3.1.3 Semi-adiabatic calorimetry

Hydration is an exothermic reaction; as such, the retardation of the temperature profile of a cementitious system under otherwise identical curing conditions indicates interference with hydration. The heat evolution of Mixes 2, 3, 4, and 5 were decreased compared to the control as plotted in Figure 29 *(overleaf).* Mixes 2 and 4 experienced a 6 % and 3 % reduction in peak temperature compared with the peak temperature of 61.5 °C (142.7 °F) in Mix 1, respectively. A slightly different trend was observed for Mixes 3 and 5. The rate of hydration was accelerated, producing a leftward shift in the graph with an overall lower peak temperature (8.5 % and 10.8 % decreases, respectively). As with setting time and compressive strength, the semi-adiabatic calorimetry results indicate an interference with the hydration reactions. However, the situation is complicated by the fact that water encapsulated in the LWA has a higher heat capacity than quartz aggregate or the other internal agents and therefore takes longer to increase in temperature.
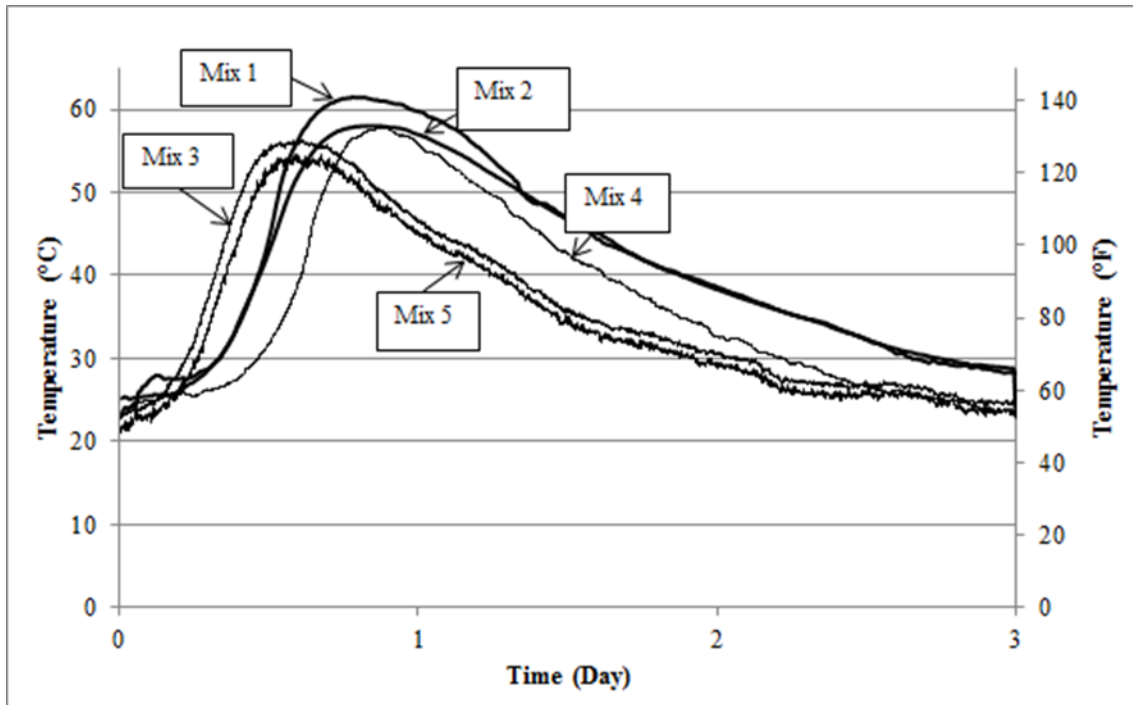
Figure 29: Semi-adiabatic calorimetry

For example, a previous study investigated the impact of nanoscale viscosity modifier in concrete as a method to increase the viscosity of the pore solution in order to decrease the diffusion rates of aggressive media such as chloride ions [72]. The viscosity modifier was added to the mixing water or was encapsulated in LWA; this study aimed to compare the use of viscosity modifiers suggested by the manufacturer and new method (through LWA). These experimental samples were then compared to a control and samples with water encapsulated with LWA. The authors determined that the addition of the viscosity modifier impacts the hydration reaction whether it is added through the conventional method or through LWA. It was determined that the cause for such results was due to the pore solution's increase in viscosity, viscosity reduced the diffusion and dissolution processes that aid in early age hydration. The sample with water encapsulated in LWA also showed an acceleration of hydration reactions where a higher heat of hydration was observed at an earlier time. This experiment has similar

58

acceleration results as in Mixes 3 and 5. Due to the smaller sample size used in the previous study (of the nanoscale viscosity modifier), an overall lower heat release is produced.

Additional studies have observed similar results. Bentz and Turpin focused on encapsulating PCMs into LWA for three possible applications: to increase energy storage capacity of concrete in commercial and residential structures with a transition temperature close to room temperature; as a method to reduce thermal cracking by transitioning the temperatures (of higher or lower temperatures) of concrete to reduce temperature rise and fall; and as a technique to reduce freeze/thaw cycles in concrete structures such as bridge decks exposed to winter climates [71]. The authors found that the PCM embedded in LWA retarded the hydration process by not as much as when PCM was added directly into the cementitious mixture.

3.1.4 Autogenous shrinkage

Autogenous shrinkage was measured to evaluate if the stored liquids (CA, PCI, or water) were being released from the pores of the LWA. The results are shown in Figure 30. Exhibiting an
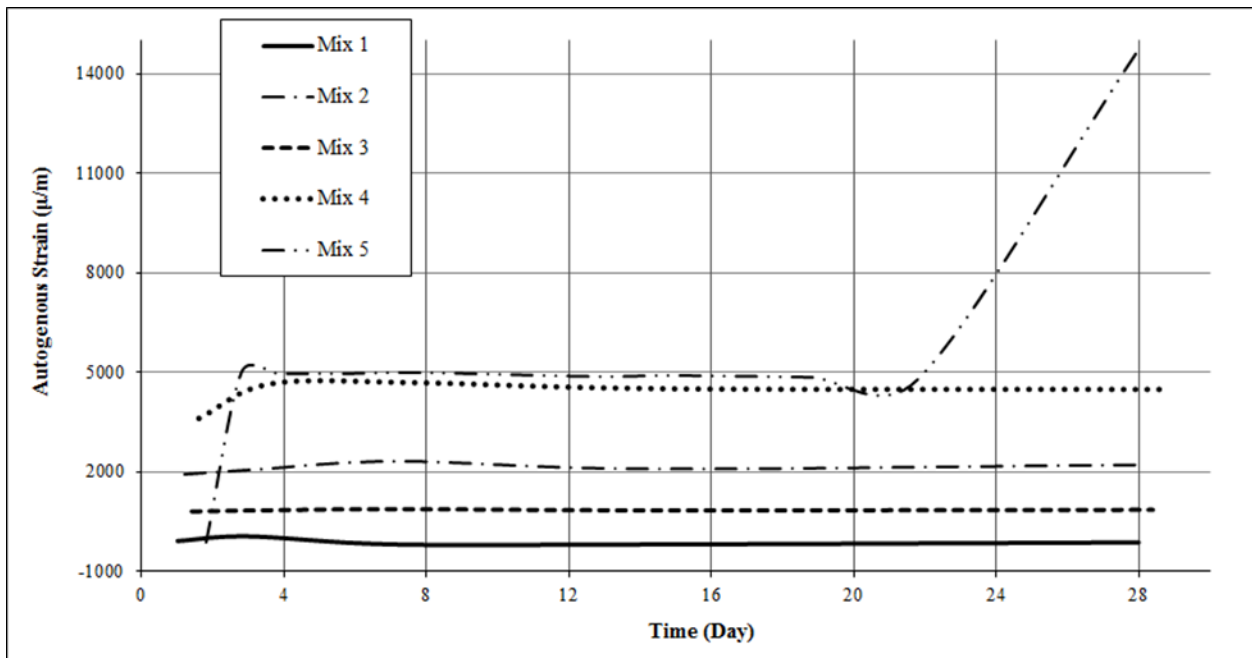
Figure 30: Autogenous strain

autogenous expansion would indicate that the liquid is being released from the LWA and entering the pore solution of the cementitious mixture. Mix 1 experienced autogenous shrinkage where initial strain observed was -77.1 µ/m to a final strain at day 28 of -122.7 µ/m due to self-desiccation. The cement was not exposed to external water and therefore the cement hydration reactions consumed the pore solution where the volume of liquid in the pores was reduced; this created menisci in the pore solution; these menisci exert an inward force that causes the sample to shrink. Mixes 2, 3, and 4 experienced slight expansions whereas Mix 5 demonstrated large and obvious expansion. Mix 2 expanded by 14.8 %, Mix 3 expanded by 5.9 %, and Mix 4 expanded by 24.1 %. Mix 5 significantly expanded and the significant increase of strain may be due to the sensitivity of the test. Due to the sensitivity of the test, large standard deviations were observed and therefore the average values are plotted. Standard deviations were omitted from Figure 30 for clarity purposes. All mixes experience a slight initial expansion which has been also been observed in previous studies [105].

Since the purpose of internal curing is to prevent early age cracking, several studies have been previously carried out and help to explain the autogenous expansion observed in Mixes 3 and 5. Bentur *et al.* performed similar autogenous shrinkage tests on high-strength concrete samples containing partial aggregate replacement of water encapsulated in LWA and compared it to a control that contained only normal weight aggregate. The authors observed expansion, apparently due to continued hydration spurred by the additional supply of water released from the LWA and the prolonged saturation of pores [105]. Similarly, Henkensiefken *et al*. observed comparable results with internal curing specimens when investigating autogenous shrinkage when using low w/c ratios [106]. Additional studies by Raoufi *et al.* and Lura on internal curing have shown similar results [107, 108].

The expansion observed in Mix 2 (containing the CA encapsulated in LWA) and Mix 4 (containing PCI encapsulated in LWA), suggests that the internal agents are diffusing from the LWA into the pores of the cementitious matrix, more completely saturating pores and reducing the surface tension of pore solution (and thus reducing shrinkage). This is the desired effect since the goal of encapsulating either CA or PCI through LWA is so that they become released to travel through the cementitious mixture and protect the reinforcing steel. However, the liquid's time of release is critical and is further investigated in Study 2 and 3.

3.1.5 Accelerated Corrosion Test (ACT)

In the ACT, a certain current flowing through the sample is required in order to keep the anodic potential constant. Currents in Mixes 1, 3, 4, 5, and 6 followed a similar trend: the current began at a range between 0.22 A and 0.26 A and gradually decreased with time as shown in Figure 31 *(overleaf)*. Eventually, a sharp and significant increase occurred, indicating the initiation of a crack and direct exposure of the rebar to the chloride solution. Mix 2 experienced the same trend but at a current of roughly 0.05 A. This may be due to the fact that CA is an organic material. Organic materials are known to have a relatively high electrical resistivity, which would serve to reduce the current [39].

The average cracking times of five of the six mixes were comparable. Mix 4 extended the time to cracking by 23 % and Mixes 3, 5 and 6 slightly decreased cracking time by 10 %, 13 %, and 15 % respectively. This may be due to the relatively short time that the inhibitor had to penetrate the samples (only 28 days) and the severity of the accelerated test. On the other hand, Mix 2, which incorporated cinnamaldehyde encapsulated in LWA, required 52.1 ± 15.9 d for the sample to crack. This may be due to creation of a protective CA film on the steel rebar.
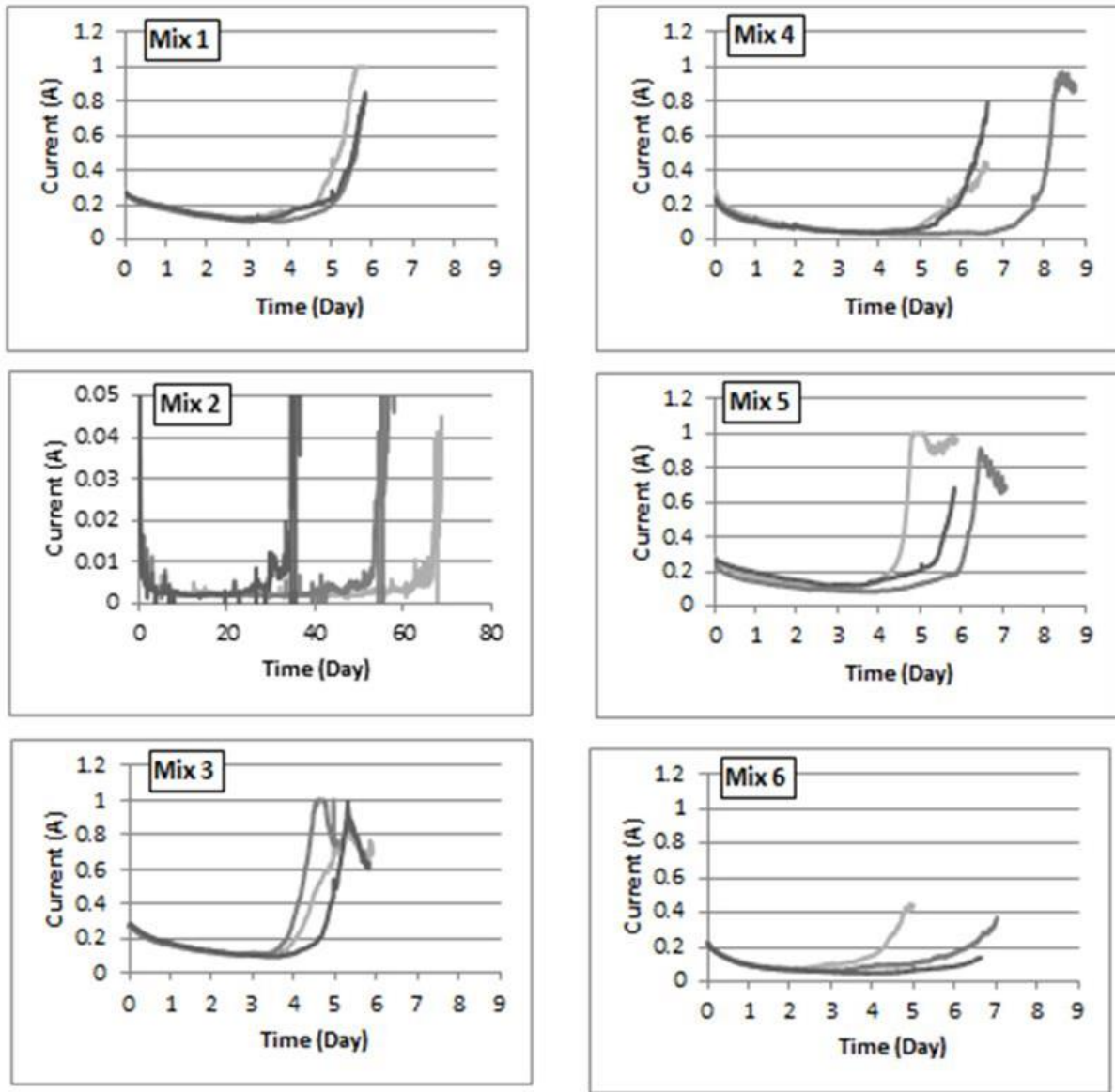
Figure 31: Accelerated corrosion test results. N.b.: for Mix 2, the x-axis is larger and the y-axis is smaller

Previous studies have shown similar results where experimental samples prolonged the time to corrosion (or cracking due to corrosion). Detwiler *et al.* investigated the impact different w/c ratios at varying temperatures had on corrosion of the steel reinforcement. It was determined that the lower the w/c ratios the longer the samples took to corrode at all temperatures. When the w/c is increased, the pore system of the cementitious mixture is more fluid allowing the chloride to penetrate through the cementitious sample and corrode the steel at a quicker rate. Additionally, an increase in curing temperature reduces the time to corrosion at all w/c ratios tested. This was due to the pore system being more continuous at increased temperatures [75]. Shaker *et al.* and Okba *et al.* used the ACT method to investigate the durability of latex modified concrete (LMC). The LMC specimen showed a significant increase in time to corrosion (230 h) compared to a control of conventional concrete (48 h) [76, 77]. Elmoaty used ACT to find that using 5 % granite dust as cement replacement could increase the time to cracking of a cementitious sample [78]. Güneyisi *et al.* investigated corrosion in chloride contaminated concretes both when metakaolin was present and not, and it was determined that the addition of metakaolin prolonged time to failure [79]. Prolonging time to failure was also observed in specimens with blended cements [80].

3.1.6 Electrical resistivity

The initial electrical resistivity values of each mix, except Mix 2, begin at around 50 $\Omega \cdot m$ as plotted in Figure 32 *(overleaf)*. A similar trend was observed for each mix: electrical resistivity increased with time until a crack initiated. A similar trend was observed by Polder and Peelen, where it was concluded that the electrical resistivity of concrete influences the likelihood of corrosion and the rate of corrosion [109]. The use of water encapsulated into LWA and PCI encapsulated into LWA did not significantly impact the resistivity; however, the use of surface

63
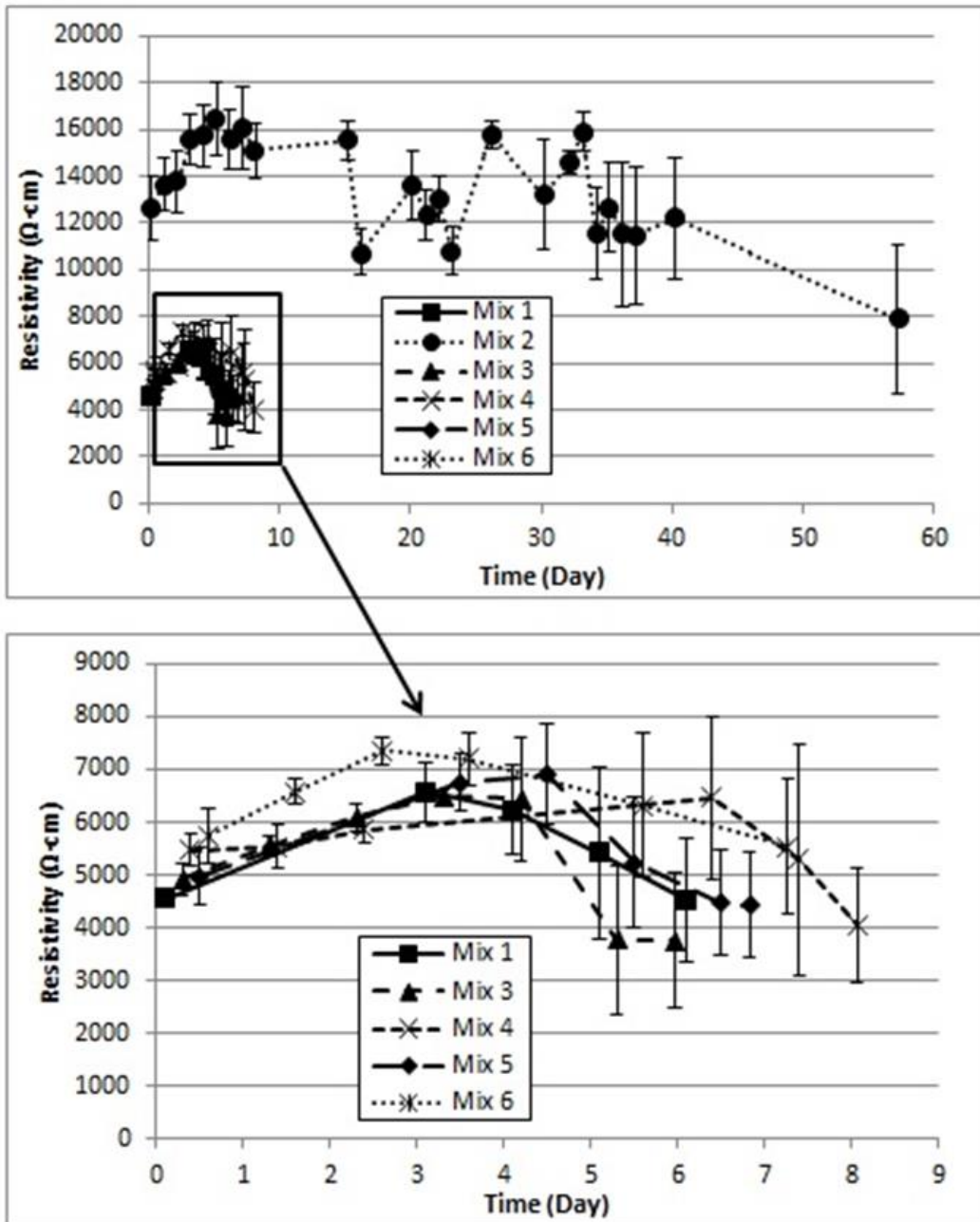
Figure 32: Electrical resistivity of lollipop samples as determined by Wenner probe. The electrical resistivity of Mixes 1, 3, 4, and 5 are enlarged in the lower plot.

applied penetrating corrosion inhibitor did cause some variation by creating a slight, overall increase in resistivity. The resistivity of Mix 2 was significantly increased, due to the cinnamaldehyde being an organic material, as previously discussed *(see section 3.1.4 Accelerated corrosion test)*. As the test progressed, low standard deviations were initially

observed for the resistivity measurements. Over time, the deviations increased due to the readings being taken on four sides of each sample. Resistivity is drastically lowered in the area of a saturated crack, causing the increase in deviation. It should be noted that resistivity values presented may not be the true resistivity values due to the possibility of ions leaching from the sample into the NaCl solution [110].

Güneyisi *et al.* observed a similar trend of a decrease in resistivity over time as chloride contamination increased when investigating corrosion in chloride-contaminated concretes with the addition of metakaolin [79]. The electrical resistivity will decrease when there is an increase in current such as when corrosion occurs; this is due to Ohm's law (*I = V/R; I = current, V = voltage, and R = resistance*).

3.1.6 Mass loss

After impressing a constant 30 V potential on the lollipop samples during the ACT, the mass loss of the reinforcing steel was calculated and compared with cracking time as illustrated in Figure 33 *(overleaf)*. The greatest steel mass loss was observed in the water encapsulated in LWA of Mixes 3 and 5 (36.5 ± 2.8 g and 37.3 ± 9.8 g, respectively). Mixes 1, 2, and 4 had similar results, with losses of 31.5 ± 5.3 g, 21.8 ± 13.2 g, and 23.4 ± 5 g, respectively. Mix 6 experienced the least amount of steel mass loss of 17.9 ± 2.9 g. This indicates that CA-LWA and PCI-LWA did not significantly impact the mass loss of the reinforcing steel during corrosion. Surface application of the penetrating corrosion inhibitor seemed to protect the rebar from losing mass, while water-soaked LWA permitted a large mass loss before failure. Elmoaty conducted a similar test on lollipop samples, determining that the high voltage (30 V) used in the ACT may affect the results [78]. If a lower voltage were used over a longer time period, more accurate results (e.g. that could be observed in the field) might be produced.
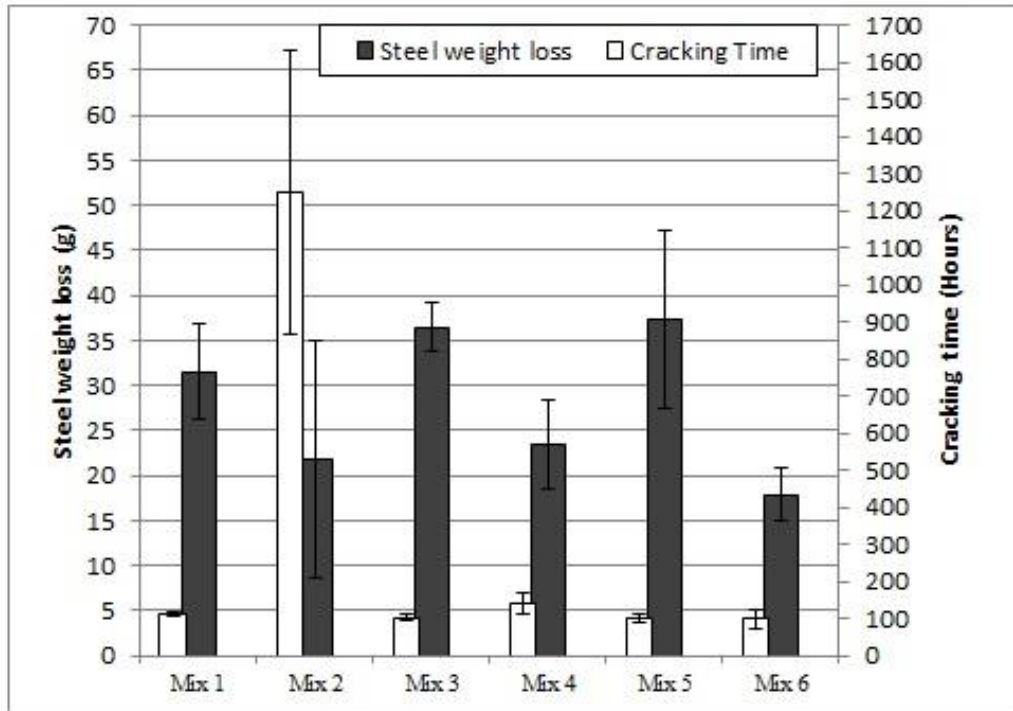
Figure 33: Mass loss of reinforcing steel and corresponding cracking time.

Summary of Study 1

After completing Study 1, there are three main conclusions that can be determined:

- Addition of CA-LWA and PCI-LWA observed mechanical weaknesses (with lower compressive strength) as well as reduced heat of hydration.

- Autogenous shrinkage showed liquids stored in LWA are being released.

- ACT establishes that CA-LWA greatly lengthens time to corrosion.

3.2 Study 2

A further study on the potential chemical and mechanical interferences with CA in a cementitious matrix was investigated by subjecting three mix designs to a set of nine tests.
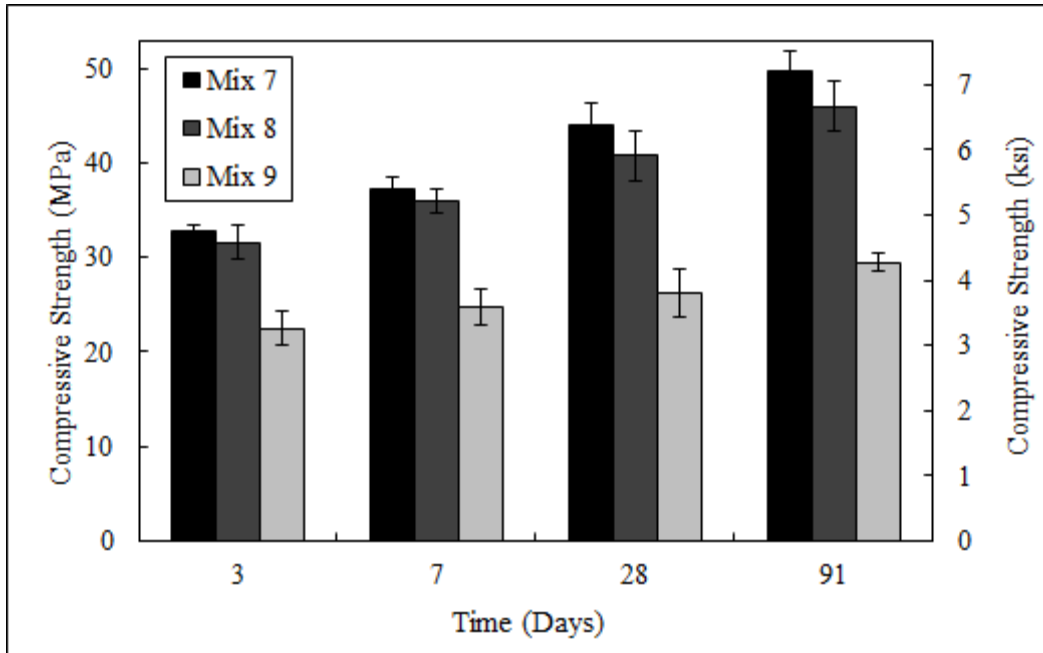
Figure 34: Compressive strength of mortars at ages 3, 7, 28, and 91 d

3.2.1 Compressive strength

Mixes containing presoaked LWA resulted in lower compressive strengths as shown in Figure 34 *(overleaf)*. Mix 8, which contained water-LWA, resulted in reduced strengths when compared to the control by 4 % at 3 d and 7 d; 8 % at 28 d; and 7 % at 91 d. This decrease in strength is likely due to the weak nature of the porous LWA as explained in Study 1 *(see section 3.1.2 Compressive strength)* [24]. When using LWA to encapsulate CA (Mix 9) larger reductions in strength were observed. Compressive strength decreased by 31% at 3 d, 33 % at 7 d, 40% at 28 d, and 41 % at 91 d, indicating that either a surplus of CA remains on the surface of the LWA (which may prevent the formation of mechanical bonds between LWA and the cementitious matrix), or LWA is releasing the CA early enough to interfere with the hydration reactions by coating cement particles and inhibiting hydration.

3.2.2 FTIR and XRD

The FTIR spectra of the three mortar mixes consisted of six similar bands: a band at 600 cm^{-1} due to Si-O vibrations; a band at 975 cm^{-1} due Si-O and Al-O vibrations; a band at 1413.8 cm^{-1} due to S-O and C-O vibrations; a band at 1643.3 cm^{-1} due to H-O-H bending; a band at 3390.8 cm^{-1} due to S-O; and a band 3643.5 cm^{-1} due to hydrated minerals; shown in Figure 35. XRD identified traces of crystalline quartz and calcite in each of the three mortar mixes shown in Figure 36 *(overleaf)*. The similarity in FTIR spectra and x-ray diffractograms indicate that any potential effects on mechanical properties in mortars containing CA are unlikely to be due to the formation of new chemical species.

These types of FTIR results were not seen by Biricik and Sarier when they investigated the characteristics of cement mortars incorporating nanosilica, silica fume, and fly ash [111,
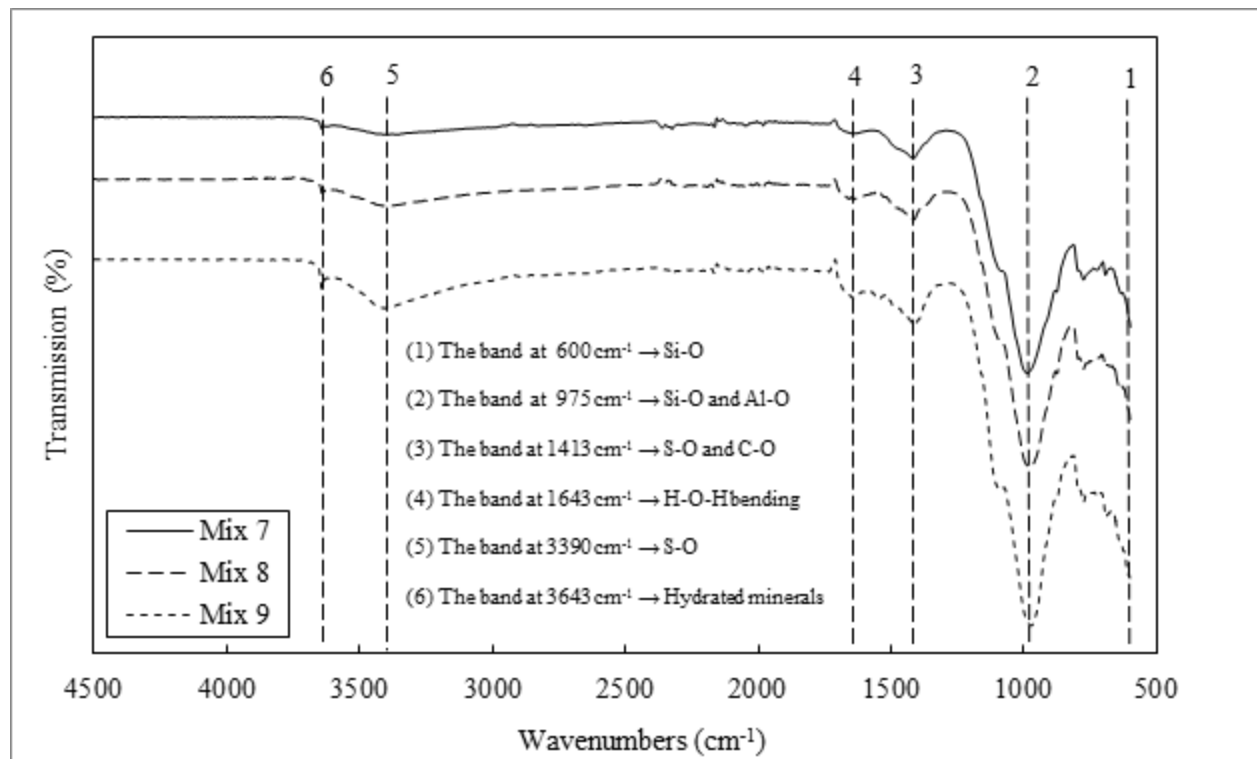
Figure 35: FTIR spectra of the mortars
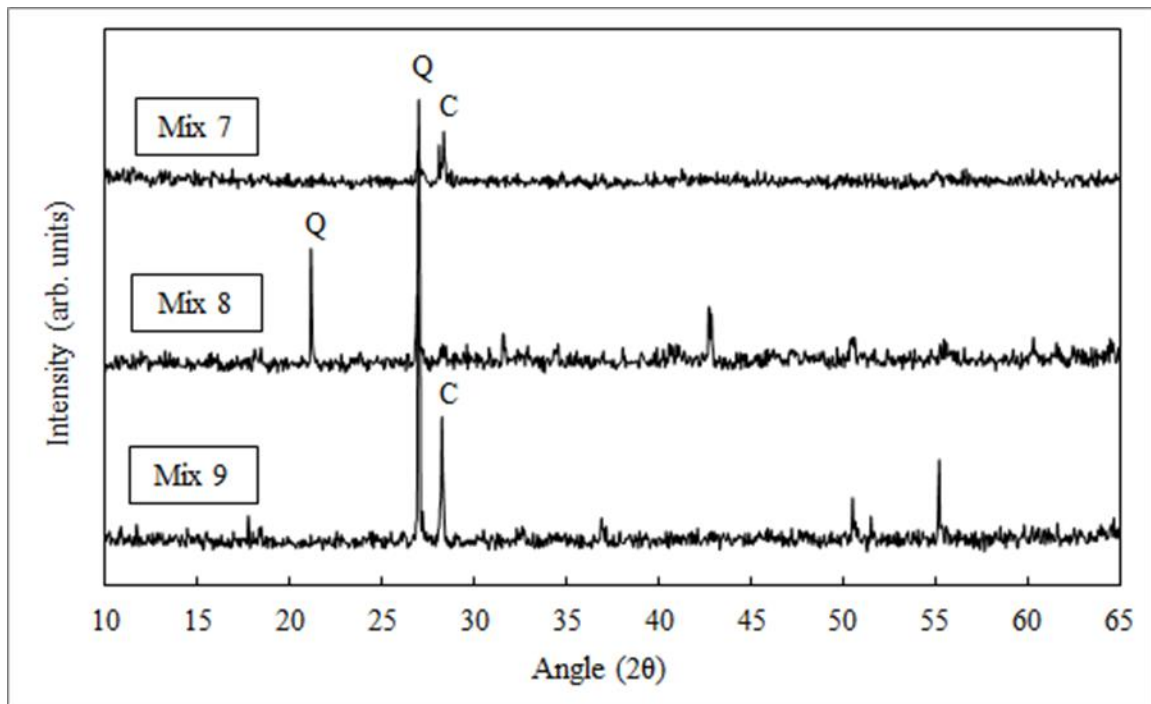
Figure 36: XRD diffractograms of mortars. Notes: Q is quartz and C is calcite

112]. Biricik and Sarier found that the mortar with nanosilica displayed evidence for the highest degree of polymerization of C_3S and C_2S phases with the formation of C-S-H phase compared to the mortars with silica fume and fly ash.

3.2.3 Isothermal calorimetry

Hydration kinetics of the mixes was observed by isothermal calorimetry as shown in Figure 37 *(overleaf)*. Mix 8 displayed a slight acceleration when compared with the control (Mix 7). This has been previously observed in a study which concluded that such behavior was due to additional hydration provided by absorbed water [113]. However, the hydration of Mix 9 was somewhat retarded, with a 14 % reduction of heat flow compared to the control. A rightward shift is also evident, indicating a significant delay in hydration. This is most likely due to CA

69
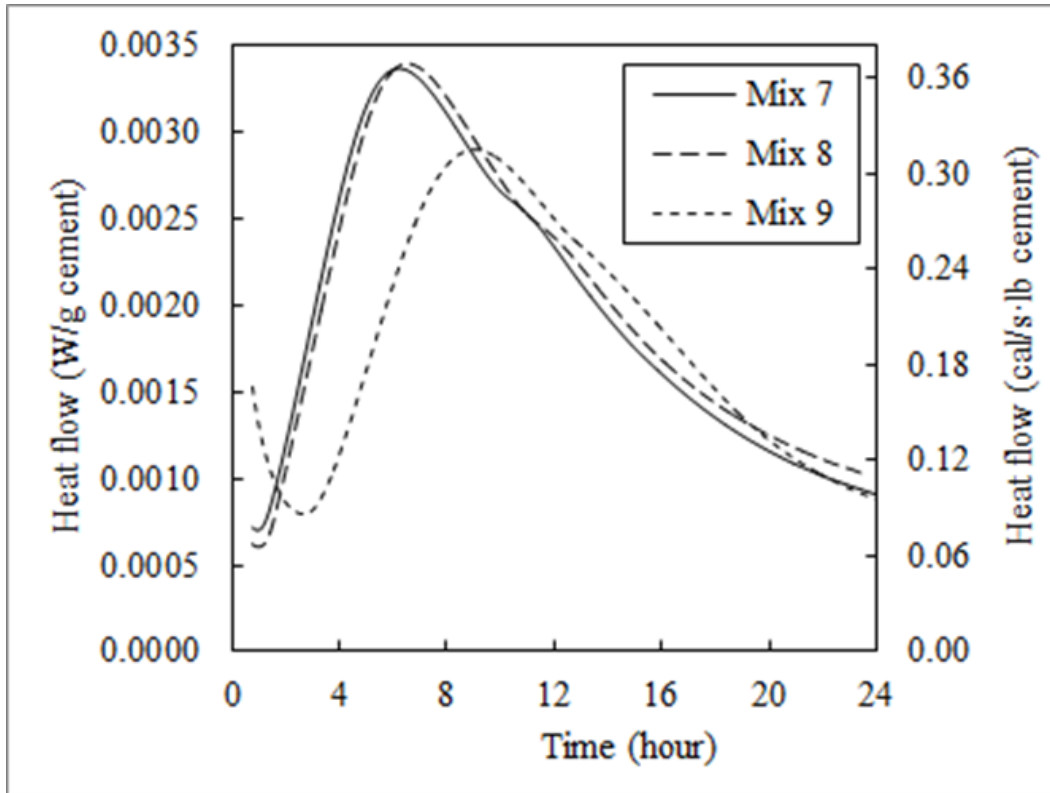
Figure 37: Isothermal calorimetry

coating the particles and hindering the hydration of cement.

3.2.4 Scanning electron microscopy (SEM)

Microscopic investigation of the mortars suggests that the addition of cinnamaldehyde interferes with the development of the cementitious matrix. Figure 38 shows gapping around the ITZ of the LWA in Mix 9. Gaps between cement paste and LWA may be due to the cinnamaldehyde remaining on the surface of the LWA and therefore preventing the adhesion of the paste to the LWA, which is a possible explanation for the reduction of compressive strength. Such gapping is not seen around the ITZ of the LWA in Mix 8. This denser microstructure was observed by Bentz and Stutzman in a study of internal curing [29]. The additional supply of water provided through internal curing reduces the ITZ in a cementitious mixture due to the porous LWA's
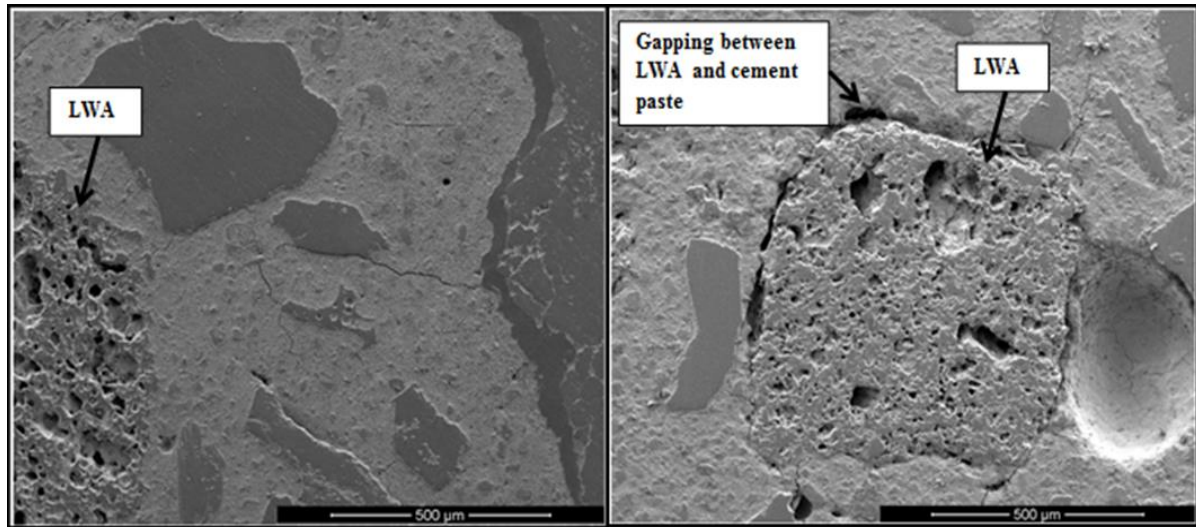
Figure 38: SEM image on left is Mix 8. No apparent ITZ is observed around the LWA. The SEM image on the right shows how Mix 3 produces a gapping space between the LWA and the cement paste. This can be a cause of the reduction in

ability to absorb some of the water that would normally build up around the aggregate due to the "wall effect".

Although gapping was found around the LWA of Mix 9, SEM provides qualitative analysis. There are several variables that could impact the images such as an artifact could disturb the sample during polishing. Moreover, SEM helps provide another possible explanation to the reduction of strength observed when including CA-LWA into a cementitious mixture. FTIR and XRD suggested that new chemical phases are not being created, and isothermal calorimetry suggested that CA is interfering with the hydration of cement. Another option is that CA is mechanically interfering with the bond between aggregate and paste.

3.2.5 Sorptivity

Sorptivity of the three mortars was investigated. The initial rates of absorption follow a linear relationship, with a correlation coefficient of 0.98 or greater shown in, Figure 39 *(overleaf)*. The sorptivity coefficient of Mix 8 was slightly larger when compared to the control (Mix 7) within the first 6 h, listed in Table 10 *(overleaf)*. Since sorptivity relates to the ability of the pore

structure to absorb liquid by capillary forces, this may explain the reason that Mix 8 has the greatest initial sorptivity [114]. Once the LWA releases the stored liquid, the pores of the LWA are empty and can therefore absorb water. However, the addition of CA (Mix 9) led to a lower initial sorptivity coefficient compared to the control. This may be due to CA filling the pores of the cementitious matrix during the initial phases of sorptivity or altering the transport properties of the pore solution (for example, by increasing the viscosity).

The secondary rate of water absorption for Mix 7 and Mix 8 did not follow a linear relationship, with correlation coefficients of 0.945 and 0.934, respectively as shown in Figure 39 *(overleaf)*. Ghafari *et al.* observed similar nonlinear coefficients when testing the sorptivity of ultra-high performance concrete; the nonlinear results were used as an approximation of sorptivity [115]. The results of the regression equations were used for estimation of the secondary rate of sorptivity, despite being nonlinear, and are listed in Table 11*(overleaf)*. Between 1 d and 7 d, the sorptivity coefficients of Mix 7 and Mix 8 decreased, a trend observed by Lo *et al.* [114]. However, the secondary rate of water absorption for Mix 9 increased slightly. This may be due to the CA fully emptying out of the LWA pores, suggesting that CA is exiting the LWA pores at a slower rate when compared with the water in Mix 8.

Table 10: Regression equations of initial rate of water absorption

Sample	Content	Regression equation	Correlation coefficient	Sorptivity coefficient $(mm/s^{1/2})$
Mix 7	Control	y = 0.0146x + 0.163	0.998	0.0146
Mix 8	Internal curing	y = 0.0159x + 0.240	0.997	0.0159
Mix 9	CA-LWA	y = 0.0061x - 0.082	0.980	0.0061

Table 11: Regression equations for secondary rate of water absorption

Sample	Content	Regression equation	Correlation coefficient	Sorptivity coefficient $(mm/s^{1/2})$
Mix 7	Control	y = 0.0045x + 2.7285	0.945	0.0045
Mix 8	Internal curing	y = 0.0042x + 3.3381	0.934	0.0042
Mix 9	CA-LWA	y = 0.0065x + 0.9166	0.980	0.0065

Henkensiefken *et al.* studied the sorptivity of mortars containing low w/c ratios as well as experimental samples containing water encapsulated into LWA [116]. It was determined that the specimens containing water-filled LWA did have lower initial and secondary sorptivity than samples that did not contain the water-filled LWA. The cause for such reduction was due to the extra hydration produced by the internal curing, creating a denser pore structure within the cementitious matrix. However, Henkensiefken *et al.* did mention that there is a possibility that the porous LWA can show an increase in sorptivity if the LWA pores are larger than the capillary pores of the cementitious matrix. This phenomenon can explain the increase observed in Mix 8 during initial sorptivity.
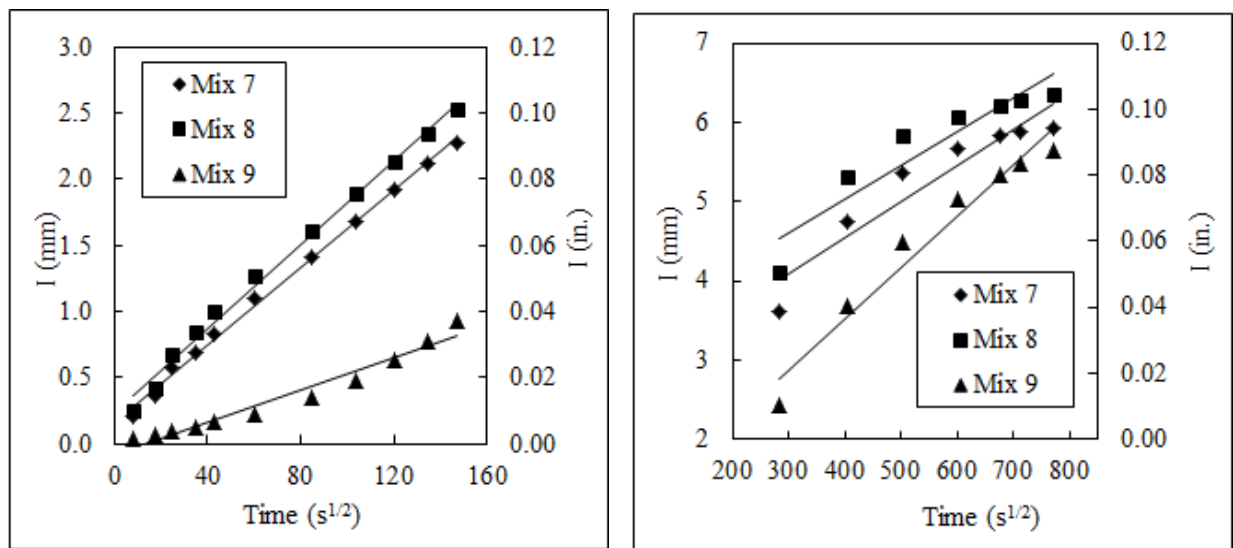
Figure 39: Initial rate of water absorption (left) and secondary rate of water absorption (right)

3.2.6 Chloride diffusion

The area (measured in percentage) through which chloride penetrated Mix 8 was 23 % less when compared with Mix 7 as shown in Figure 41. This may be due to the LWA creating a denser ITZ microstructure due to additional hydration. The diffusion of chlorides through Mix 9 was 17 % less than Mix 7, possibly due to the CA filling the pores within the cementitious matrix and altering the transport properties of the pore solution. (Figure 41*(overleaf)* shows cylinder mortar samples split lengthwise and sprayed with silver nitrate in order to measure the chloride diffusion.)

A previous study observed that when viscosity modifier was encapsulated into LWA, it experienced the least amount of chloride penetration in the specimens when compared to both the viscosity modifier being added in the traditional manner (where it was mixed into the cementitious matrix) and a control containing normal weight aggregates [72]. The results were explained that the LWA creates a denser microstructure as well as the pore solution becomes
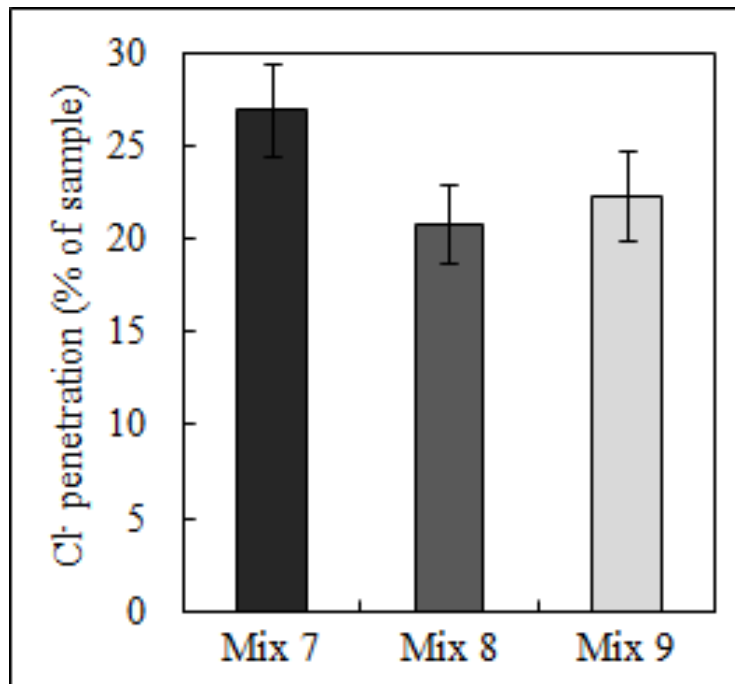
Figure 40: Chloride penetration of split cylinders in terms of the percentage of the mortar sample.
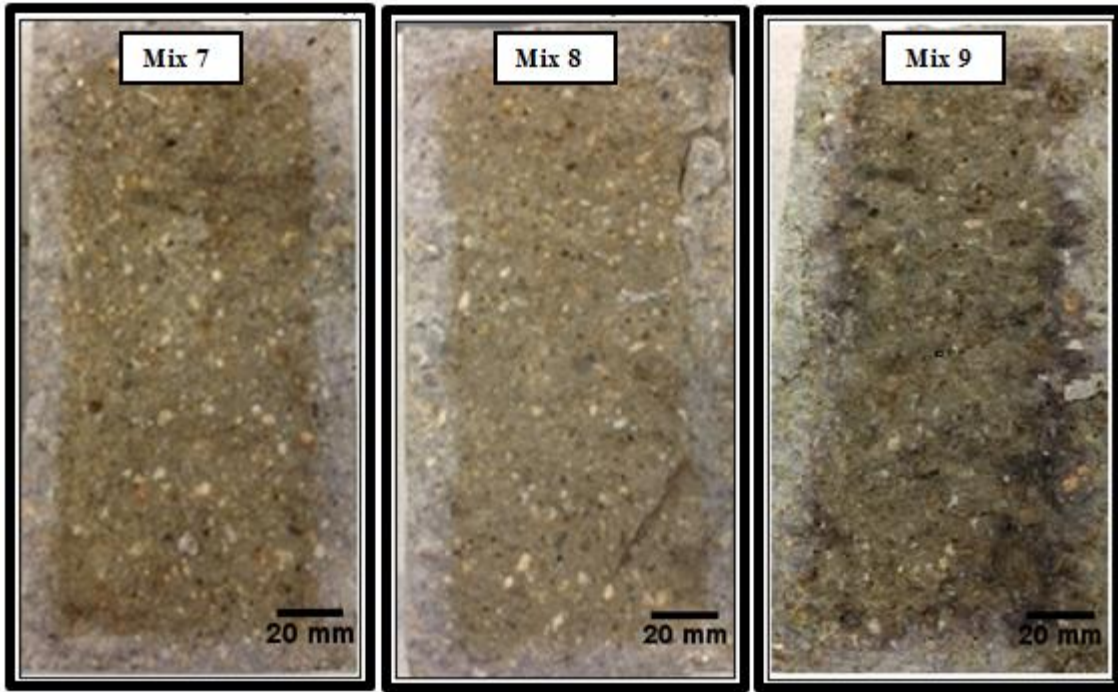
Figure 41: Samples of cylinders split lengthwise and sprayed with silver nitrate after exposed to NaCl solution bath for 3 m.

filled from the viscosity modifier. Additionally, water-filled LWA also reduces the chloride penetration due to its denser microstructure, as discussed.

3.2.7 Chloride threshold level (CTL)

The times to initiation of corrosion of the samples are listed in Table 12. The resulting times for corrosion initiation of Mixes 7 and 8 were roughly similar; however, it took Mix 9 roughly 91 % longer for the corrosion initiation process to begin. This has previously been observed in Study 1 and is likely due to the cinnamaldehyde creating a protective film on the reinforcing steel as well as slowing the ingress of chloride. Mix 8 had a slightly greater chloride concentration from the

Table 12: Time to corrosion initiation of samples

Sample	Content	Average (day)	Standard Deviation (day)
Mix 1	Control	2.9	± 0.08
Mix 2	Internal curing	2.9	± 0.08
Mix 3	CA-LWA	32.1	± 18.4
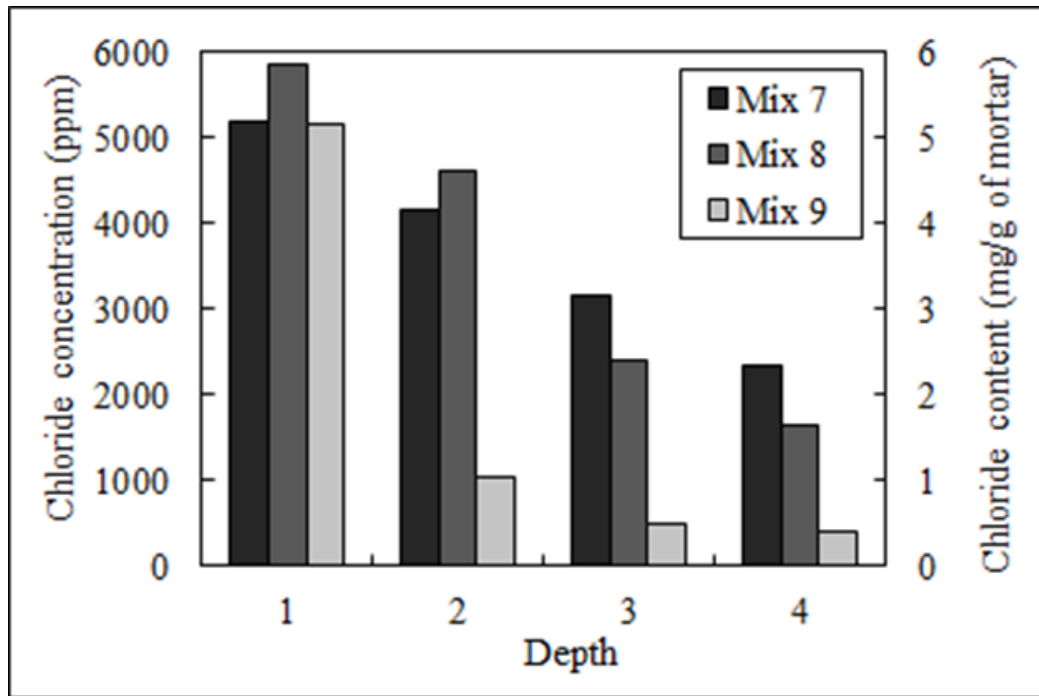
Figure 42: Chloride concentration at varying depth within the lollipop sample. The depths refer to Fig. 4 where : (1) is the powdered mortar collected from the depth of surface to ½ in.; (2) is the powdered mortar collected from the depth of ½ in. to 1 ½ in.; (3) is the powdered mortar collected from the depth of 1 ½ in. to 2 in.; (4) is the powdered mortar collected along the length of the mortar-rebar interface. Error bars are excluded for clarity purposes.

surface to ½ in. (12.7 mm) and 1 ½ in. (38.1 mm) than the control (Mix 7) but lower concentrations at 2 in. (50.8 mm) and along the length of the mortar-rebar interface. Mix 9 has the lowest concentration of chloride at all depths. Figure 42 graphs the chloride concentration at each depth for the three mixes. The lower chloride concentrations combined with the lengthened time to corrosion indicates that the CA increases the CTL of the sample. Due to the sensitivity of the test, large standard deviations were observed and were omitted from the figure for clarity purposes – as such, the values should be taken as only potentially indicative of an increase in the CTL.

3.2.8 Bond strength

The bond strengths between the matrix and rebar were determined for each mix. Figure 43 shows the results of the rebar pullout test where Mix 8 has the greatest bond strength. The failure pattern of Mix 8 also reveals gradual failure, with plateau-like behavior, prolonging the time to failure. This may be due to the denser microstructure of the mix. Mix 9 yields the lowest bond stress with a sharp failure mode (as opposed to the plateaus observed in Mix 8) due to the cinnamaldehyde coating the rebar. Further studies are needed to fully determine the reasons for such failures, and it is likely that the reduced rebar/matrix bond strength would have to be overcome before this system could have any practical applications.

Previous studies demonstrated that bond strength is dependent on the material used to coat the reinforcement. Chen *et al.* observed a reduction of bond strength when testing epoxy
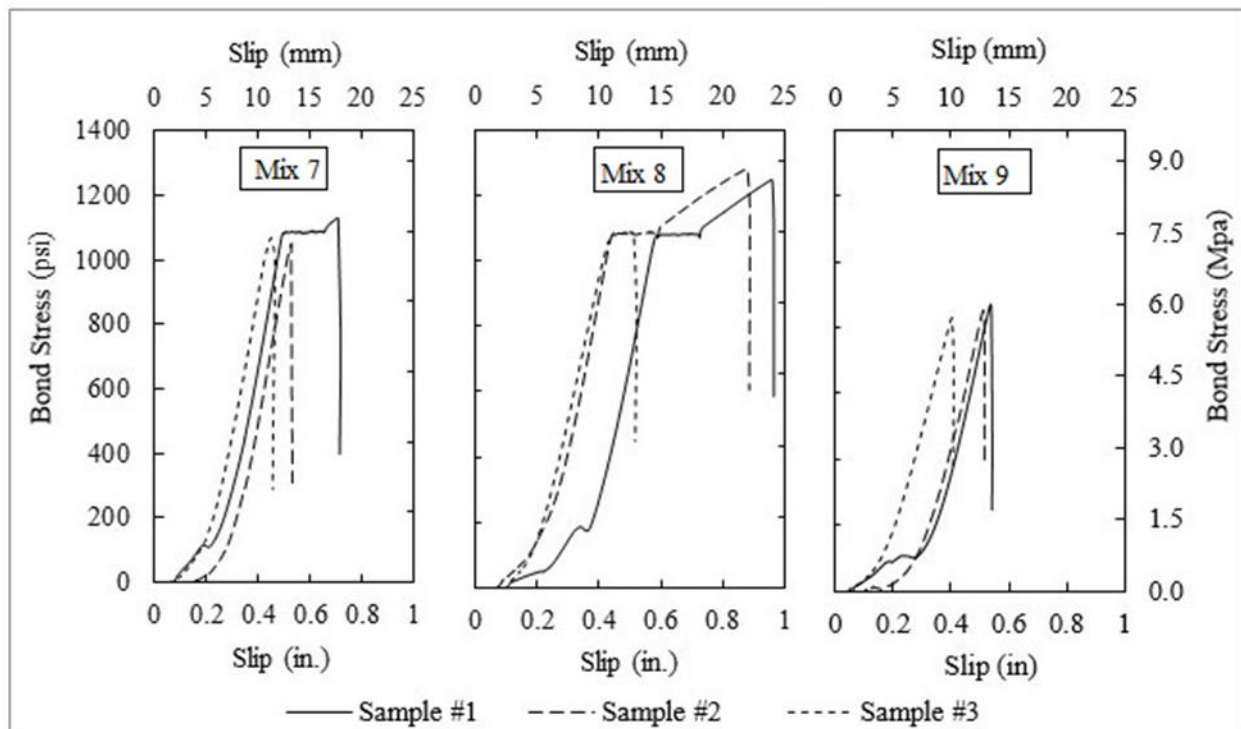
Figure 43: Rebar pullout results plotted as bond stress over slip

coated reinforcement but an increase in bond strength when coated with enamel [95]. Similar results have been observed by Jorge *et al.*[97]*,* De Lorenzis *et al.* [94]*,* Baena *et al.* [93],and Mo *et al.* [96].

Summary of Study 2

After completing Study 2, there are four main conclusions that can be determined:

- FTIR and XRD suggested that new chemical phases are not being created in experimental sample.

- SEM provided another option that CA may mechanically interfere with the bond between aggregate and paste.

- CA-LWA causes low bond stress.

- CA-LWA raises the CTL.

3.3 Study 3

Study 3 investigated five mix designs. This study focused on vacuum encapsulation of the liquid (either CA or water) in LWA. Since the previous two studies (Studies 1 and 2) showed interference of CA on the hydration of cement, Study 3 investigated the impact of coating LWA with cement to provide an additional barrier and prevent the negative interference effects.

3.3.1 Compressive strength

The compressive strength of the five mix designs are presented in Figure 44 *(overleaf)*. The vacuum encapsulation of the CA into LWA (Mix 11) did not improve the compressive strength. However, the compressive strengths in the samples including LWA pre-wet with CA (Mix 12) and coated with cement were promising. The strength of Mix 12 at 28 d was 41.2 ± 1.4 MPa (5975.6 ± 203.1 psi) surpassing that of the control (Mix 10 with a 28 d strength of 40.8 ± 2.3

78
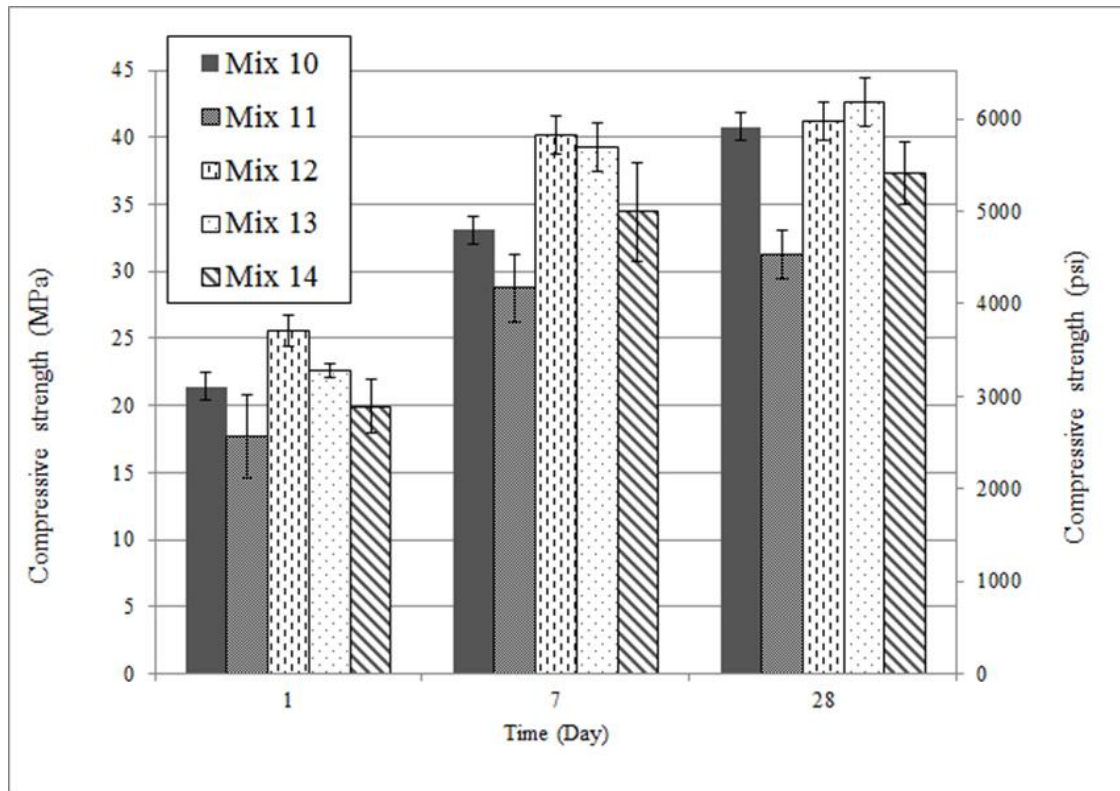
Figure 44: Compressive strength of Study 3

MPa (5917.5 ± 333.6 psi)). This indicates that a thin cement coating can be used a method for encapsulating CA into LWA. It can prevent the contact of CA with the bulk cement and therefore allow proper hydration of the cement since the cement particles do not become coated with CA to hinder the hydration. The negative effects to compressive strength seen in Studies 1 and 2 are reduced. The internal curing specimen showed similar results seen in both Studies 1 and 2 where strength profiles were similar to the control. However, when the internal curing samples were coated with cement, reduced strengths were produced. This may be due to a premature hydration of the coated cement with the water remaining on the surface of the LWA. As a result, premature hydration can interfere with the processes that would usually occur in internal curing specimen.
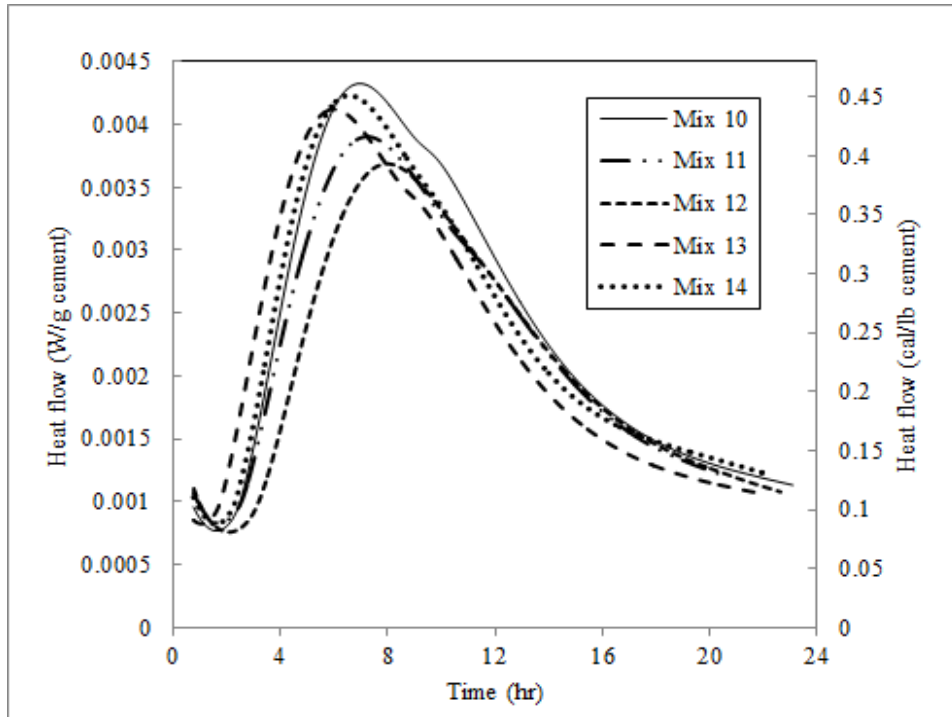
Figure 45: Isothermal calorimetry results from Study 3

3.3.2 Isothermal Calorimetry

The results from isothermal calorimetry are shown in Figure 45. The heat evolution of Mixes 11 and 12 were reduced by 9.7 % and 14.8 % respectively when compared to the control. These results are similar to Mix 9 in Study 2 where a 14 % reduction was observed. CA is still somewhat hindering the heat evolution. However, the difference between the result of Mix 9 in Study 2 and the result of Mix 12 in Study 3 is that although a reduction in heat evolution occurs in Mix 12, the compressive strength was not impacted by this reduction. Mixes 13 and 14 also observed reductions in heat evolution of 4.7 % and 2.2 %, respectively. Although Mix 13 experienced a reduction of heat evolution, the reduction did not impact the compressive strength of the mixture. Such results with a reduction of heat evolution in internal curing samples were observed in Study 1 (semi-adiabatic calorimetry of Mix 2 and 4 were reduced but the compressive strength was not impacted).

80

Summary of Study 3

After completing Study 3, there is one main conclusion that can be determined:

- CA-LWA with cement coating improved in compressive strength but interferences were shown in isothermal calorimetry.

CHAPTER 4: CONCLUSIONS

Corrosion of steel reinforcement in concrete has been a major issue since the 1960s and remains a critical issue; $100 billion worth of corrosion-related damages still occur each year. Although there have been advances with research and commercially available products to alleviate this great issue, billions of dollars are still being expended annually on maintaining and repairing corrosion-related damages. There is yet no product that effectively mitigates corrosion. Therefore, new and innovative corrosion prevention methods are a necessity. This research program focused on developing a new approach to corrosion mitigation by incorporating CA, a natural bioactive agent, through encapsulation of LWA as a method for corrosion prevention in concrete.

Through a series of ACTs in Studies 1 and 2, the use of LWA pre-wet with CA raised the CTL and extended the specimens' time to corrosion by 91 %. Although the corrosion results were promising, mechanical weaknesses (with lower compressive strength) as well as reduced heat of hydration in CA-LWA samples were observed. SEM images showed gapping around the ITZ of CA- LWA, and therefore CA may mechanically interfere with the bond between aggregate and paste. FTIR and XRD suggested that new chemical phases are not being created and therefore can be ruled out. Moreover, weaker bond strength could be due to the CA coating the rebar.

In Study 3, however, the compressive strength of CA-LWA improved when a thin coating of cement was placed on the surface of the LWA. Although mechanical strength developed, the heat of hydration still indicated retardation. Further studies such as bond strength and autogenous shrinkage are needed to understand the behavior of cement-coated CA-LWA in a

cementitious matrix. SEM images would be necessary to investigate the ITZ of the coated CA-LWA.

The use of CA in concrete as a method of corrosion prevention is promising. It has shown to significantly increase the time to corrosion by creating a protective film on the steel reinforcement. This could mean that by using CA in concrete, the premature deterioration of concrete could be alleviated. However, there remains some concerns such as reduction of strength and therefore more studies are necessary before CA can be used as corrosion prevention method in the practice.

Future studies

This research program was the first of its kind to bring attention to the use of natural bioactive agents as a method for corrosion prevention in concrete. Although a suitable method to use CA as a corrosion mitigation technique was not established, favorable results were found. Future work includes further studies to determine the optimum method to include CA into concrete. Additional investigations are needed regarding the advantages of including CA encapsulated in LWA. Such advantages include the possibility that the formation of rust could expand into the pores of the LWA and alleviate tensile stresses; petrographic analysis shown in Figure 46 [117]
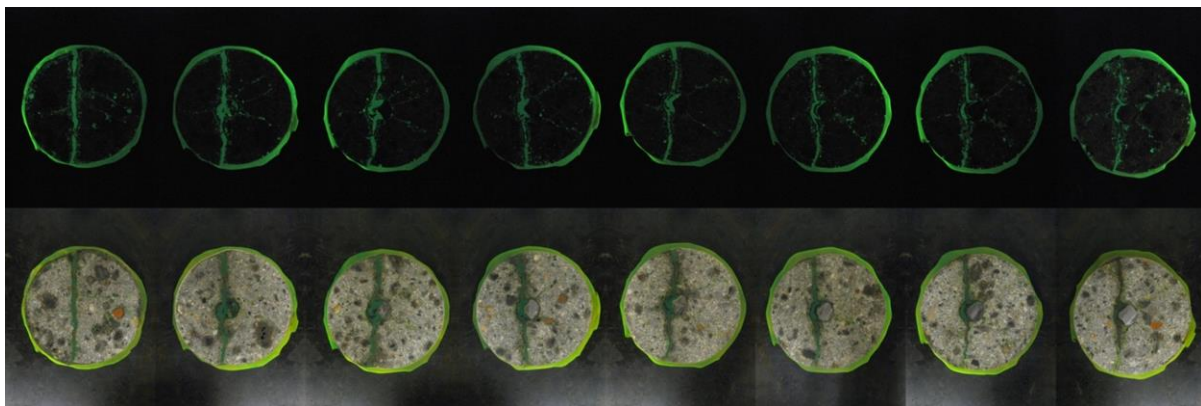
Figure 46: Petrographic slide of corroded lollipop sample [117]

of "lollipop" samples could help indicate such behavior. Figure 46 shows a corroded lollipop sample which is thinly sliced across the samples diameter and impregnated with a florescent dye. Moreover, other bioactive agents, such as vanillin could be tested to be incorporated into a cementitious matrix for corrosion prevention. Also, a different carrier such as super absorbent polymers (SAP) could be tested (as opposed to LWA as a carrier). If a viable method of incorporating CA into a cementitious matrix is determined, corrosion can be mitigated.

As an extension to the research conducted at WPI on premature deterioration of concrete, a Fulbright grant led to the study of historic infrastructure materials of the old city of Fès, Morocco. Fès is a UNESCO world heritage site and under restoration.

Background

The historic city of Fès, Morocco was founded in the ninth century by Idriss II and quickly developed into a prosperous and booming city. Fès was methodically established in a valley – one which was commonly used for trade routes and particularly had access to a river [118]. Formerly, it was particularly noted for its architecture, artisanal craftsmanship, and labyrinth of narrow streets. It was the capital of Morocco and the home to the oldest university in the world, *Al-Qarawiyyin University,* shown in Figure 47. Today, however, Fès has come to be known as a city in need of critical restoration due to the deterioration of its structures. In 1981 UNESCO classified Fès as a site for the Heritage of Mankind [119].
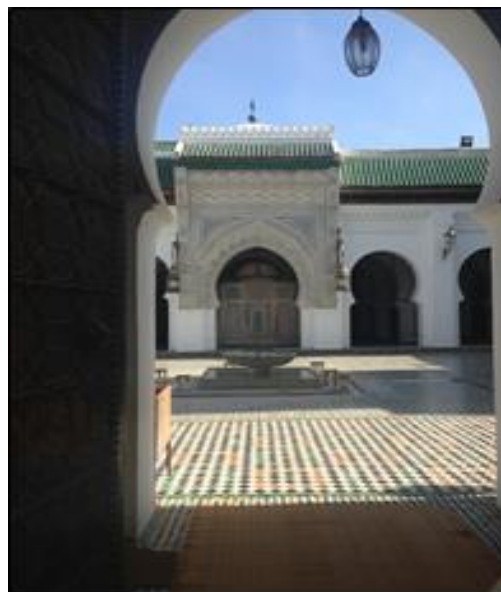
Figure 47: Al-Qarawiyyin University

The deterioration of the *medina qdima* (old city) of Fès is partly due to changing times. In order to truly understand the decay of the *medina* and therefore the process to preserve[2] and restore it, the history of the *medina* must first be discussed and understood. This research program gives a brief history of the *medina* of Fès, current preservation efforts, materials used in restoration projects, and finding the balance of integrating traditional and 'new' materials. This project was completed while working alongside ADER (Agence pour la Dédensification et la Réhabilitation de la Médina de Fès) as well as individual restorers. This research program took a new direction regarding the rehabilitation efforts; previous studies have focused on preservation of the Fès *medina* but few studies have looked at the materials used in its preservation.

Methodology

A holistic approach was taken to investigating the building materials of the *medina*. A four-step conservation plan presented by D'Ayala and Copping was used as a guide; D'Ayala and Copping examined the rehabilitation of *founduks* (caravanserai) of Salè, Morocco [120]. Steps 1-4 are described as follows:

1. **Understand;** the history of the city in terms of its conservation and what the *medina* is like today.

2. **General assessment;** of the value tied to a specific site as well as the materials used in its construction.

3. **Vulnerability**; looking at the social context as well as reasons for specific materials used

4. **Next step**; looking forward and recommendations

The collected data and reported outcomes are a compilation of interviews and observations. Interviews were conducted in both English and Darija (Moroccan Arabic); interviewees

---

[2] For this research program, the terminology of preservation, conservation and rehabilitation will be used interchangeably although a clearer definition will be provided further in the paper.

consisted of the head architect and assistant from ADER as well as a well-known individual restorer in Fès. Additionally, conversations relating to restoration were carried out with local craftsmen when observing ongoing projects onsite.

Understand

In order to fully grasp the importance of the Fès *medina* along with how and why it is crucial for preservation, the history of its development must be discussed. As Radoine describes, the general history can be broken into three main parts [121]:

- Pre-colonial period (prior to 1912)

- Colonial period (1912-1956)

- Post-colonial period

During the pre-colonial period, each ruler of Fès kept the edifices successfully built by previous rulers; however, at the same time, each ruler wanted to compete with their preceding ruler. Fès was a city of continuous growth and construction of new infrastructure; this could range from building a new *mosque*, *founduk*, *madrassa* (school), etc. The period focused on development and progress rather than destruction and, in return, preserved the fabric of the city.

However, the colonial era hindered the growth of the *medina*. The French colonized Morocco from 1912-1956 and used the conservation of the *medina* as a tactic in their favor. They took a 'culturalist' approach by first understanding the Moroccan people and culture. In doing so, they realized the cultural heritage sites of the *medina* were valued by the Moroccans and therefore they left those sites as is; this way opposition could be avoided. Instead, the French created a new section of the city (Ville Nouvelle) on a plateau above the walled *medina*. The *medina* was no longer a place for growth and development as in previous times. Rather, it

became a place where those from the countryside, hired for colonial industrialization, would reside. It became home to the poor and quickly overpopulated.

Once Morocco achieved independence (post-colonial period), the *medina* was left as a place with no hope to prosper leading to its decay. An example can be shown in Figure 48 where a structure was left to fall apart. Additionally, the wealthier residents began moving to the Ville Nouvelle, leaving many of the poorer migrants in the *medina*. These migrants would reside in formerly prominent homes (which were many times large) and could not afford the upkeep of these homes. This led to homes initially intended for the use of one family being transformed into multifamily residences. Residences quickly became overpopulated, increased in poor hygiene and in turn was not preserved [121, 122].

Preservation efforts

The importance of Fès expands beyond an acknowledgement of its history but a place where private investors are willing to fund major restoration projects. This is due to the many unique qualities it possesses including its architectural value, craftsmanship, its geographical location

Figure 48: A decayed structure in the medina. The entire building has been sheared off

(with springs and rivers), an area that spans 800 acres (323.7 ha) surrounded by a 20 kilometer (65616.8 ft.) wall, as well as its existing pedestrian roads [123]. Although the *medina* of Fès was left in crumbles due to the French colonization, international organizations saw the value and significance of preserving the craftsmanship and architecture of this historic city. UNESCO became interested in Fès; in 1972 they sent two experts to evaluate the *medina*. Initially it was thought that simply restoring the main sites in the *medina* (i.e. *mosques, founduks, madarssas,* etc.) would be enough – until they arrived in the *medina*. They realized that in order to restore the monuments, the entirety of the old city needed to be restored since the city works in cohesion [122, 124]. In 1981 Fès was declared as a world heritage city where it was described as significant part of Moroccan history [119]:

'The Medina of Fez [sic] preserves in its old, densely monumental, parceling the memory of the capital founded in 192 of the Hegira (808 AD) by Idriss II… Fez is at once an astonishing city-museum and one of the largest Islamic metropole where various demographic strata determined the greatest variety of architectural forms and urban landscapes.'[125]

By UNESCO recognizing Fès, it brought attention to the importance of the city as well raised interest to private investors.

ADER Fès

ADER Fès began in 1989 as a semi-private organization meant to safeguard the historical and cultural value of Fès. Along with preserving the structures of the *medina,* ADER has the goal preserving the artisanal trade and craftsmanship, which was a disappearing due to it being mainly oral knowledge passed down from generations. There are 13,385 buildings in the *medina*, of which 11,601 are historic and 3,000 are historic monuments (historical monuments are buildings such as *mosques, founduks, and madarssas* whereas historic structures are places such as homes).

Currently, there are a total 3,666 structures which are structurally deficient in the Fès *medina;* ADER is currently working on 1,241 structures and they have completed 1,062 to date [126].

ADER has a geographical information system (GIS) that identifies all the buildings of the *medina*. The GIS has at least 30 details regarding each site. ADER is known to be associated with major historic restorations such as the *Founduk Nejjarin* shown in Figure 49 [127]. Additionally a list of 27 historical monuments listed in

Table 13 *(overleaf)* were declared by Morocco's King Mohammed VI of significant importance and are either completed in restoration, in the process, or will be worked on in the near future. With monuments and building of such caliber of importance, attention to the details of the materials used is magnified. The best craftsmen are hired and work with traditional materials.

Moreover, there many structures within the medina which are in need for repair but do not

Figure 49: Founduk Najjarin restored

necessarily have historical value as in the monuments; ADER operates in terms of conserving the

Table 13: 27 historical monuments

Historic monuments
Madrasa Sahrij
Mesbahia Madrasa
Madrasa Sbaiyine
Seffarine Medersa
Hammam Ibn Abbad
Bridge Khrachfiyine
Bridge Terrafine
Dar Dmana
Dar Lazrak
Borj Sidi Bouafae
Borj Neffara
Borj Boutouil
Borj Al Kawkab
Foundouk Achiche
Foundouk Kettanine
Foundouk Sagha
Ain Azliten Tannery
Tannery Sidi Moussa
Bab Makina
Wall-Bab Chems
Jenifer Wall
Jnane Drader-Lahid-Bab Mausoleum
Sidi Hrazem
Kissariat Al Kifah (traditional part)
Dar Dbagh Chouara
Souk Sebbaghine
Al Quaraouiyine library

city. Every day, technicians are on site in the *medina* conducting visual inspections and noting possible structures needing repair or restoration. Residents can also come to the ADER offices and let the organization know that their home may need repair. In such cases, ADER sends an architect to evaluate the structure. For residential restorations, ADER can allot residents up to 80,000 MAD for repair. If accepted by ADER, the residents receive an architect from ADER but must hire the craftsmen and an engineering company (ADER architects must approve all potential changes to the structure as well check on the developments made during construction) [128]. An example of a *dar* (home) that was funded by ADER for its restoration is shown in

Figure 50: Restored *dar* with partial funding from ADER

Figure 50 (a picture of the home prior to the restoration was not available by ADER chose to show this home as an example since it was in poor condition prior to restorations).

In 1997, ADER partnered with Harvard University's Graduate School of Design Unit for Housing and Urbanization and the World Bank to present a case study of the rehabilitation of Fès [129]. 240m MAD ($23.6m USD) from the public sector and $14m USD (142m MAD) from the World Bank were secured for rehabilitation projects. This resulted in a report detailing the practicality as well as the essential job opportunities that could come out of preservation efforts in Fès. The report listed seven potential results:

1. Enhancements to current circulation network

2. Design of an emergency vehicular network

3. Environmental progress such as moving industries causing pollution to other industrial locations outside the *medina*

4. Growth of current programs in order to advance the built environment, such as the removal of ruins, creation of community facilities, and urban landscaping

5. Establishment of an incentive program to encourage private investment in developments to the medina and involve residents in the rehabilitation process

6. Design for tourist routes and the restoration of monuments

7. Poverty mitigation through the employment opportunities

Vulnerability

Although private investments and other preservation efforts exist in Fès, the social context must be discussed. Once this concept is developed, the reasons for specific materials used in both the construction and conservation of the city can be investigated.

Defining 'preservation'

The terminology 'preservation' is many times thrown around and has been quite widely used in this paper. However, it is important to define the term. One definition is that it is critical to keep structures in their original condition as much as possible whereas some consider it essential to adjust accordingly to changes in time [130]. Alberts and Hazen explain that there are varying methodologies regarding preservation [131, 132]. "Preservation/conservation" is described as leaving the structure in its original state and only making necessary changes to prevent further damage to the site. "Restoration" is about bringing the structure into its original state while trying to keep all components as much as possible (i.e. use original beams). "Reconstruction" is a structure built to replicate a historic building. "Adaptation" is the modification of a structure in order to accommodate for modern usages [132]. These definitions are provided just as reference and not intended to categorize the *medina* Fès.

93

The projects of the Fès *medina* can be considered as a culmination of the definitions described above. At times, it is necessary to preserve, restore, reconstruct, and adapt the *medina* sites. When attempting to rehabilitate the structures of the *medina* it is critical to understand and know what materials are used and why. Many times the materials used to rehabilitate structures are overlooked and therefore may cause premature deterioration and may hinder the aesthetics. The materials used when initially building the *medina* were methodically chosen and had a purpose. Therefore, it is critical to know the reasoning behind the materials originally used in order to help in the preservation/restoration projects.

Traditional Building Materials

Construction of buildings - a monument, a *dar*, a *madrassa*, a *fouduk* - in Fès all had a purpose and the city was well planned out [133]. This also goes for the materials[3] used in building these structures. Although the structures of the *medina* have need for restoration, these structures have remained standing after all this time and neglect, and the reason comes down to the materials that were used. Traditional walls were made from *jeer* (lime), *ramal* (sand), and *liyajoor beldi* (bricks). For the supportive beams, *ilerz* (cedar wood) was placed [134, 135]. Two of the three important building materials are studied for this research program: lime and cedar wood.

Lime has the following properties [136]:

- **Breathability:** Lime is highly porous and permeable. This allows for the flow of moisture through a building and therefore avoiding issues related to condensation.

- **Autogenous healing:** Small, thin cracks are commonly found in lime based structures (as opposed to large cracks found in cement based ones). These small cracks can self-heal when water penetrates into the cracks depositing small amounts 'free' lime on

---

[3] This paper discusses solely the materials used in the buildings - the building methods (i.e. architectural styles and purposes) are not within the scope of this paper.

the surface. Once the water evaporates, the lime is left and 'heals' the cracks. This phenomenon can be noticed in many old structures that deform rather than immediately fail. This is particularly important since Fès is in an earthquake zone.

- *Low thermal conductivity:* The low thermal conductivity of lime impacts the temperature inside a building, leading to the inside of structures feeling warmer when outside temperatures are cooler. This is something important in Fès because of the temperature drop in the winters.

- *Soft texture:* Lime, having a soft texture, acts as a cushion between bricks and stones. This type of buffer avoids the potential issues such as cracking of the brick.

- *Workability:* Lime-based binders are easily molded and can form easily during construction.

The support beams of structures in the Fès *medina* are mainly made of cedar wood shown in

Figure 51: Cedar beams (in circle) in a tradition building

Figure 51. This wood came from the cedar trees of the Rif, Mid Atlas, and High Atlas ranges [137, 138]. The properties of cedar wood are:

- Cedar is resistant to insects and rot.

- Has dimensional stability where it will not expand or contract in size even in weather, humidity, or temperature changes.

- Since cedar is porous it can absorb noise.

Finding the balance between the traditional and new materials

It is ideal to use all traditional building materials and techniques when restoring structures of the Fès *medina* because each material serves a purpose. However, realistically, many factors come into play. The cost of using traditional materials is at many times far too expensive. For example, cedar is about 14,000 MAD/m^3 ($38.90 USD/ft^3) and traditional bricks are around 1,700 MAD/m^3 ($4.72 USD/ft^3) built. In addition, the cost of hiring a craftsman is more expensive due to their rarity. Craftsmen are mainly taught through apprenticeship and are a disappearing trade due to changes of time such as technology. This culmination would mean that the structures, even though partially funded by ADER, would be quite difficult to complete. Thus, it is important to find that balance and recognize when and where it is acceptable to use 'new' materials.

The term 'new material' refers to a building material that was not previously used in the original construction of Fès. The common replacements to cedar are steel beams, and the replacement for lime is cement (ordinary portland cement) as a binder. If not careful with the proper use of these 'new' materials, the 'new' materials could visually affect the structure or even be significantly detrimental (i.e. cause premature deterioration). *Note: when observing the*

Figure 52: Slab using cement for flooring

materials of the medina, it can be very difficult to analyze just by a quick visual check. However, the following observations were noticed during ongoing construction projects.

The use of cement has grown quite popular within the construction sites of the *medina*. Cement has a quicker set time than lime and is less expensive. However, the use of cement can be very destructive to these historic structures if not used correctly. Figure 52 shows the use of cement in an appropriate way. The second floor of a house had a cement slab placed as new flooring. The structure is not impacted or harmed due to the fact that the cementitious flooring does not impact its surrounding materials. The properties that would be beneficial of using lime (such as breathability) are insignificant in this case. Figure 53 *(overleaf)* shows two images of concerning uses of cement. Cementitious mortar is simply 'slapped' on the surface of these homes. Using cement in this manner will cause severe problems in the future by producing early failure of the material. Cement is impervious and rigid, and if it begins cracking, large cracks

97

Figure 53: Cement mortar mixed inappropriately with traditional lime mix

could occur and progress rapidly. Adding cement to a porous, flexible lime mortar will cause spalling and early deterioration.

Some of the structures undergoing restoration need to have additional supports to load since a lot of the columns and beams are no longer capable of doing so. One example is in Figure 54. A *founduk* under construction has a C-column added for support. However, the architect has made sure to consider the original column and will insert the original column inside the new steel

Figure 54: a) *Founduk* under restoration; b) C-column put in place for structural purposes; c) The original columns that will be placed in the C-column to keep original look

Figure 55: Under passage with steel beam exposed

column. This will give the *founduk* its original look but will now be structurally safe. However, in Figure 55, an under passage has been restored (by ADER) but the steel beams are left exposed which becomes aesthetically displeasing and an eyesore.

The topic of sustainability in terms of continual use of cedar wood is also brought about by expert preservationists [126, 139]. Additional to the high cost of cedar, trees may be destroyed. One solution would be to determine if there is a material comparable in properties as cedar that could be used. In terms of aesthetics, the reuse of old cedar is another answer.

Individual restoration projects

Individuals including non-Moroccans can buy and restore homes within the *medina*. The concept of purchasing a *riad* (a traditional, Moroccan guest house with a courtyard and garden in the center), and renovating it has increased in popularity and has been referred to as '*riad* fever' [140]. This phenomena has become trendy and the *riads* are used as vacation homes or even become hotels for those who want a traditional experience when visiting Fès [140]. These traditional homes are at times bought in bad physical condition and restored beautifully.

However, independent restorers are generally not experts in the field of restoration nor many cannot decipher whether the restoration is completed with quality. They usually are not funded by ADER and do not have an expert architect to oversee their project. This brings about the question of how these independent restorers find craftsmen and complete their restorations. Usually, craftsmen are found by word of mouth. There is no network to really know if that craftsman is actually a quality one. Many times it can be a trial-and-error type of project [135]. This phenomenon needs to be addressed and further studied by organizations such as ADER.

Next step

The Fès *medina* is a rich and defined part of Moroccan history. Preserving it takes more than one initiative. Organizations currently present such as ADER and private investors are making great strides. If the materials used in these preservation projects are brought to light and further investigated, the quality of restoration can be improved as well as may increase the life cycle of these structures. Future studies on material testing are needed. By having both the chemical and material analyses of traditional and 'new' materials and reviewing the results, awareness on restoration materials can be raised. In doing so, the Fès *medina* can continue to be preserved in a manner that will last generations.

REFERENCES

1. Lea, F.M., *The chemistry of cement and concrete.* 1970.
2. Garboczi, E.J., and Bentz, D.P, *Multi-scale picture of concrete and its transport properties: Introduction for non-cement researchers*. 1996: National Institute of Standards and Technology Internal Report
3. Menn, C., *Prestressed concrete bridges*. 2012: Birkhäuser.
4. Aldred, J. *Burj Khalifa–a new high for high-performance concrete*. in *Proceedings of the Institution of Civil Engineers-Civil Engineering*. 2010. Thomas Telford Ltd.
5. Hilsdorf, H. and J. Kropp, *Performance criteria for concrete durability*. Vol. 12. 2004: CRC Press.
6. ASCE, *2013 Report Card for America's Infrastructure*. 2013.
7. Chen, Z., *Effect of reinforcement corrosion on the serviceability of reinforced concrete structures.* Master's thesis, Department of Civil Engineering, University of Dundee, UK, 2004.
8. Li, F., Y. Yuan, and C.-Q. Li, *Corrosion propagation of prestressing steel strands in concrete subject to chloride attack.* Construction and Building Materials, 2011. **25**(10): p. 3878-3885.
9. Neville, A.M., *Properties of concrete*. 1995.
10. Kosmatka, S.H.K., Beatrix; Panarese, William C, *Design and Control of Concrete Mixtures* ed. PCA. 2008, Skokie, IL Portland Cement Association
11. Bertolini, L., et al., *Corrosion of steel in concrete: prevention, diagnosis, repair*. 2013: John Wiley & Sons.
12. Popovics, S., *Concrete materials: properties, specifications, and testing*. Vol. 2nd. 1992, Park Ridge, N.J: Noyes Publications.
13. Lea, F.M., P.C. Hewlett, and C. Books24x7 EngineeringPro, *Lea's chemistry of cement and concrete*. Vol. 4th. 1998, New York;London;: Arnold.
14. Wang, C.-K.S., Charles G.; Pincheira, Jose A. , *Reinforced concrete design* 7th ed. 2007 Hoboken, NJ John Wiley & Sons, Inc. .
15. Li, Z.D. and C. Ebrary Academic, *Advanced concrete technology*. Vol. 1. 2011, Hoboken, N.J: Wiley.
16. Koch, G.H., et al., *Corrosion cost and preventive strategies in the United States*. 2002.
17. Emmons, P.H.a.D.J.S., *The State of the Concrete Repair Industry, and a Vision for its Future.* Concrete Repair Bulletin, 2006: p. 7-14.
18. Ahmad, S., *Reinforcement corrosion in concrete structures, its monitoring and service life prediction—a review.* Cement and Concrete Composites, 2003. **25**(4–5): p. 459-471.
19. Söylev, T. and M. Richardson, *Corrosion inhibitors for steel in concrete: State-of-the-art report.* Construction and Building Materials, 2008. **22**(4): p. 609-622.
20. Böhni, H., *Corrosion In Reinforced Concrete Structures*. 2005: Woodhead pub.
21. Park, D.C., *Carbonation of concrete in relation to CO2 permeability and degradation of coatings.* Construction and Building Materials, 2008. **22**(11): p. 2260-2268.
22. Talukdar, S., N. Banthia, and J.R. Grace, *Carbonation in concrete infrastructure in the context of global climate change – Part 1: Experimental results and model development.* Cement and Concrete Composites, 2012. **34**(8): p. 924-930.
23. Houst, Y.F. and F.H. Wittmann, *Depth profiles of carbonates formed during natural carbonation.* Cement and Concrete Research, 2002. **32**(12): p. 1923-1930.

24.	Broomfield, J.P., *Corrosion of steel in concrete: understanding, investigation and repair*. 1997: Spon Press.

25.	Raupach, M., *Chloride-induced macrocell corrosion of steel in concrete—theoretical background and practical consequences.* Construction and Building Materials, 1996. **10**(5): p. 329-338.

26.	Lindquist, W.D., et al., *Effect of cracking on chloride content in concrete bridge decks.* ACI Materials Journal, 2006. **103**(6): p. 467.

27.	Şahmaran, M. and V.C. Li, *De-icing salt scaling resistance of mechanically loaded engineered cementitious composites.* Cement and Concrete Research, 2007. **37**(7): p. 1035-1046.

28.	Tuutti, K., *Corrosion of steel in concrete*. 1982.

29.	Cusson, D., Z. Lounis, and L. Daigle, *Benefits of internal curing on service life and life-cycle cost of high-performance concrete bridge decks–A case study.* Cement and Concrete Composites, 2010. **32**(5): p. 339-350.

30.	Manning, D.G., *Corrosion performance of epoxy-coated reinforcing steel: North American experience.* Construction and Building Materials, 1996. **10**(5): p. 349-365.

31.	Virmani, Y.P. and G.G. Clemena, *Corrosion protection-concrete bridges*. 1998.

32.	Kepler, J.L., D. Darwin, and C.E. Locke Jr, *Evaluation of corrosion protection methods for reinforced concrete highway structures*. 2000, University of Kansas Center for Research, Inc.

33.	Manning, D.G., N.R.C.T.R. Board, and N.C.H.R. Program, *Waterproofing Membranes for Concrete Bridge Decks*. 1995: National Academy Press.

34.	Russell, H.G., *Waterproofing Membranes for Concrete Bridge Decks*. Vol. 425. 2012: Transportation Research Board.

35.	Kepler, J.L., D. Darwin, and C.E. Locke, *Evaluation of Corrosion Protection Methods for Reinforced Concrete Highway Structures*. 2000, Kansas Department of Transportation.

36.	Pike, R., *Nonmetallic coatings for concrete reinforcing bars.* Public Roads, 1973. **37**(5).

37.	Clifton, J., H. Beighly, and R. Mathey, *Final Report: Non-metallic coatings for concrete reinforcing bars Federal Highway Administration Rep*. 1974, FHWA-RD-74-18.

38.	May, C., *Epoxy resins: chemistry and technology*. 1987: CRC press.

39.	Kilareski, W., *Epoxy coatings for corrosion protection of reinforcement steel*, in *Chloride Corrosion of Steel in Concrete*. 1977, ASTM International.

40.	Smith, L., R. Kessler, and R.G. Powers, *Corrosion of epoxy-coated rebar in a marine environment.* Transportation Research Circular, 1993(403).

41.	Baddoo, N.R., *Stainless steel in construction: A review of research, applications, challenges and opportunities.* Journal of Constructional Steel Research, 2008. **64**(11): p. 1199-1206.

42.	NÜRNBERGER, U., *Stainless steel in concrete structures.* Corrosion in reinforced concrete structures, 2005: p. 135.

43.	El-Reedy, M.A. and EngnetBase, *Steel-reinforced concrete structures: assessment and repair of corrosion*. 2008, Boca Raton: CRC Press.

44.	Pedeferri, P., *Cathodic protection and cathodic prevention.* Construction and Building Materials, 1996. **10**(5): p. 391-402.

45.	Saricimen, H., et al., *Effectiveness of concrete inhibitors in retarding rebar corrosion.* Cement and Concrete Composites, 2002. **24**(1): p. 89-100.

46. Bjegovic, D., *Migrating corrosion inhibitor protection of concrete.* Materials performance, 1999. **38**(11): p. 52-56.

47. Tritthart, J., *Transport of a surface-applied corrosion inhibitor in cement paste and concrete.* Cement and Concrete Research, 2003. **33**(6): p. 829-834.

48. Söylev, T.A., C. McNally, and M.G. Richardson, *The effect of a new generation surface-applied organic inhibitor on concrete properties.* Cement and Concrete Composites, 2007. **29**(5): p. 357-364.

49. SCHIEGG, Y., F. HUNKELER, and H. UNGRICHT. *The Effectiveness of Corrosion Inhibitors–a Field Study.* in *IABSE Congress Report.* 2000. International Association for Bridge and Structural Engineering.

50. Growcock, F. and W. Frenier, *Kinetics of Steel Corrosion in Hydrochloric Acid Inhibited with trans-Cinnamaldehyde.* Journal of The Electrochemical Society, 1988. **135**(4): p. 817-823.

51. A Negm, N., M. A Yousef, and S. M Tawfik, *Impact of Synthesized and Natural Compounds in Corrosion Inhibition of Carbon Steel and Aluminium in Acidic Media.* Recent Patents on Corrosion Science, 2013. **3**(1): p. 58-68.

52. Rieger, K.A. and J.D. Schiffman, *Electrospinning an essential oil: Cinnamaldehyde enhances the antimicrobial efficacy of chitosan/poly (ethylene oxide) nanofibers.* Carbohydrate Polymers, 2014.

53. Subash Babu, P., S. Prabuseenivasan, and S. Ignacimuthu, *Cinnamaldehyde—a potential antidiabetic agent.* Phytomedicine, 2007. **14**(1): p. 15-22.

54. Jafferji, H.K., Gregory T.; Schiffman, Jessica D.; Sakulich, Aaron R., *Preliminary Investigations of Essential Oils as Corrosion Inhibitors in Steel Reinforced Cementitious Systems.* Proceeding of the Thrity-Fifth Conference on Cement Microscopy, USA, 2013: p. 40-48.

55. Jafferji, H. and A.R. Sakulich. *Impact of Corrosion Inhibitors on Design.* in *Proceedings of the 2nd International Workshop on Design in Civil and Environmental Engineering.* 2013. Mary Kathryn Thompson.

56. Bremner, T. and J. Ries, *Stephen J. Hayde: Father of the Lightweight Concrete Industry.* Concrete international, 2009. **31**(08): p. 35-38.

57. Bentz, D.P. and W.J. Weiss, *Internal curing: A 2010 state-of-the-art review.* 2011: US Department of Commerce, National Institute of Standards and Technology.

58. ASTM, *Standard Test Method for Sieve Analysis of Fine and Coarse Aggregates C136.* West Conshohocken, PA.

59. Alexander, M. and S. Mindess, *Aggregates in concrete.* 2010: CRC Press.

60. Kosmatka, S.H., B. Kerkhoff, and W.C. Panarese, *Design and control of concrete mixtures.* 2011: Portland Cement Assoc.

61. Bentz, D.P., P. Lura, and J.W. Roberts, *Mixture proportioning for internal curing.* Concrete International, 2005. **27**(2): p. 35-40.

62. Sika, *Sika® FerroGard®-903+The Unique Multi-Functional Surface Applied Corrosion Inhibitor for Reinforced Concrete.*

63. Sakulich, A. and D. Bentz, *Incorporation of phase change materials in cementitious systems via fine lightweight aggregate.* Construction and Building Materials, 2012. **35**: p. 483-490.

64.   Castro, J., et al., *Absorption and desorption properties of fine lightweight aggregate for application to internally cured concrete mixtures.* Cement and Concrete Composites, 2011. **33**(10): p. 1001-1008.

65.   ASTM, *Standard Test Method for Chemical Shrinkage of Hydraulic Cement Paste.*

66.   Tazawa, E.-i., S. Miyazawa, and T. Kasai, *Chemical shrinkage and autogenous shrinkage of hydrating cement paste.* Cement and concrete research, 1995. **25**(2): p. 288-292.

67.   ASTM, *Standard Test Method for Compressive Strength of Hydraulic Cement Mortars (Using 2-in. or [50-mm] Cube Specimens).*

68.   ASTM, *Standard Test Methods for Time of Setting of Hydraulic Cement by Vicat Needle C191.*

69.   Hewlett, P., *Lea's chemistry of cement and concrete.* 2003: Butterworth-Heinemann.

70.   ASTM, *Standard Test Method for Air Content of Hydraulic Cement Mortar.*

71.   Bentz, D.P. and R. Turpin, *Potential applications of phase change materials in concrete technology.* Cement and Concrete Composites, 2007. **29**(7): p. 527-532.

72.   Bentz, D.P., K.A. Snyder, and M.A. Peltz, *Doubling the service life of concrete structures. II: Performance of nanoscale viscosity modifiers in mortars.* Cement and Concrete Composites, 2010. **32**(3): p. 187-193.

73.   ASTM, *Standard Test Method for Autogenous Strain of Cement Paste and Mortar*

74.   Tazawa, E.-i., *Autogenous shrinkage of concrete.* 1999: CRC Press.

75.   Detwiler, R.J., K.O. Kjellsen, and O.E. Gjorv, *Resistance to chloride intrusion of concrete cured at different temperatures.* ACI Materials Journal, 1991. **88**(1).

76.   Shaker, F., A. El-Dieb, and M. Reda, *Durability of styrene-butadiene latex modified concrete.* Cement and concrete Research, 1997. **27**(5): p. 711-720.

77.   Okba, S., A. El-Dieb, and M. Reda, *Evaluation of the corrosion resistance of latex modified concrete (LMC).* Cement and concrete research, 1997. **27**(6): p. 861-868.

78.   Elmoaty, A. and A.E. Mohamed, *Mechanical properties and corrosion resistance of concrete modified with granite dust.* Construction and Building Materials, 2013. **47**: p. 743-752.

79.   Güneyisi, E., et al., *Corrosion behavior of reinforcing steel embedded in chloride contaminated concretes with and without metakaolin.* Composites Part B: Engineering, 2013. **45**(1): p. 1288-1295.

80.   Güneyisi, E., T. Özturan, and M. Gesoğlu, *A study on reinforcement corrosion and related properties of plain and blended cement concretes under different curing conditions.* Cement and Concrete Composites, 2005. **27**(4): p. 449-461.

81.   Gowers, K. and S. Millard, *Measurement of Concrete Resistivity for Assessment of Corrosion Severity of Steel using Wenner Technique* ACI Materials Journal, 1999. **96**(5).

82.   Al-Zahrani, M., et al., *Effect of waterproofing coatings on steel reinforcement corrosion and physical properties of concrete.* Cement and Concrete Composites, 2002. **24**(1): p. 127-137.

83.   Scrivener, K.L., A.K. Crumbie, and P. Laugesen, *The interfacial transition zone (ITZ) between cement paste and aggregate in concrete.* Interface Science, 2004. **12**(4): p. 411-421.

84.   Ollivier, J., J. Maso, and B. Bourdette, *Interfacial transition zone in concrete.* Advanced Cement Based Materials, 1995. **2**(1): p. 30-38.

85.   ASTM, *Standard Test Method for Measurement of Rate of Absorption of Water by Hydraulic-Cement Concretes*

86. Ismail, I., et al., *Influence of fly ash on the water and chloride permeability of alkali-activated slag mortars and concretes.* Construction and Building Materials, 2013. **48**: p. 1187-1201.

87. Baroghel-Bouny, V., et al., *AgNO3 spray tests: advantages, weaknesses, and various applications to quantify chloride ingress into concrete. Part 1: Non-steady-state diffusion tests and exposure to natural conditions.* Materials and structures, 2007. **40**(8): p. 759-781.

88. Baroghel-Bouny, V., et al., *AgNO3 spray tests: advantages, weaknesses, and various applications to quantify chloride ingress into concrete. Part 2: Non-steady-state migration tests and chloride diffusion coefficients.* Materials and Structures, 2007. **40**(8): p. 783-799.

89. Aldea, C.-M., et al., *Effects of curing conditions on properties of concrete using slag replacement.* Cement and Concrete Research, 2000. **30**(3): p. 465-472.

90. NIH, *Image J program*

91. Ann, K.Y. and H.-W. Song, *Chloride threshold level for corrosion of steel in concrete.* Corrosion Science, 2007. **49**(11): p. 4113-4133.

92. Yeih, W., et al., *A pullout test for determining interface properties between rebar and concrete.* Advanced Cement Based Materials, 1997. **5**(2): p. 57-65.

93. Baena, M., et al., *Experimental study of bond behaviour between concrete and FRP bars using a pull-out test.* Composites Part B: Engineering, 2009. **40**(8): p. 784-797.

94. De Lorenzis, L., A. Rizzo, and A. La Tegola, *A modified pull-out test for bond of near-surface mounted FRP rods in concrete.* Composites Part B: Engineering, 2002. **33**(8): p. 589-603.

95. Chen, G., et al., *Coated Steel Rebar for Enhanced Concrete-Steel Bond Strength and Corrosion Resistance.* 2010.

96. Mo, K.H., et al., *Feasibility study of high volume slag as cement replacement for sustainable structural lightweight oil palm shell concrete.* Journal of Cleaner Production, 2015. **91**: p. 297-304.

97. Jorge, S., D. Dias-da-Costa, and E. Júlio, *Influence of anti-corrosive coatings on the bond of steel rebars to repair mortars.* Engineering Structures, 2012. **36**: p. 372-378.

98. Soylev, T. and R. François, *Quality of steel–concrete interface and corrosion of reinforcing steel.* Cement and Concrete Research, 2003. **33**(9): p. 1407-1415.

99. Henkensiefken, R., et al., *Internal curing improves concrete performance throughout its life.* Concrete InFocus, 2009. **8**(5): p. 22-30.

100. Lura, P., et al., *Influence of shrinkage-reducing admixtures on development of plastic shrinkage cracks.* ACI Materials Journal, 2007. **104**(2): p. 187.

101. Uchikawa, H., D. Sawaki, and S. Hanehara, *Influence of kind and added timing of organic admixture on the composition, structure and property of fresh cement paste.* Cement and Concrete Research, 1995. **25**(2): p. 353-364.

102. Bentz, D.P., *Internal curing of high-performance blended cement mortars.* ACI Materials Journal, 2007. **104**(4): p. 408.

103. De la Varga, I., et al., *Application of internal curing for mixtures containing high volumes of fly ash.* Cement and Concrete Composites, 2012. **34**(9): p. 1001-1008.

104. Sakulich, A.R. and D.P. Bentz, *Increasing the service life of bridge decks by incorporating phase-change materials to reduce freeze-thaw cycles.* Journal of Materials in Civil Engineering, 2011. **24**(8): p. 1034-1042.

105.   Bentur, A., S.-i. Igarashi, and K. Kovler, *Prevention of autogenous shrinkage in high-strength concrete by internal curing using wet lightweight aggregates.* Cement and concrete research, 2001. **31**(11): p. 1587-1591.

106.   Henkensiefken, R., et al., *Volume change and cracking in internally cured mixtures made with saturated lightweight aggregate under sealed and unsealed conditions.* Cement and Concrete Composites, 2009. **31**(7): p. 427-437.

107.   Raoufi, K., et al., *Parametric assessment of stress development and cracking in internally cured restrained mortars experiencing autogenous deformations and thermal loading.* Advances in Civil Engineering, 2011. **2011**.

108.   Lura, P., *Autogenous deformation and internal curing of concrete.* 2003.

109.   Polder, R.B. and W.H. Peelen, *Characterisation of chloride transport and reinforcement corrosion in concrete under cyclic wetting and drying by electrical resistivity.* Cement and Concrete Composites, 2002. **24**(5): p. 427-435.

110.   Weiss, J., et al., *Using a saturation function to interpret the electrical properties of partially saturated concrete.* Journal of Materials in Civil Engineering, 2012. **25**(8): p. 1097-1106.

111.   Biricik, H. and N. Sarier, *Comparative study of the characteristics of nano silica - , silica fume - and fly ash - incorporated cement mortars.* Materials Research, 2014. **17**: p. 570-582.

112.   Miranda Júnior, E.J.P.d., et al., *Increasing the compressive strength of Portland cement concrete using flat glass powder.* Materials Research, 2014. **17**: p. 45-50.

113.   Bentz, D.P., *Influence of internal curing using lightweight aggregates on interfacial transition zone percolation and chloride ingress in mortars.* Cement and concrete composites, 2009. **31**(5): p. 285-289.

114.   Lo, T.Y., et al., *The effects of air content on permeability of lightweight concrete.* Cement and concrete research, 2006. **36**(10): p. 1874-1878.

115.   Ghafari, E., et al., *The effect of nanosilica addition on flowability, strength and transport properties of ultra high performance concrete.* Materials & Design, 2014. **59**: p. 1-9.

116.   Henkensiefken, R., et al., *Water absorption in internally cured mortar made with water-filled lightweight aggregate.* Cement and Concrete Research, 2009. **39**(10): p. 883-892.

117.   Peterson, K., *Petrographic study (image)*

118.   Bianca, S., *Fez: The Ideal and the Reality of the Islamic City.* The Moroccan Ministry of Housing and Urban Planning, 1981.

119.   UNESCO. *Medina of Fez.*   [cited 2015 December 8]; Available from: http://whc.unesco.org/en/list/170/.

120.   D'Ayala, D. and A.G. Copping, *Holistic approach to the rehabilitation of Foundouks in Morocco.* APT Bulletin, 2007. **38**(2/3): p. 39-46.

121.   Radoine, H., *Conservation-based cultural, environmental, and economic development: The case of the walled city of Fez.* 2003: na.

122.   Bianca, S., *Conservation and rehabilitation projects for the old city of fez*, in *Adaptive reuse: integrating traditional areas into the modern urban fabric*. 1983, The aga khan program for islamic architecture. p. 47-59.

123.   Radoine, H., *Urban conservation of Fez-Medina: a post-impact Appraisal.* Global Urban Development Magazine, 2008. **4**(1): p. 1-12.

124.   UNESCO, *International Campaignin for Safegaurd of the Medina of Fez*, in *Cultural Heritage Division* 1998.

125. Sites, I.C.o.M.a., *World Heritage List N° 170*. 1980.
126. ADER, *Interview with architect of ADER Fès*. 2015-2016.
127. Radoine, H., *Medina: evolution of an urban tyology*. L'Architecture d'Aujourd'hui, 2015(408): p. 104-107.
128. Jafferji, H., *Interview with ADER*. 2015-2016.
129. pour la Dedensification, A., *Case Study: Fez, Morocco Rehabilitation of the Fez Medina.*
130. Tyler, N., T.J. Ligibel, and I.R. Tyler, *Historic preservation: An introduction to its history, principles, and practice*. 2009: WW Norton & Company.
131. Alberts, H.C. and H.D. Hazen, *Maintaining authenticity and integrity at cultural world heritage sites*. Geographical Review, 2010. **100**(1): p. 56-73.
132. Aplin, G., *Heritage identification, conservation and management*. 2002: Oxford University Press.
133. Radoine, H., *Planning paradigm in the madina: order in randomness*. Planning Perspectives, 2011. **26**(4): p. 527-549.
134. Grillo, A., *Traditional Building Techniques in Fes*. 1988, Environmental.
135. Jafferji, H., *Interview with David Amster*. 2015-2016.
136. Holmes, S.W., Michael, *Building with Lime* 2008: Intermediate Technology Publications.
137. Brunetti, M., et al., *Natural durability, physical and mechanical properties of Atlas cedar (Cedrus atlantica Manetti) wood from Southern Italy*. Annals of forest science, 2001. **58**(6): p. 607-613.
138. Navarro-Cerrillo, R.M., et al., *Structure and spatio-temporal dynamics of cedar forests along a management gradient in the Middle Atlas, Morocco*. Forest Ecology and Management, 2013. **289**: p. 341-353.
139. Architecte, K.R., *Interview with Kamal Raftani* 2015-2016.
140. Lee, J., *Riad fever: Heritage tourism, urban renewal and the medina property boom in old cities of Morocco*. E Review of Tourism Research, 2008. **6**(4): p. 66-78.